Department of Physiology and Pharmacology "Vittorio Erspamer"

PhD Program in Pharmacology

XXX cycle

'Dosis sola facit, ut venenum non fit'

A novel selective cell-permeable peptide disrupts presynaptic JNK2-STX1a interaction, providing neuroprotection and preventing glutamate-mediated *excitotoxicity*

A Dissertation Submitted in Fulfilment of the Requirements

for the Degree of Doctor of Philosophy in Pharmacology

by

Serena Marcelli

Thesis Supervisor

Prof. Robert G. Nisticò

Thesis Co-supervisor

Dott. Marco Feligioni

Academic year 2016/2017

I do not know what I may appear to the world, but to myself I seem to have been only like a child playing on the seashore, and diverting myself in now and then finding a smoother pebble or a prettier shell than ordinary, whilst the great ocean of truth lay all undiscovered before me.

- Sir Isaac Newton

To strive, to seek, to find, and not to yield.

CONTENTS

ABSTRACT

L-glutamate is the major excitatory neurotransmitter in the central nervous system of vertebrates. By playing a dual role as amino acid and neurotransmitter, glutamate fulfils a large array of physiological functions supporting neuronal development and cognitive performances. Consequently, the alteration of glutamate signaling entails profound detrimental effects that give rise to disease conditions, including *excitotoxicity* induced by cerebral ischemia.

Although plenty of reports have so far investigated the effects of cerebral ischemia at postsynaptic sites, little is known concerning the mechanisms activated by the ischemic injury at the presynaptic terminal.

NMDA receptors have been classically implicated in both postsynaptic and presynaptic pathways sustaining *excitotoxicity*. Recently, their intracellular association with the c-Jun *N*-terminal kinase (JNK) has also been involved in such pathological mechanisms.

Our previous findings already underlined a specific and unique involvement of the JNK2 isoform as a pivot player in glutamate release, when focusing on presynaptic sites.

In the present dissertation we furthermore unveil the selective protein-protein interaction between JNK2 and Syntaxin-1a (STX1a), emphasizing their unexplored contribution in the docking and release of synaptic vesicles at the basis of the NMDA-evoked *excitotoxicity*.

On purpose, we have developed *JGRi1*, a cell-permeable peptide able to selectively disrupt JNK2/STX1a interplay and pharmacologically prevent the downstream ischemic cascade.

To uphold our hypothesis, we tested *JGRi1* in several experimental settings, achieving a convincing neuroprotective effect also in a murine model of ischemia over a conveniently long therapeutic window.

Conclusively, we analysed the presence of three single nucleotide polymorphisms (SNPs) on the *STX1A* gene in a cohort of stroke patients, evidencing a haplotype correlated with increased susceptibility to cerebral ischemia.

Overall, we here confirm JNK fundamental implication in glutamate release at presynaptic level, moreover presenting for the first time *JGRi1*, a selective inhibitor of the JNK2/STX1a interaction that may represent a new therapeutic tool able to modulate glutamate overflow in various conditions, including neurodegenerative diseases and ischemia-linked pathologies.

INTRODUCTION

1. Ischemia: definition and classification

Stroke is a medical condition characterized by a severe reduction of blood flow to the brain that impedes the attainment of a proper metabolic demand and the clearance of waste toxins.

This emergency condition results in cerebral hypoxia and initiation of the ischemic cascade, ultimately leading to delayed neuronal vulnerability or cell death, depending on the severity and duration of the insult (*https://www.nhlbi.nih.gov/health/health-topics/topics/stroke*).

In the 1970s the *World Health Organization* defined stroke as a "neurological deficit of cerebrovascular cause that persists beyond 24 hours or is interrupted by death within 24 hours" (World Health Organisation, Geneva 1978). This statement was devised to reflect the potential reversibility of tissue damage in less severe and manageable conditions, although the time frame of 24 hours was chosen arbitrarily.

Cerebral blood flow in healthy human brain is about 50–55 mL/100 g tissue/minute, although neurons can still survive in a quiescent state at 23 mL/100 g tissue/minute. Below this value, the ischemic cascade is set into motion. Dropping down to 12 mL/100 g tissue/minute cell death occurs rapidly and the injury gets irreversible (Harper, 1965).

Two main types of stroke are diagnostically recognized (**Fig. 1**):

- *ischemic stroke*, caused by decrease or lack of blood supply to the brain, possibly due to either thrombosis, embolism or systemic hypoperfusion. In this context, focal ischemia indicates a condition confined to a specific region of the brain whereas global ischemia, presumably due to cardiac arrest, encompasses wider areas.
- *hemorrhagic stroke*, due to bleeding at either intracerebral or subarachnoid compartments.

Roughly 90% of the strokes are ischemic while the others are hemorrhagic.

Additionally, the hemorrhagic transformation of ischemic infarction is a well-recognized consequence of cerebral stroke (*https://www.nhlbi.nih.gov/health/health-topics/topics/stroke/types*; Roger et al., 2011).

To what concern this dissertation, the first type of stroke, *i.e.* ischemia, will be mainly taken into consideration, although both share common pathological mechanisms.

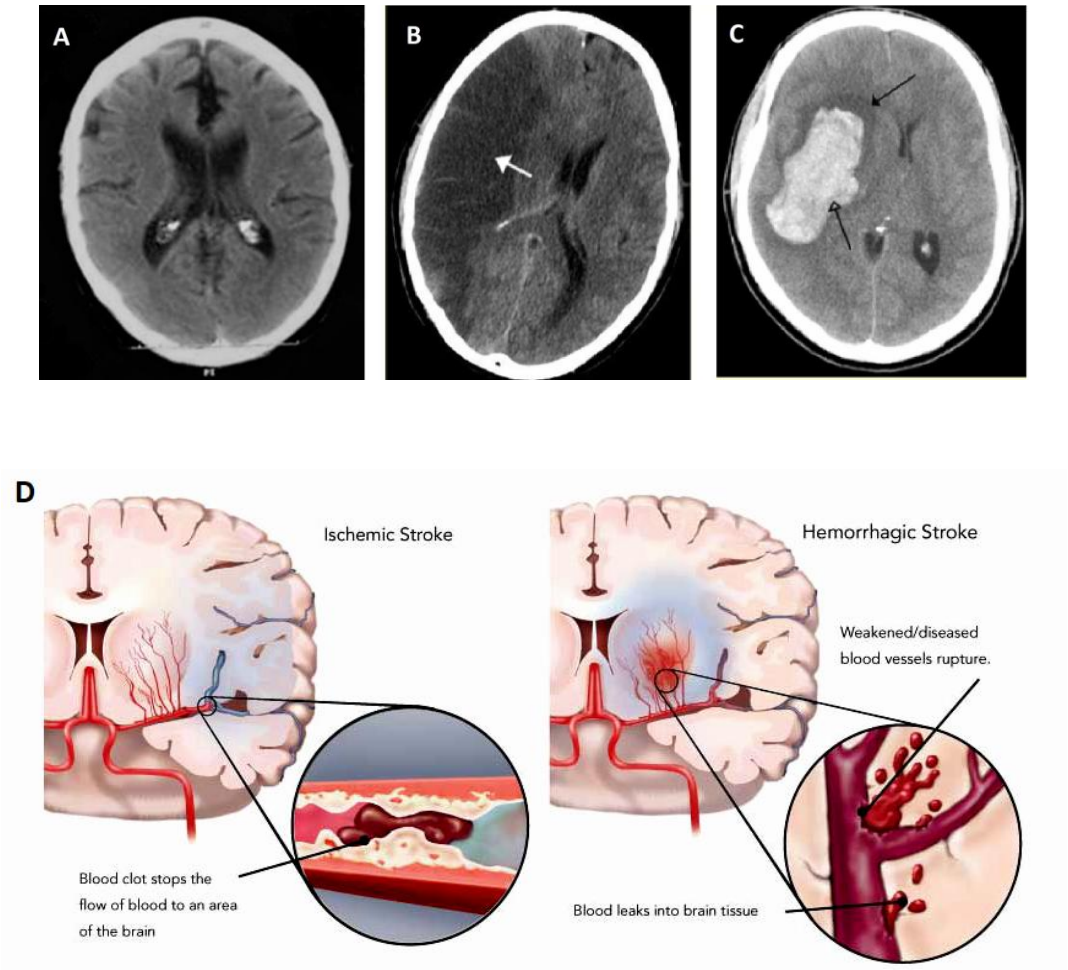

Fig. 1
Ischemic vs. Hemorrhagic stroke.
CT scans of a healthy control subject (**A**), and patients with ischemic (**B**) or hemorrhagic (**C**) stroke, as indicated by the arrows.
D) Blockade of a blood vessel and lack of blood flow to a brain area is the major cause underlying ischemic stroke (left panel). Hemorrhagic stroke is instead due to the rupture of a blood vessel with subsequent blood leakage within the cerebral parenchyma (left panel).

1.1 Epidemiology

According to estimates from the 'Global Burden of Diseases, Injuries and Risk Factors Study 2010', ischemic stroke is recognized as the second leading cause of premature death in the developed countries, responsible for substantial health care costs (3–7% of the total health-care expenditure in high-income countries) and worldwide long-term disability (Wang et al., 2016).

Basically, every 40 seconds an ischemic event occurs, every 4 minutes a person dies from stroke, more than 10% of deaths every year are due to stroke, and, among survivors, approximately half of people who have had a stroke live less than one year more (Mozaffarian et al., 2016).

The NHLBI *Framington Heart Study* for stroke estimated a global prevalence and mortality respectively accounting for 33 million and 6.5 million cases annually, with an incidence supposed to more than double in each successive decade, especially for males over the age of 55 (Bramlett and Dietrich, 2004; Wolf et al., 1977).

Incidence is subjected to a large geographical variation, and is worryingly increasing in developing countries, due to lack of good health services and social policy for stroke prevention and/or care (*i.e.* smoking cessation, blood pressure control, proper dietary regimen, accessibility to health services in terms of treatment availability, rehabilitation strategies, secondary and long-term prevention). Consequently, although stroke mortality rates and mortality-to-incidence ratios have generally decreased in the past two decades, the global burden of stroke in terms of absolute number of people affected every year and related deaths is increasing and ultimately accounting for an epidemiological transition, with most of the burden actually gathered in developing countries (**Fig. 2**).

Additionally, although stroke has been traditionally thought as a disease of elderly, the proportion in people younger than 65 years is substantial, and more than 83.000 children and youths younger than 20 years are affected by stroke annually.

If these trends in stroke incidence and mortality will continue, by 2030 there will be almost 12 million of stroke deaths per year (Feigin et al., 2014).

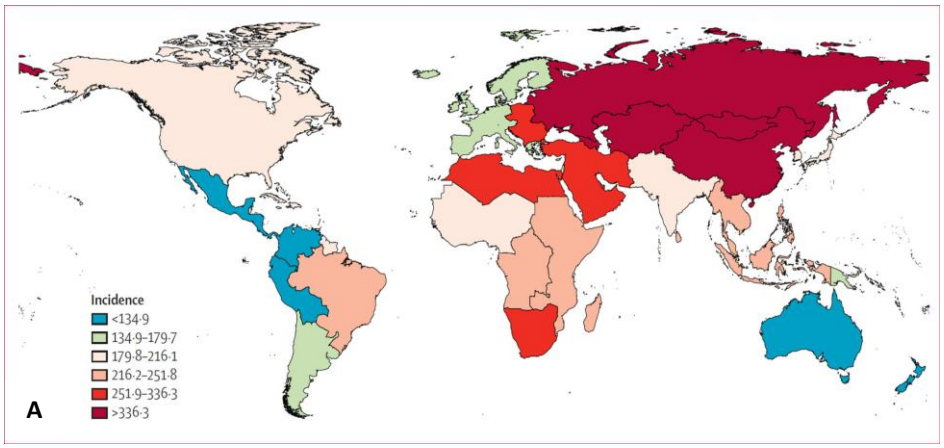

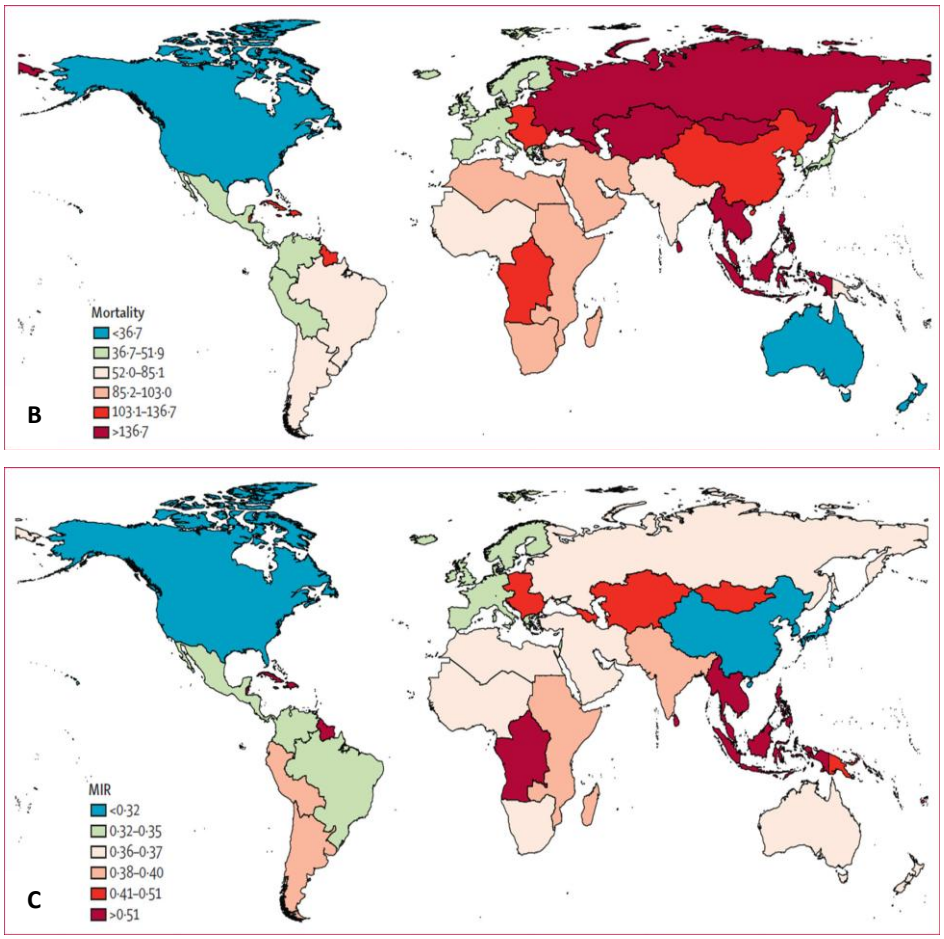

Fig. 2
Stroke epidemiology.
A) Age-standardized stroke incidence per 100 000 person/year for 2010.
B) Age-standardized stroke mortality per 100 000 people for 2010.
C) Stroke mortality-to-incidence ratio (MIR) for 2010.
(Adapted from Feigin et al., 2014).

1.2 Risk factors and preventive care

As a cardiovascular based disease, the main modifiable risk factors for stroke are chronic hypertension and atrial fibrillation, followed by thromboembolism and coagulation impairment, vascular disease and cerebral microangiopathology, hypercholesterolemia and dyslipidemia, obesity, diabetes mellitus, hyperhomocysteinemia, active and passive cigarette smoking, alcohol and amphetamine-like drugs abuse, lack of physical activity, and unhealthy diet, especially rich in processed red meat (Bailey, 2017; Meschia et al., 2014).

In addition, genetic predisposition (congenital heart defects, familial increased Von Willebrand factor), environmental factors and gender may undermine ischemia pathomechanisms, with premenopausal women presenting for instance lower stroke incidence and better recovery compared to men (Bramlett and Dietrich, 2004; Roof and Hall, 2000).

Primary prevention is generally less effective than secondary prevention for recurrent episodes. However updated and detailed guidelines have been published for both conditions by the *American Heart Association/American Stroke Association* (Kernan et al., 2014; Meschia et al., 2014).

35–50% of stroke risk is accounted only by high blood pressure, indeed a reduction of 10 mmHg systolic pressure may lower ischemic occurrence up to 40% in both primary and secondary prevention.

Statins were shown to reduce the risk of stroke by about 15% (O'Regan et al., 2008). On the other hand, although oral anticoagulants and antiplatelet drugs have been the mainstay of stroke prevention for over 50 years, they are by now mostly indicated in secondary prevention after stroke or transient ischemic attack, in order to avoid unsolicited bleeding. Among those drugs, warfarin and aspirin have been respectively the most used, with lower aspirin doses (50–150 mg daily) resulting as effective as higher daily doses, but with lesser unwanted side effects. Thienopyridines including clopidogrel and ticlopidine used in monotherapy might be slightly more effective than aspirin and showed a lower risk of gastrointestinal bleeding. Dipyridamole in association with aspirin provided tiny additional therapeutic benefits, therefore it is currently recognized as a secondary therapeutic option for the prevention of recurrent ischemic events (Diener, 2006; Kirshner, 2008).

The recourse to carotid endarterectomy or carotid angioplasty can be ultimately evaluated to remove atherosclerotic stenosis of the carotid artery, particularly to prevent secondary occurrence (Rothwell et al., 2003).

1.3 Causes

Cerebral ischemia has been linked to a variety of diseases or abnormalities. Individuals with sickle cell anemia, compressed blood vessels, ventricular tachycardia, plaque build-up in the arteries, blood clots, extremely low blood pressure as a result of heart attack, and congenital heart defects have for instance a higher predisposition to brain ischemia in comparison to healthy counterparts (Sveinsson et al., 2014).

Overall, the main causes accounting for ischemic events, as reported above, have been identified in:

- Thrombosis
- Embolism
- Cerebral hypo-perfusion

Additionally, a small percentage of cases is represented by ischemic stroke of unknown etiology and therefore referred to as *cryptogenic* stroke (Bailey et al., 2012; Scullen et al., 2015).

Atherosclerosis may for instance disrupt the blood supply by narrowing arterial lumen, directly forming blood clots within the vessels, or indirectly promoting the release of small emboli through the disintegration of atherosclerotic plaques (Lyaker et al., 2013).

Embolic infarction occurs when a thrombus in the circulatory system (typically in the heart as a consequence of atrial fibrillation or in the carotid arteries) breaks off, enters the cerebral circulation and lodges in, blocking brain perfusion and preventing oxygen or glucose in properly reaching brain areas.

The fall of metabolic supply to the cellular milieu following those events leads to failure of energy-dependent processes and initiates a complex cascade of molecular pathogenic events that endanger cell survival and ultimately produce cell injury and death (see paragraph 2 – "Pathophysiology of cerebral ischemia").

On the other hand, silent strokes can also occur without any outward symptoms. Despite patients are typically unaware they have had a stroke, brain damage may obviously present and place the patient at increased risk for both transient ischemic attack and major stroke in the future.

1.4 Signs and symptoms

Sudden-onset face weakness, arm drift and abnormal speech are the warning signs mostly evaluated in order to correctly diagnose stroke. These assessments are rapid and easy to make, therefore they are deeply valuable in acute conditions. Apart from neurological and neuropsychiatric consequences, ischemia also induces immediate immune depression, generally reflected in the fever and sometimes pneumonia suffered within few days by about 60% of patients. Additionally, association with severe headache or vomiting may occasionally present in case of hemorrhagic stroke.

A scoring system called ROSIER (*Recognition of Stroke in Emergency Room*) has been recommended in emergency settings to identify features belonging to the medical history and physical examination of the patient (Nor et al., 2005).

Stroke symptomatology typically starts suddenly, over seconds to minutes, and strictly depends on the specific areas of the brain affected. Consequently, the wider the ischemic area, the higher the number of cerebral functions likely to be lost.

If cerebral areas affected contain one of the three prominent central nervous system pathways, *i.e.* spinothalamic tract, corticospinal tract, and dorsal column (**Fig. 3**), symptoms may include hemiplegia and facial muscle weakness with initial flaccidity followed by spasticity, numbness, sensory depletion. A brainstem stroke may produce symptoms related to deficits in the cranial nerves, including altered smell, taste, hearing, or vision, nystagmus, ptosis and weakness of ocular muscles, decreased reflexes (*i.e.* gag, swallow, pupil reactivity to light), weakness in tongue, balance problems, altered breathing and heart rate. On the other hand, cortical ischemia may be responsible for aphasia, dysarthria, apraxia, visual field defects, memory deficits, disorganized thinking, confusion, lack of proprioceptive insight. Finally, cerebellum infarction is linked with ataxia, altered movement coordination, vertigo and disequilibrium.

Most symptoms generally affect only one side of the body, usually contralateral with respect to the brain area where ischemia has occurred.

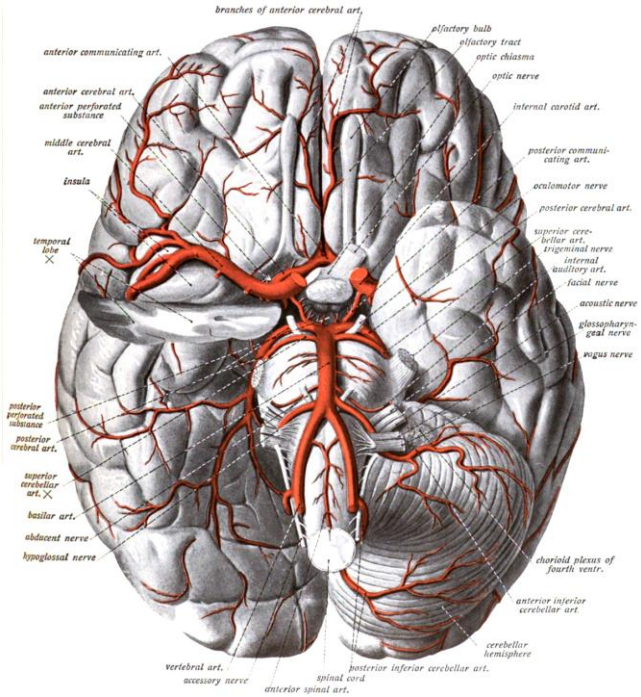

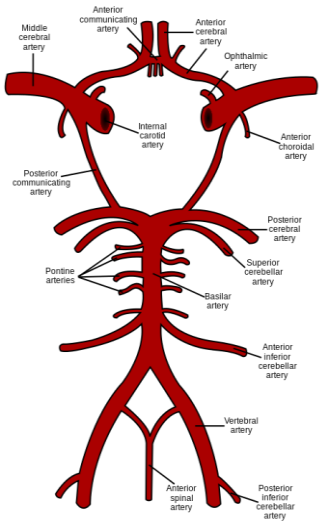

Fig.3

The Circle of Willis and the cerebral vasculature.

Inferior aspect of the arteries at the basis of the brain, depicting the Circle of Willis and its main vessels. The temporal lobe and the cerebellar hemisphere have been removed on the right side of the left image. According to the patient symptomatic presentation, it is possible to speculate the anatomical site where the ischemic insult has occurred.

(Adapted from "*Atlas and Text-book of Human Anatomy Volume III Vascular System, Lymphatic system, Nervous system and Sense Organs"*).

1.5 Diagnosis

Diagnosis for stroke is typically assessed by imaging techniques, including MRI (Magnetic Resonance Imaging) and multimodal CT (Computed Tomography) scans, along with a neurological and physical examination *(https://www.nhlbi.nih.gov/health/health-topics/topics/stroke/diagnosis*).

Structural imaging has been classically used to assess the presence and extent of ischemia or to evaluate a differential diagnosis. At present, however, the improvement in functional imaging approaches including perfusion-CT or Diffusion-Weighted Imaging (DWI) has revolutionized both diagnosis and management of acute ischemic stroke that has thereby been redefined from an all-or-none process to a dynamic and evolving process.

Particular concern is nowadays focused on the diagnostic discrimination between ischemic core and *penumbra*. Additionally, several studies have been converted into clinical practice, opening the possibility to select patients on the basis of imaging criteria for favourable clinical outcomes with conventional thrombolytic therapy (Leiva-Salinas and Wintermark, 2010).

As a matter of fact, the most important service that imaging provides is to rapidly identify those ischemic patients who are most likely to benefit from immediate treatment. This sub-population includes patients with severe neurological symptoms due to an occlusion of a major artery and who are candidates for recanalization using intravenous thrombolysis or intra-arterial intervention to remove the occlusion.

Outcomes for these patients are determined by symptom severity, specific artery occluded, size of the infarct at the time of presentation, and overall treatment efficacy (Ginsberg, 2016; González, 2012) (**Fig. 4**).

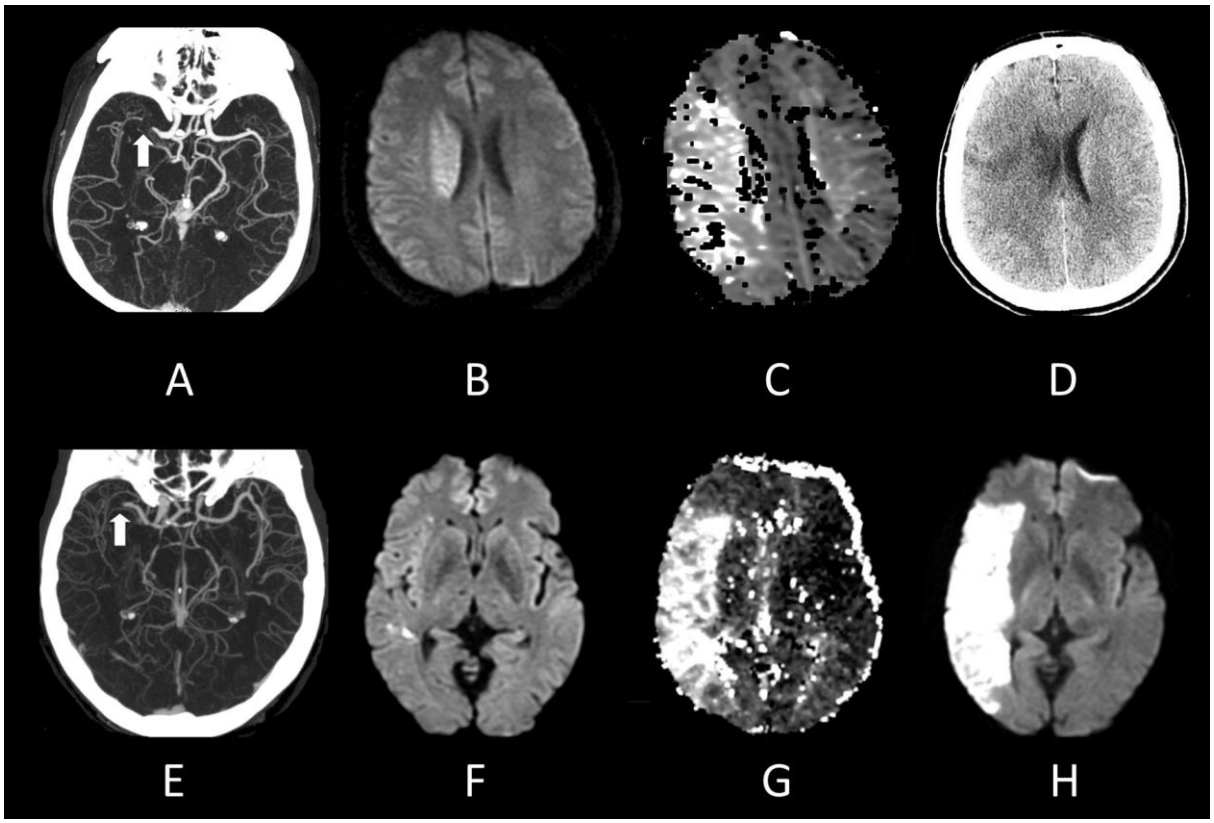

Fig. 4
Ischemic stroke to right middle cerebral artery (MCA) in 2 patients.
(Top row) 38-year-old man with severe left-sided paralysis of unknown time of onset.
A) CT angiography demonstrates occlusion of the right MCA (arrow).
B) Diffusion MR imaging shows a small diffusion abnormality in the right hemisphere.
C) Perfusion MR imaging displays abnormalities involving the entire right MCA territory. Because of the large diffusion/perfusion mismatch and the likely poor long-term outcome, the decision was made to proceed to intra-arterial thrombolysis, which was successful.
D) A follow-up head CT scan shows infarction in the region of the right corona radiata and a small portion of cerebral cortex. The patient made a complete recovery.

(Bottom row). 61 year old male with mild left sided weakness that began 12.7 hours earlier.
E) CT angiography demonstrates a proximal right MCA occlusion (arrow).
F) Initial DWI reveals multiple punctate foci of diffusion abnormality in the right hemisphere.
G) Mean transit time (MTT) MR perfusion map demonstrates a large volume of poor perfusion involving the majority of the right MCA territory. The patient did not undergo thrombolytic therapy because of the long time between stroke onset and imaging.
H) The patient condition worsened to severe paralysis, and follow-up MRI showed a large area of infarction.
(Adapted from González, 2012).

Doppler ultrasound and arteriography, electrocardiogram, echocardiogram, and blood tests may be added to determine risk factors, confirm the supposed diagnosis or rule out other

possible underlying causes. For the assessment of stable strokes, SPECT (Single Photon Emission Computed Tomography) is used to evaluate cerebral blood flow whereas PET (Positron Emission Tomography) estimates the metabolic activity of neurons.

The *National Institute of Health Stroke Scale* (NIHSS) is a validated tool used by healthcare providers to objectively quantify the impairment caused by acute stroke and document patient neurological status in order to predict lesion size as well as both short- and long-term disability.

The NIHSS is composed of 11 items evaluating levels of consciousness, language, neglect, visual-field loss, extraocular movement, motor strength, ataxia, dysarthria, and sensory loss, scoring each specific ability between 0 and 4. Higher scores are indicative of some level of impairment. The individual scores from each item are summed up in order to calculate the patient's total NIHSS score, with 42 being the highest value, correlated with higher stroke severity (Ortiz et al., 2008).

1.6 Clinical management

In auspicious situations wherein sufficient circulation is restored within short periods of time, symptoms may be transient. Conversely, if a significant amount of time passes before perfusion restoration, brain damage may be permanent.

The management of acute ischemic stroke patients is driven by the catchphrase *"time is brain"*. Indeed, as reported in a renowned paper, an average of 1.8 million neurons is lost every minute that appropriate treatment is not given (Saver, 2006) (**Fig. 5**).

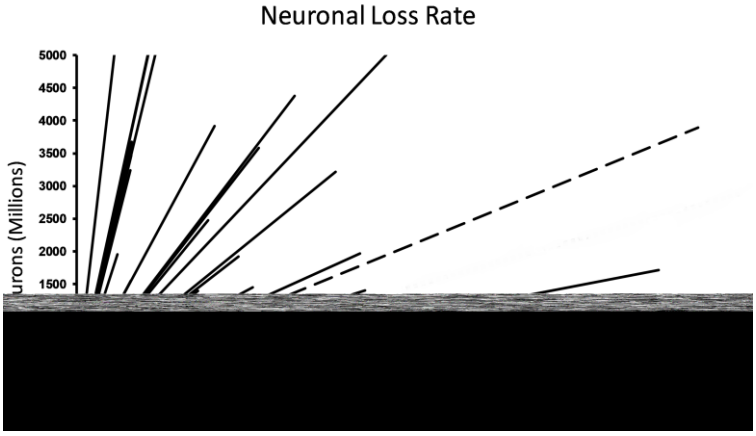

TIME	NEURONS LOST	SYNAPSES LOST	ACCELERATED AGING
1 second	32 000	230 million	8.7 ore
1 minute	1.8 million	14 billion	3.1 weeks
1 hour	120 million	830 billion	3.6 years
Avg. stroke	1.2 billion	8.3 trillion	36 years

Fig. 5
Time is brain, but each patient has his own time.
Neuronal loss estimated from 68 patients who presented to the emergency room within 24 hours from stroke onset. The mean for all 68 patients is the dashed line (Adapted from González, 2012).
The table shows indicative values of loss in terms of neurons, synaptic connections and years of life in relation to time window without therapeutic intervention.

Immediate reperfusion appears essential to effectively provide neuroprotection, although reperfusion injury may occur when the restoration of blood supply is provided to the ischemic tissue (see paragraph 2.6 – "Reperfusion injury") (Nour et al., 2013).

When ischemic stroke is detected within 3 to 4 hours from the onset, the usage of systemic thrombolysis, *i.e.* intravenous administration of recombinant tissue plasminogen activator (rt-PA; Alteplase®) might be beneficial in order to break down eventual clots formation (Hacke et al., 2008; Saver, 2006). Indeed, the administration of thrombolytic drugs within the first 3 hours from stroke onset provided neuroprotection and improved functional outcomes versus placebo (*i.e.* a modified Rankin scale score of 0 or 1 at 3–6 months), although overall mortality was not affected. On the other hand, thrombolysis proved to worsen patients outcome if applied 4.5 hours after ischemia onset (Alper et al., 2015; Emberson et al., 2014; Wardlaw et al., 2014).

Recent evidence moreover underlined the efficacy of mechanical endovascular thrombectomy over intravenous thrombolysis, due to the complete vessel recanalization showed in three of four treated eligible patients (Chamorro et al., 2016; Goyal et al., 2015; Jovin et al., 2015). Additionally, thrombolysis may not be ideal for various restrictions and complications, limiting to 10% or less the percentage of patients treatable within the appropriate time window. Surgical removal of the blood clot may also improve the outcome if done within 7 hours from the onset, but again, only eligible patients could benefit (Saver et al., 2016).

Recent evidence from randomized trials confirmed that aspirin is a key drug for reducing up to 13% the long-term risk of recurrent stroke (Diener, 2006; Rothwell et al., 2016). On the other hand, tight blood sugar and blood pressure control in the first few hours did not provide evidence for improved functional outcomes.

Stroke rehabilitation has been formulated to support stroke patients in overcoming disabilities and possibly regaining the skills of everyday living. Moreover, rehabilitation helps stroke survivors to adapt to challenges, prevent secondary complications and educate family members to play a supportive role.

The rehabilitation team is usually multidisciplinary and involves staff with different skills, including physicians trained to rehabilitation medicine, clinical pharmacists, nurses, physiotherapists, occupational therapists, speech and language therapists, orthotists and psychologists.

Based on current experience, the rehabilitation should start as quickly as possible since important functional benefits have been mostly seen in the first few months, with little chance for further improvement after the sixth month. Physical exercise and a proper diet may positively contribute to the rehabilitation success, although a complete recovery is unusual (Barclay et al., 2015; Brady et al., 2016; Saunders et al., 2013).

In this context, the *modified Rankin Scale*, introduced in 1957 by Dr. Rankin (Rankin, 1957) and subsequently modified to its currently accepted form by Prof. Warlow, is by now the commonly used scale to categorize the degree of disability in daily activities for patients who have suffered a stroke or akin neurological disabilities. The Rankin scale ranges from 0 to 6, running from perfect health to death. The evaluation has been recently implemented with a structured questionnaire during the interview process, becoming the most widely used clinical outcome measure for the assessment of ischemia in clinical trials (Bruno et al., 2010).

Similarly, the *Barthel Index*, introduced in 1965 (Mahoney and Barthel, 1965) but lately updated, is an ordinal scale used to measure patients performances concerning their independence in activities of daily living (ADL). Each of the ten performance item describes ADL and mobility and is rated with a given number. Higher scores are associated with greater likelihood of being able to live at home with a respectable degree of independence following discharge from hospital. The scale is regarded as a reliable tool to predict the functional outcomes related to stroke for in-patient rehabilitation and occupational therapy. Its use in clinical stroke trials has been only recently reconsidered (Ohura et al., 2017).

Ultimately, novel virtual reality and video games for rehabilitation are under evaluation for potential future use (Balasubramanian et al., 2010). In addition, self-management programs are special trainings currently used to educate stroke survivors to cope with everyday challenges and meet their own goals during their recovery process (Fryer et al., 2016).

1.7 Prognosis

As reported above, ischemia is a severe condition with no cure at the moment, recognized as second leading cause of worldwide death, and accounting for a 0.35 mortality-to-incidence ratio (Wang et al., 2016). 75% of stroke survivors are limited by the inability to employability due to disability at physical, mental, and emotional level, depending on the anatomical location and size of the ischemic lesion (Edwardson and Dromerick, 2017).

In this frame, physical disability can include muscle weakness, numbness, incontinence, apraxia, pain, appetite, speech and vision loss. Cognitive deficits resulting from stroke include perceptual disorders, aphasia, dementia, anosognosia, impairments of attention and memory. Moreover, up to 10% of patients may develop seizures, therefore anticonvulsants may be a supportive therapeutic option (Gilad, 2012).

Emotional problems may be due to direct damage of emotional centres in the brain or to frustration from adaptation to post-ischemic challenges. 30 to 50% of stroke survivors suffer post-stroke depression. Additionally, anxiety, panic attacks, sleep disturbances, flat affect, apathy, disruption of self-identity, social isolation, mania, and ultimately psychosis may thereby present (Dhamoon et al., 2010).

2. Pathophysiology of cerebral ischemia

Cerebral ischemia results from the severe or prolonged decrease of blood flow supplying nervous tissues, following the transient or permanent occlusion of a cerebral artery.

The consequent hemodynamic deprivation of oxygen and glucose thereupon elicits the transition to anaerobic metabolism, characterized by fall in the synthesis of high energy phosphate compounds such as ATP, and release of lactic acid by-products. Metabolic stress, energy depletion, ionic imbalances and build-up of potentially toxic substances follow. Furthermore, vascular perturbations, platelet aggregation, cerebral cells swelling, vasogenic

edema, tissue vulnerability and peri-infarct depolarization subsequently occur, promoting a complex cascade of biochemical and molecular pathogenic events finalized toward neuronal death (Bramlett and Dietrich, 2002; Danton et al., 2002; Dewar et al., 2003).

The ischemic core is generally enclosed by an area known as *penumbra*, wherein still salvageable neurons do not receive enough blood to communicate, although they do receive sufficient oxygenation to avoid cell death for a limited period of time.

As a consequence, the *penumbra* has become a milestone in stroke research, being a tissue potentially recoverable. Conversely, neurons from the central core of dense ischemia almost inexorably will die.

Clinically, ischemic *penumbra* may be recognized through precise hemodynamic and electrophysiological parameters, being declaimed as a diagnostic territory for neuroprotection, neurorepair and brain plasticity, ultimately allowing an extension of the window for therapeutic intervention (Ramos-Cabrer et al., 2011).

Neuroimaging devices are currently providing optimized functional thresholds to differentiate ischemic core and *penumbra* in acute ischemic stroke patients. Cerebral perfusion-CT has for instance recently allowed a fine discrimination comparing baseline profiles from both areas, in order to select eligible patients for efficacious reperfusion therapy (Yu et al., 2016) (**Fig. 6**).

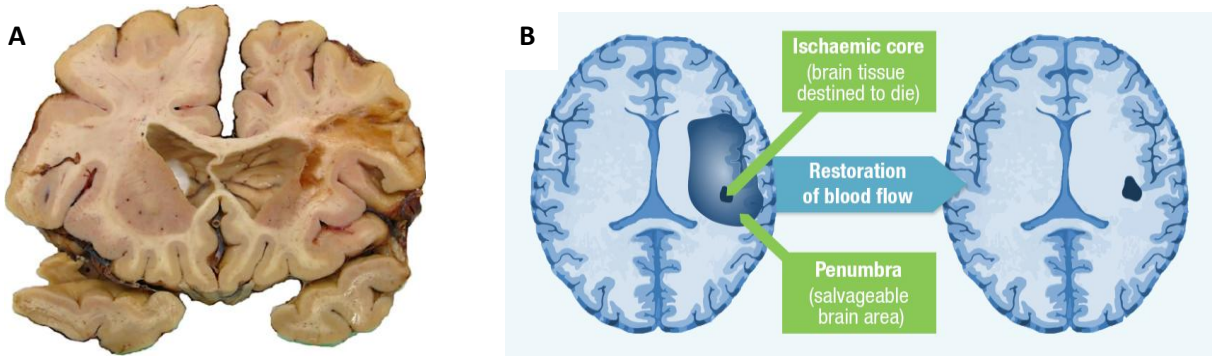

Fig. 6
Human brain ischemia, ischemic core and *penumbra*.
A) Cerebral infarction with liquefactive necrosis is shown in the upper right of this image, within the distribution territory of the middle cerebral artery.
B) Schematic representation of ischemic core and *penumbra*, an area bearing potential to reverse neurologic impairment with post-stroke therapy

2.1 Molecular mechanisms underlying pathophysiology: *excitotoxicity*, inflammation, oxidative stress

Although the adult human brain constitutes only 2% of total body weight, nerve cells account for 25% of basal metabolism and exhibit exceedingly high metabolic rates, consuming 20% of the total oxygen intake.

Consequently, immediate loss of consciousness ensues already 10 seconds after oxygen deprivation, while any cerebral activity ceases if interruption of blood flow proceeds for more than 60 to 90 seconds. After few minutes of hypoxia neurons generally suffer irreversible injury and possibly death, as also detected by electroencephalographic demise (Lee et al., 2000).

Various pathological molecular mechanisms have been ascribed as potentially underlying the ischemic neuronal death, including oxidative stress and generation of reactive oxygen species (ROS), mitochondrial dysfunction, aberrant nitrosylation, delayed inflammation, and, ultimately, caspase3-driven apoptosis or necrosis (Chamorro et al., 2016; Iadecola and Alexander, 2001; Shi et al., 2013). In particular, the exact percentage of cells dying through apoptosis versus necrosis depends upon several factors including stroke severity and duration, with necrotic neuronal damage occurring early after severe ischemic insults, while apoptotic cell death may be observed with milder insults and longer survival periods (Bramlett and Dietrich, 2004).

Besides those possible concomitant causes, scientific consensus presently recognizes a major culprit in *excitotoxicity*, a term coined by John Olney in 1970 to indicate the neuronal impairment specifically driven by glutamatergic storm persisting in the synaptic cleft (Borsello et al., 2003a; Lee et al., 2000; Olney, 1969) (**Fig. 7**).

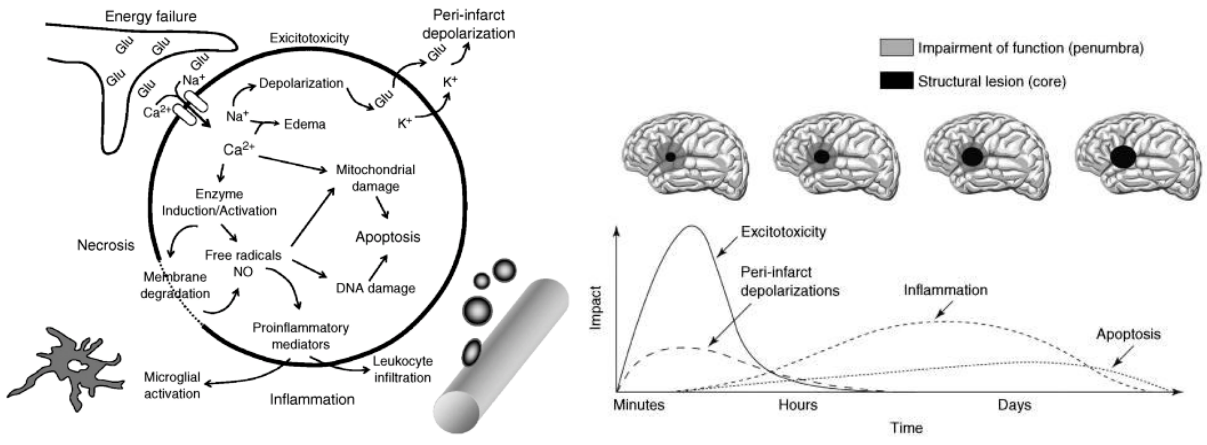

Fig. 7
Molecular mechanisms underlying the pathophysiology of ischemia,
A) Schematic overview of the molecular mechanisms involved in brain ischemia, including *excitotoxicity*, inflammation and oxidative stress (see text for further details).
B) (Top) Evolution of the expanding volume of the ischemic core over the salvageable *penumbra*, during ischemic cerebral demise. (Bottom) Time-course of the damaging events in focal cerebral ischemia, represented as a function of time and impact of the insult on final outcome.
(Adapted from Dirnagl et al., 1999).

2.2 *Excitotoxicity*

Notwithstanding the ubiquitous nature of L-glutamate, *excitotoxicity* is a pathological state exclusively confined to the central nervous system.

The massive shutdown of neural activity upon blood flow reduction is primarily induced by K^+ efflux from neuronal voltage-gated potassium channels, leading to membrane hyperpolarization. The ensuing abrupt redistribution of ions results in anoxic depolarization, relief of Mg^{2+} block from *N*-methyl-D-aspartate (NMDA) receptors, intracellular free Ca^{2+} influx and ultimately excessive release of excitatory neurotransmitters, especially glutamate.

Due to its versatile and ubiquitous role in neuron-to-neuron communication, neuronal growth and axon guidance, differentiation, migration and survival, as well as in synaptic transmission and plasticity (Collingridge and Lester, 1989; Nisticò et al., 2015; Yang et al., 2012), the concentration of this abundant dicarboxylic amino acid in the cerebrospinal fluid is physiologically strictly regulated on the order of 10 μM. During ischemia, however, as a consequence of the transmembrane ion gradient rundown, both synaptic vesicles from nerve terminals and reversed glutamatergic transporters from astrocytes massively release glutamate in the extracellular space to a concentration up to 10-fold increased with respect to physiological conditions.

This near-millimolar extracellular glutamate overflow turns out to be deeply harmful yet neurotoxic, indeed producing overactivation of ionotropic glutamate receptors, especially the NMDA subtype. The further induction of K^+ efflux together with a rapid Ca^{2+} influx relentlessly trigger neuronal death, waving from the ischemic core out toward the margins of the ischemic *penumbra* (Dirnagl et al., 1999; Zipfel et al., 2000). Conclusively, the spreading of membrane shunting exacerbates both metabolic demand and energy failure, further enhancing glutamate release and breaking into harmful cytotoxic cascades, in a vicious

downward spiral that leads to neuronal cell body swelling and eventually death, either apoptotic or necrotic (**Fig. 8**).

In addition to these damaging effects, ischemia also results in loss of structural integrity of cerebral tissue, blood vessels and blood brain barrier (BBB) architecture. The release of proteases including matrix metalloproteases, namely zinc- and calcium-dependent enzymes that break down collagen, hyaluronic acid, and connective tissue, may indeed contribute to cerebral edema and inflammation, secondarily exacerbating ongoing brain injury (Lakhan et al., 2013; Yang and Rosenberg, 2015).

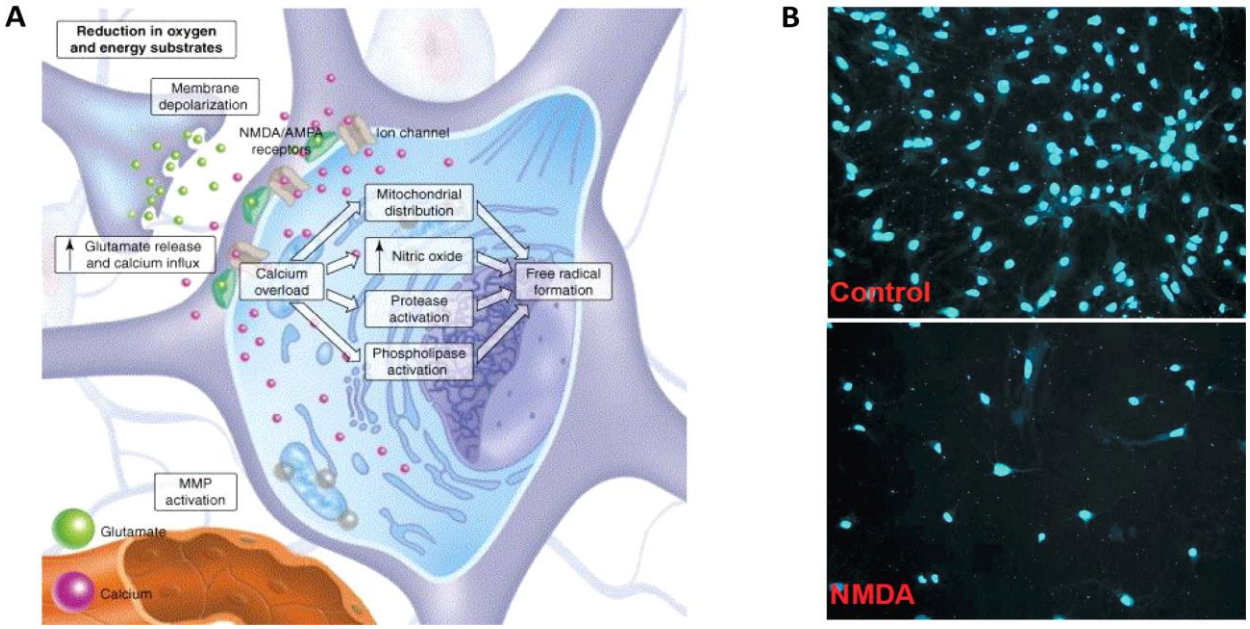

Fig. 8
***Excitotoxicity*: the insult driven by glutamate spillover.**
A) Schematic representation of the *excitotoxic* cascade within a neuronal cell (see text for further details).
B) Micrographs show Hoechst-stained neurons 24 h after treatment with NMDA 100 µM. Cellular death is evidenced by the decreased level of cellular nuclei (Adapted from Borsello et al., 2003a).

2.3 Glutamate and NMDA receptors

Interest in *excitotoxicity* arose almost sixty years ago when the food additive monosodium glutamate was found to be neurotoxic. Starting from the pioneering work conducted by Van Harreveld in 1959 (Harreveld, 1959), further evidence subsequently corroborated and then

unequivocally confirmed the hypothesis that glutamate is not only the primary excitatory neurotransmitter in the adult brain, responsible for neuronal depolarization and action potentials firing, but also that glutamate-mediated *excitotoxicity* is a primary contributor to ischemic neuronal death (Lai et al., 2014; Mangia et al., 2012).

Glutamate exerts its biological activity mainly through the activation of the ionotropic glutamate-gated NMDA receptor (NMDAR), a cerebral hub that detects and processes extracellular glutamate signals into diverse intracellular signaling outputs (Green and Nayeem, 2015). NMDARs are calcium-permeable ion channels that also allow the entry of monovalent cations such as Na^+ and K^+. As a result, NMDARs activation mostly produces excitatory postsynaptic responses, generally slower but longer-lasting than those produced by AMPA or kainate receptors.

To be opened, beside the two agonist molecules of glutamate, NMDARs additionally require the presence of a co-agonist (the amino acid glycine) as well as the removal of the Mg^{2+} block within the pore channel, achieved by postsynaptic neuronal depolarization following repetitive firing of the presynaptic cell (**Fig. 9**).

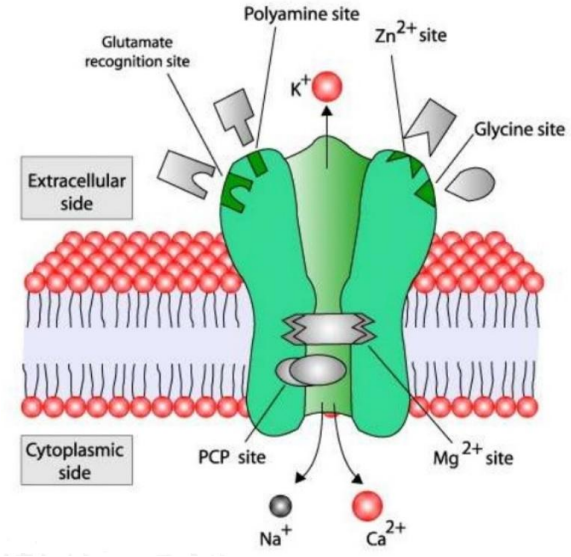

Fig. 9

NMDA receptor model illustrating important binding and modulatory sites.

Activation of NMDA receptors requires binding of glutamate with the co-agonist glycine for the efficient opening of the ion channel. The most relevant modulatory sites are the magnesium (Mg^{2+}) site within the ion channel and an S-nitrosylation site located toward the extracellular *N*-terminal of the receptor. Other modulatory sites include binding sites for Zn^{2+}, polyamines, and drugs like phencyclidine (PCP), memantine, MK-801.

NMDAR exhibits therefore a dual input requirement (both a sufficiently strong depolarization and a presynaptic release of glutamate) that together with the slow activation and deactivation kinetics allow the accurate integration and codification of incoming patterns of synaptic activity and the consecutive transduction into enduring alterations in synaptic strength.

These events are at the basis of NMDARs pivotal activity in regulating physiological synaptic plasticity and cognitive processes, as well as in NMDARs association with psychiatric disorders, neurodegenerative diseases, and neurodevelopmental dysfunctions (Gonda, 2012).

Since ‘80s, studies performing intracerebral injection of the NMDAR blockers such as 2-amino-7-phosphonoheptanoic acid (AP-7) evidenced a prevention of neuronal death following cerebral ischemia in murine animal models (Simon et al., 1984), providing the first hint that glutamate, and particularly its action on the NMDARs, is a condition necessary for ischemic brain damage.

Apparent agreement from recent studies claims that NMDARs may fulfil a dual-effect depending on the level of receptor activity. As shown in both *in vitro* and *in vivo* assays, high levels of NMDA stimulation induce neuronal death, while survival is promoted by low levels of NMDA stimulation (Brassai et al., 2015). The specific function and localization of many synaptic and extra-synaptic proteins further corroborated the hypothesis that, in turn, synaptic and extra-synaptic NMDARs can be functionally coupled to different downstream pathways, conferring such differential functional outputs on neurons.

To confirm, the propensity for synaptic NMDARs to support synaptic activity and thereby neuronal survival is accompanied by the activity-driven activation of the downstream survival pathway involving the ERK kinase, the transcription factor CREB and the survival-promoting protein BDNF (Brassai et al., 2015). Conversely, extra-synaptic NMDARs have been correlated with downstream death pathways and are persistently activated when abrupt glutamate spillover circulates within the brain, such as during cerebral ischemia. As a consequence, extra-synaptic NMDARs induce the shut-off of CREB and BDNF production, while PTEN, cdk5, DAPK1, calpains and JNK are downstream activated, leading to neuronal failure (Lai et al., 2014) (**Fig. 10**).

Recent findings however underlined a possible contribution also of synaptic NMDARs in *excitotoxicity* in primary hippocampal neurons (Wroge et al., 2012), underlining the urgency to clearly determine the mechanisms by which the location of these receptors may promote their coupling to specific downstream signaling proteins and biochemical cascades.

The molecular cloning of NMDAR subunits has provided improved understanding of the receptor pharmacology.

The most accepted theory describes NMDARs as heterotetramers composed of an essential NR1 subunit that is functionally coupled to at least one of the $NR2_{A-D}$ subunits and, less commonly, to an NR3 subunit, in order to fully establish the ionotropic activity of the channel (Gambrill and Barria, 2011; Stephenson, 2006). The specific subunit composition confers specific channel kinetics, agonist affinity, sensitivity to channel blockers, and differential brain localization.

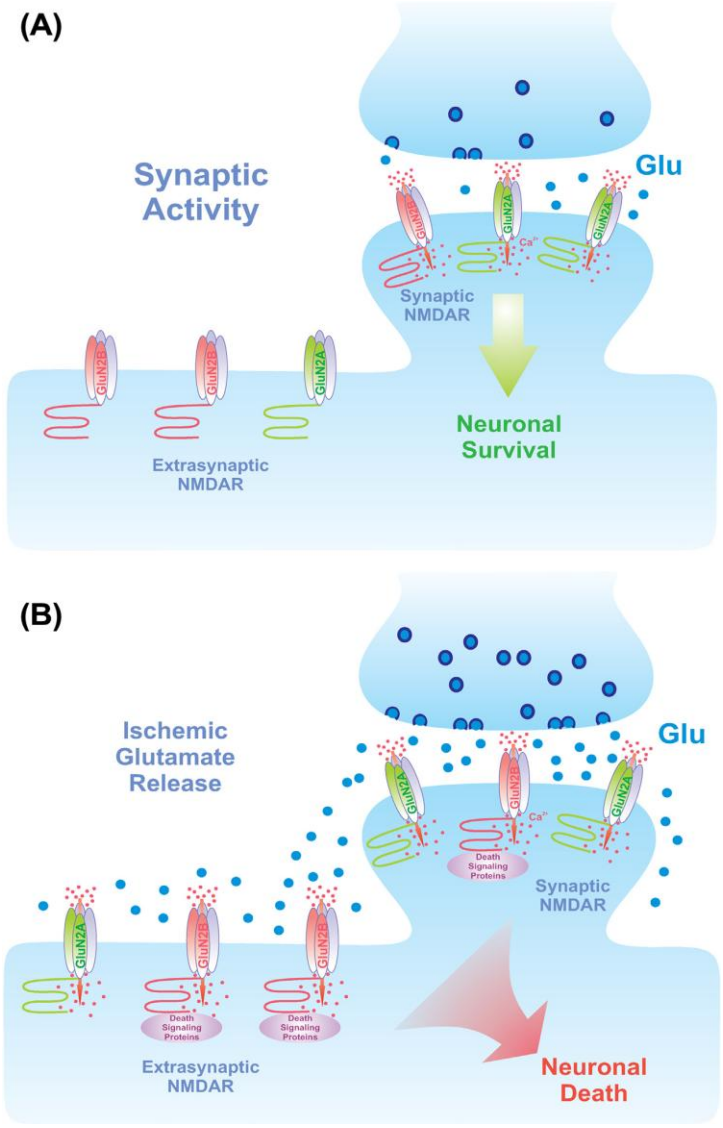

Fig. 10

Distinct subpopulations of the NMDA receptor mediate neuronal death and survival.

A) Under normal conditions, synaptic activity maintains neuronal survival via activation of the synaptic NMDAR. This pro-survival effect is dependent on the calcium influx through the receptors.

B) During cerebral ischemia, excessive release of glutamate into the synapses and extra-synaptic sites causes global stimulation of NMDAR at both locations. The *C*-terminal domain of the GluN2B (NR2B) subunit acts as a major hub for recruiting death-signaling proteins, which in turn is activated by calcium influx through the receptors to induce neuronal death.
(Adapted from Lai et al., 2014).

Additionally, the physiological role of NMDAR subunits depends expressly on their large and distinct cytoplasmic tails that mediate intracellular signaling (Ryan et al., 2008).

On this line, synaptic receptors containing the NR2B subunit proved to be sufficient for the induction of neuronal death, whereas the synaptic NR2A protects against the *excitotoxic* insult. Similarly, extra-synaptic NR2A subunit is pro-survival while NR2B yields widespread neuropathy (Liu et al., 2007).

Consistent with the extra-synaptic localization of the NR2B-containing NMDAR, there may be several advantages in selectively inhibiting the NR2B receptor subtype and its downstream death signaling pathways (Hardingham et al., 2002; Vizi et al., 2010, 2013).

Ifenprodil® and derived compounds (*i.e.* eliprodil®, traxoprodil®) are for instance a distinct class of NMDAR antagonists that act non-competitively at the NR2B NMDAR with high subunit specificity (Tajima et al., 2016; Williams, 1993). These NR2B-selective compounds provided therapeutic efficacy against ischemic neuronal death *in vitro* and *in vivo*, circumventing nonspecific blockade of the pro-survival NR2A NMDAR and without presenting the psychotomimetic side effects commonly seen with conventional NMDAR antagonists (Kalia et al., 2008).

Nevertheless, a major pitfall affecting such selective blockade is the non-trivial physiological function developed also by NR2B NMDAR, including their role in the extinction of fear memory, the manifestation of stress responses, and the learning of new memory. Secondly, also these specific NMDAR blockers are only effective when administered immediately following stroke, and they quickly lose their efficacy when treatment is delayed, thereby limiting the time window for effective drug administration.

Overall, this emerging evidence points to distinct NMDAR subpopulations that may differentially promote either neuronal death or survival.

A deeper identification of those distinct intracellular pathways may lead to the development of novel and more therapeutically practical pharmacological agents able to convincingly target the molecular pathways affecting the ischemic brain.

2.4 The role of calcium toward death or survival

Calcium is a crucial signaling molecule in cell biology and its tight regulation via sequestration or extrusion is fundamental for cellular function. Additionally, this cation plays an essential role in glutamate-mediated *excitotoxicity*, therefore any dysfunction of calcium homeostatic machinery is expected to exacerbate neuronal overload and to contribute to the ischemic injury.

In particular, the initial calcium overload following *excitotoxic* glutamate spillover is the signal that triggers the secondary intracellular calcium influx in an NMDAR-mediated mechanism, actually correlating with neuronal death. In this context, also the sodium-calcium exchanger (NCX), an important regulator of intracellular Ca^{2+} levels that extrudes calcium using the driving force from sodium influx, fails in recovering the intracellular calcium concentration back to physiological levels (Chen and Li, 2012). Additionally, the mitochondrial maintenance of intracellular calcium homeostasis collapses, due to the failure of direct calcium uptake or indirect facilitation of ATP-dependent calcium extrusion (Szydlowska and Tymianski, 2010). As a result, upon *excitotoxic* stimulation, the mitochondrial uptake of calcium results in reactive oxygen species production, breach of the permeability transition pore followed by mitochondrial depolarization, worsening of calcium deregulation, and final induction of neuronal death (Khatuh et al., 2013; Nishio et al., 2013).

In a fashion similar to the mechanisms previously described, high calcium loading induced by glutamate via NMDARs results to be neurotoxic when compared with the equivalent transient overflow induced by tonic depolarization via voltage-gated calcium channels that is instead neuroprotective. Such divergent effects on neuronal death or survival may again be explained by the differential effects of Ca^{2+} inputs on gene expression, as well as by the diverse sources of the calcium (Szydlowska and Tymianski, 2010). It might be possible that some calcium-dependent death-signaling proteins are closely associated or rather physically bound to the *C*-terminal domain of NMDARs, thereby generating these opposing functional outputs at the basis of neuronal functionality in physiological and/or pathological conditions.

2.5 Oxidative stress and inflammation as secondary ischemia contributors

As a consequence of such deranged orchestra of glutamate-driven detrimental signaling, several downstream pathways peaking in oxidative stress and phlogosis deeply compromise and challenge brain integrity.

Upon the ischemic insult, the conspicuous Ca^{2+} released progressively accumulates into the mitochondrial matrix, promoting the production of ROS, inhibiting the synthesis of ATP and enhancing mitochondrial membrane permeability. Contextually, due to neuronal phospholipid membrane damage, free fatty acids and arachidonic acid are released during ischemia upon phospholipase C and phospholipase A_2 activation, in turn activated following NMDAR stimulation respectively by depolarization and increased Ca^{2+} concentration, contributing to failure of ion partitioning and free radical–mediated cytotoxicity (White et al., 2000).

Besides the critical involvement in energy production, mitochondria are also primary mediators of apoptosis due to death factors located in the mitochondrial matrix, including cytochrome c, caspases and the apoptosis inducing factor (AIF) (Singh et al., 2010). Considering the substantial amount of oxygen consumed by the brain, its high propensity in generating ROS, the relative low levels of endogenous antioxidants, and the large amount of polyunsaturated fatty acids and transition metals available to fuel Haber Weiss and Fenton reactions, brain vulnerability to oxidative stress appears obvious. Thereby, the disruption of neuronal bioenergetics leads to the opening of the mitochondrial permeability transition pore, with release of cytochrome c, and finally, apoptotic cell death (Abeti and Abramov, 2015; Giorgio et al., 2013).

Toxic free radicals including superoxide anion ($O_2^{\bullet -}$), hydrogen peroxide (H_2O_2), hydroxyl radical ($HO^{\bullet}$), nitrogen dioxide ($NO_2^{\bullet}$) and peroxynitrite ($ONOO^-$) are readily produced by infiltrating phagocytes, pericytes and glial cells mostly in *penumbral* regions, further prompted during reperfusion, thus perpetrating neurotoxicity (Nishio et al., 2013; Ramos et al., 2017) (**Fig. 11**).

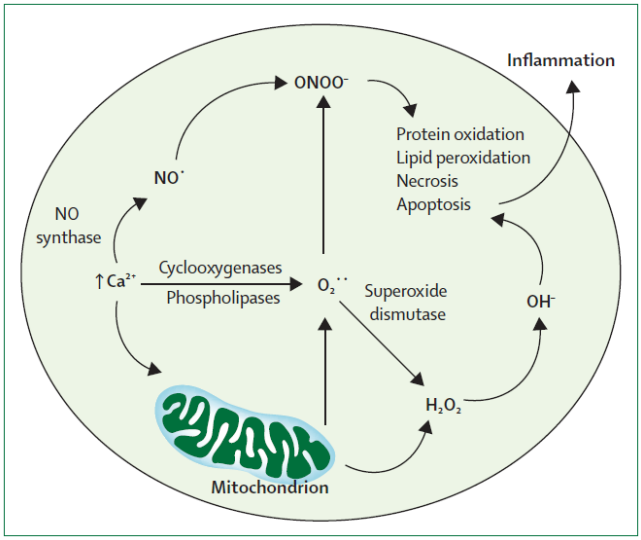

Fig. 11

Deleterious role of the mediators of oxidative and nitrosative stress in cerebral ischemia.
Calcium overload within mitochondria promote the increased generation of superoxide anion ($O_2^{\bullet-}$), hydrogen peroxide (H_2O_2), hydroxyl radical (OH^-), nitric oxide ($NO^\bullet$), or peroxynitrite ($OONO^-$) in the core and penumbral tissue. Hydroxyl radicals and peroxynitrite, which results from the interaction between nitric oxide and superoxide, lead to protein oxidation and nitration, lipid peroxidation, mitochondrial and cellular DNA damage, activation or inhibition of various signaling pathways that ultimately favour inflammatory responses, apoptosis, and necrosis.
(Adapted from Chamorro et al., 2016).

On the other hand, the production of the metastable free radical nitric oxide ($NO^\bullet$), may result both beneficial and detrimental, depending upon source, location and duration of release (Förstermann et al., 1998; Pacher et al., 2007). This diffusible neurotransmitter plays indeed important physiological roles in vasodilation, blood pressure regulation and facilitated neurotransmission when produced by the endothelial nitric oxide synthase (eNOS). Conversely, high intracellular concentrations promoted by neuronal (nNOS) and inducible (iNOS) synthases have been related to depletion of cellular NAD^+ and energy stores and further production of $ONOO^-$, which in turn elicits single-strand DNA breakage, harmful protein nitration and oxidation, stimulation of mitogen-activated protein kinases, lipid peroxidation and breakdown of blood brain barrier (del Zoppo et al., 2000; Shi et al., 2013; Yenari and Han, 2012).

Under this perspective, the association between the neuronal NOS isoform with *excitotoxic* cell death is corroborated by the fact that nNOS is physically tethered to the NMDA receptor and activated by Ca^{2+} influx, thereby explaining the increased levels of nitric oxide found in stroke animal models (Lipton, 2004). Thereupon, increased nNOS activity is related to *excitotoxic* cell death.

In this frame of damaging biological events, phlogosis is generally triggered as well, with acute inflammatory events secondarily participating in the injurious process, while delayed chronic inflammation may rather be reparative (Bethea and Dietrich, 2002; Dziedzic, 2015).

The infiltration of immune cells into the brain parenchyma begins from microglia and neutrophils, and is orchestrated by time-related release of different cytokines and chemokines including IL-1β, IL-6, and TNF-α that promote matrix metalloproteases activity and further aggravate oxidative stress and BBB damage (Gelderblom et al., 2009; Kolaczkowska and Kubes, 2013). Platelets, in turn, interact with the endothelium and facilitate pro-thrombotic

pathways through the altered expression of cell surface signaling molecules and adhesion molecules such as selectins and ICAM-1, complicating the ongoing microvascular obstruction operated by neutrophils (del Zoppo et al., 2000). Additionally, activated glial cells release mediators that further attract neutrophils, monocytes, and lymphocytes, dramatically aggravating the lesion and contributing to endothelial and parenchyma damage via increased production of nitrites, myeloperoxidases, prostaglandins, and proinflammatory cytokines, in a vicious circle (Jiang et al., 2017; Taylor and Sansing, 2013) (**Fig. 12**).

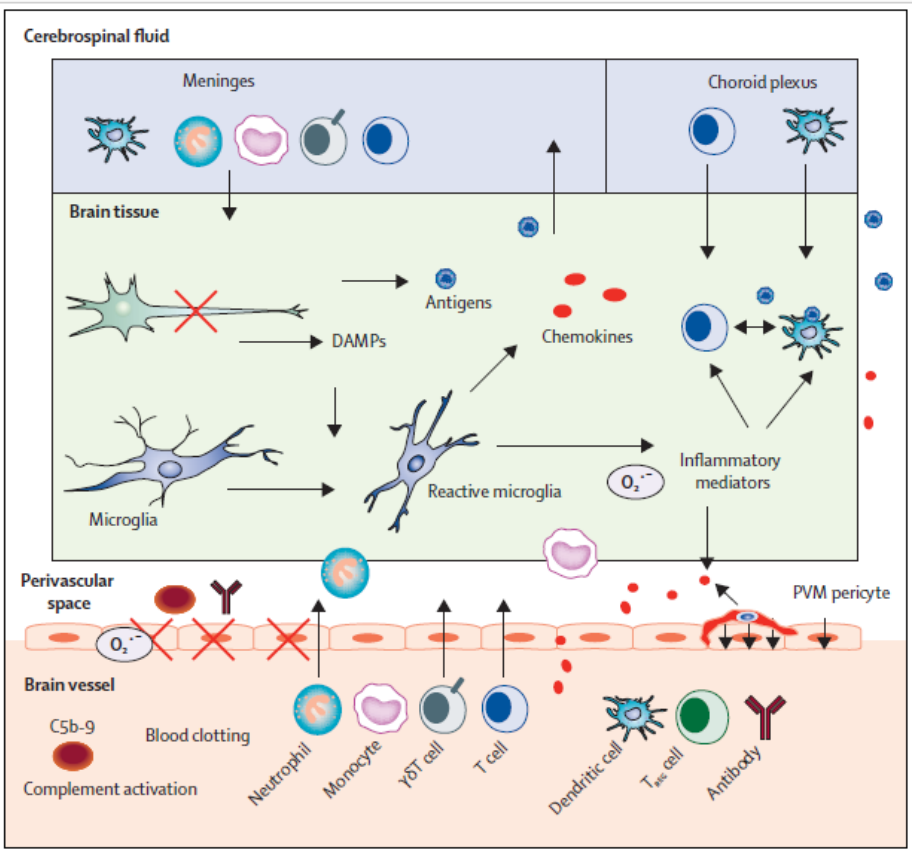

Fig. 12
Inflammation in the pathogenesis of cerebral ischemia.
Circulating monocytes, monocyte-derived macrophages, dendritic cells, natural killer cells, and lymphocytes regulate inflammatory responses and might favour thrombo-inflammation, which defines the dysfunction of the cerebral microvasculature caused by increased interaction of leucocytes with the ischemic brain endothelium and platelets. The first cells to respond to *excitotoxicity* are brain-intrinsic microglia, which release mediators that further attract neutrophils, monocytes, and lymphocytes, followed by neutrophils that exacerbate oxidative stress ($O_2^{\bullet -}$), and damage the BBB. Cerebral antigens released during brain ischemia might reach regional lymph nodes through the drainage pathways of the interstitial and cerebrospinal fluid, favouring either tolerogenic or autoimmune responses. This process also enables the recognition of cerebral antigens during ischemia to locally activate autoreactive memory T cells.
DAMPs = damage-associated molecular patterns. PVM = perivascular macrophage.
(Adapted from Chamorro et al., 2016).

2.6 Reperfusion injury

Although the ultimate therapeutic goal in ischemic stroke is addressed, as said, toward thrombolysis or mechanical recanalization, restoration of blood flow may at times collapse in the so-called "*cerebral reperfusion injury*". Indeed, while reperfusion may reduce infarct size and improve clinical outcome in some subjects, a subset of patients paradoxically experience disastrous outcomes in the form of fatal edema or intracranial hemorrhage that extend beyond the sole failure of cellular energy supply to neurons (Chen and Nuñez, 2010; Eltzschig and Eckle, 2011) (**Fig. 13**).

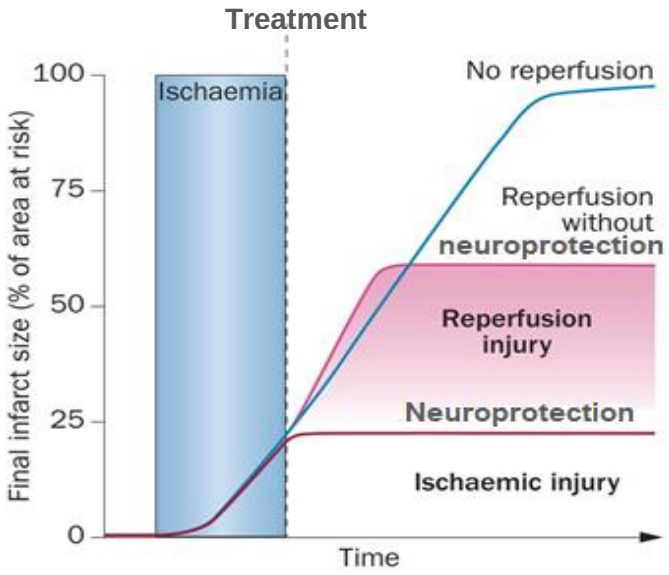

Fig. 13
Reperfusion injury.
When a cerebral artery is occluded, brain tissue becomes ischemic (blue rectangle), and death spreads exponentially. If the vessel is not reperfused using appropriate treatment, a huge brain area will be injured (blue line). If reperfusion occurs in a reasonable time, the infarct size is reduced (pink line). However, if reperfusion occurs together with neuroprotection to reduce reperfusion injury (pink shading), the infarct size is further attenuated (red line).
(Adapted from Sanz-Rosa et al., 2012).

Reperfusion is characterized by vascular restoration and concomitant reoxygenation of ischemic tissues that may nevertheless undergo cellular changes including nuclear fragmentation, chromatin condensation and neuronal cell body shrinkage, often accompanied by phospholipidic membrane alteration (Balasubramanian and Schroit, 2003; Broughton et

al., 2009). Multiple pathological molecular mechanisms are believed to be implicated in this injurious process, involving both innate and adaptive immune responses as well as complement system, platelets and coagulation factors (Nour et al., 2013). As a consequence, cell death can occur either by necrosis or apoptosis (Hotchkiss et al., 2009), thereby further stimulating the inflammatory system and exacerbating the ongoing injury (Chen and Nuñez, 2010; Elliott et al., 2009).

In the frame of such impaired cellular milieu, activated leukocytes interact with endothelial cells and extravasate from capillaries, infiltrating brain tissue and releasing leukotrienes, prostaglandins and other proinflammatory cytokines.

Several studies also suggested a negative involvement of platelets after cerebral ischemia and reperfusion (Ishikawa et al., 2004; Pan et al., 2007). Beside the mechanical obstruction, platelets can cause vasospasm through serotonin, thromboxane A2, and free radicals release. In addition, activated platelets promote chemotaxis and migration of leukocytes, emphasizing the inflammatory cascade.

The plunge into the inflammatory cascade and the release of neutrophil-derived oxidants and proteolytic enzymes increase the permeability of the vascular bed and eventually disrupt BBB integrity, ultimately deteriorating also the salvageable ischemic *penumbra*.

Moreover, *excitotoxicity*-mediated inhibition of astrocytic repair function also disables the BBB, functionally correlating with the severity of patients outcome (Liu and Chopp, 2016; Schaller and Graf, 2004).

In this inward spiral, the depletion of cellular metabolic resources leads to anaerobic glycolysis and lactic acidosis, further release of glutamate, cytotoxic edema, and excessive generation of free radicals that overwhelm the system, collapsing in irretrievable cellular demise (Dirnagl et al., 1999; Lee et al., 2000).

Reactive radical oxide species play a major role in this hypoxic context (Olmez and Ozyurt, 2012). Inducible nitric oxide synthase (iNOS) is activated during cerebral ischemia, leading to nitric oxide and peroxynitrite production, DNA damage, fall of ATP production and, ultimately, either p53 upregulation or Bcl-2 downregulation in case of, respectively, necrotic or apoptotic cell death (Shen et al., 2003).

Besides the oxidant harm, ROS may directly alter BBB permeability, causing long-lasting edema and exacerbating the impedance to adequate tissue perfusion, possibly contributing to the hemorrhagic transformation of ischemic stroke (Bektas et al., 2010; Wang and Lo, 2003).

Although no study has so far finely quantified these events in stroke patients, animal stroke models have extensively recapitulated the concept of reperfusion injury at molecular and cellular level. Injury from reperfusion has been indeed observed to last beyond the period of ischemia and to extend wider in the *penumbra*, with evidence of sustained oxidative stress on pericytes in the microvasculature, and in spite of arterial recanalization in MCAo (Middle Cerebral Artery occlusion) murine models (Yemisci et al., 2009). Furthermore, neutrophil accumulation at the site of neuronal injury with consequent increase in infarct volume has been shown to occur earlier and to greater extent in reperfused areas than in tissue permanently deprived of blood supply, starting already 6 hours after restoration of cerebral circulation (Zhang et al., 1994).

As current revascularization approaches have become highly successful and continue to improve, reperfusion injury has obtained a prominent interest for patient treatment and supportive care. On purpose, a better understanding of the mechanisms undermining cerebral ischemia and reperfusion injury has provided several potential strategies to limit or rather prevent further brain damage during reperfusion. Clinical trials ranged from inhibition of apoptosis to promotion of angiogenesis, targeting T-cells, inhibiting reactive oxygen species production and modulating cellular metabolic apparatus (Eltzschig and Eckle, 2011).

Several interventions have targeted leukocyte infiltration by means of anti-neutrophil antiserum or anti-neutrophil monoclonal antibodies, showing improved recovery and reduced infarct size after cerebral reperfusion in both rats and rabbits (Pan et al., 2007). On the same line, monoclonal antibodies anti-adhesion molecules like ICAM-1 (*i.e.* enlimomab®) reduced neutrophil infiltration and lesion size after reperfusion in rats, although the translation of these promising agents into effective therapies in humans has been disappointing (Enlimomab Acute Stroke Trial Investigators, 2001).

Additionally, given the major role of free radicals in hypoxic reperfusion, several studies have tailored neuroprotective interventions to target these players. Among those, modulation of superoxide dismutase and NADPH oxidase proved to limit injury in animal models of ischemia-reperfusion (Kahles and Brandes, 2012; Radermacher et al., 2013).

Dextran sulfate, unfractionated heparin and fingolimod, a sphingosine-1 phosphate receptor agonist, also reduced infarct volume after reperfusion and provided improved functional neurological outcomes, paving a potential role for these agents alongside conventional therapeutic options (Wei et al., 2011).

Besides these drug therapies, management strategies including inhalation of hydrogen or nitric oxide gases, brain cooling and conditioned blood perfusion are under clinical evaluation due to the possibility to modulate several pathways involved in reperfusion injury (Stowe et al., 2011; Yenari and Hemmen, 2010).

In this context, neuroimaging is currently being effectively used to provide real-time, clear-cut, non-invasive, easily reproducible measures of potential success for therapeutic strategies implied in injury recovery (Nour et al., 2013; Pan et al., 2007).

However, despite preclinical success of several previously described agents, clinically convincing benefits are still far from attainment, therefore a deeper understanding of revascularization beyond the concept of recanalization alone is strongly required.

3. Symptomatic and disease modifying treatments

The main reasonable aim of acute stroke treatment is the rescue of hypoperfused yet still viable ischemic *penumbra* surrounding the infarcted core. Indeed, since 1974 when Hossmann and Zimmermann demonstrated that ischemia induced in mammalian brains for up to an hour can be at least partially recovered, the possibility of intervening after the ischemic insult but before the damage becomes irreversible has been multifariously addressed (Raichle, 1983).

On purpose, similarly to what previously said regarding reperfusion injury, relevant areas of interest include the search for safe and effective treatment strategies that combine neuroprotection, reperfusion, better use of advanced brain imaging for patient selection, and wider implementation of pre-hospital conducted trials.

Despite this pressing clinical emphasis, acute thrombolysis using intravenous rt-PA is the only therapeutic strategy currently approved by the *Food and Drug Administration*, at least in the subpopulation of stroke patients that reperfuse adequately in the brain microvasculature. Indeed, as said before, rt-PA administered within 3 hours after stroke onset succeeded at lysing the arterial thrombus and restoring cerebral blood flow, although no additional implementations have been so far achieved.

Thereupon, *excitotoxicity*, inflammation, and oxidative stress are key ischemia culprits to be targeted. Frustratingly, despite promising preclinical results, several hundred phase II studies and dozens of phase III randomized clinical trials failed to confirm the therapeutic benefits of the related pharmacological agents (Chamorro et al., 2016; Lo et al., 2005; O'Collins et al.,

2006). An implemented search for new treatments appears thereby imperative to overcome these barriers and progress in stroke research (**Fig. 14**).

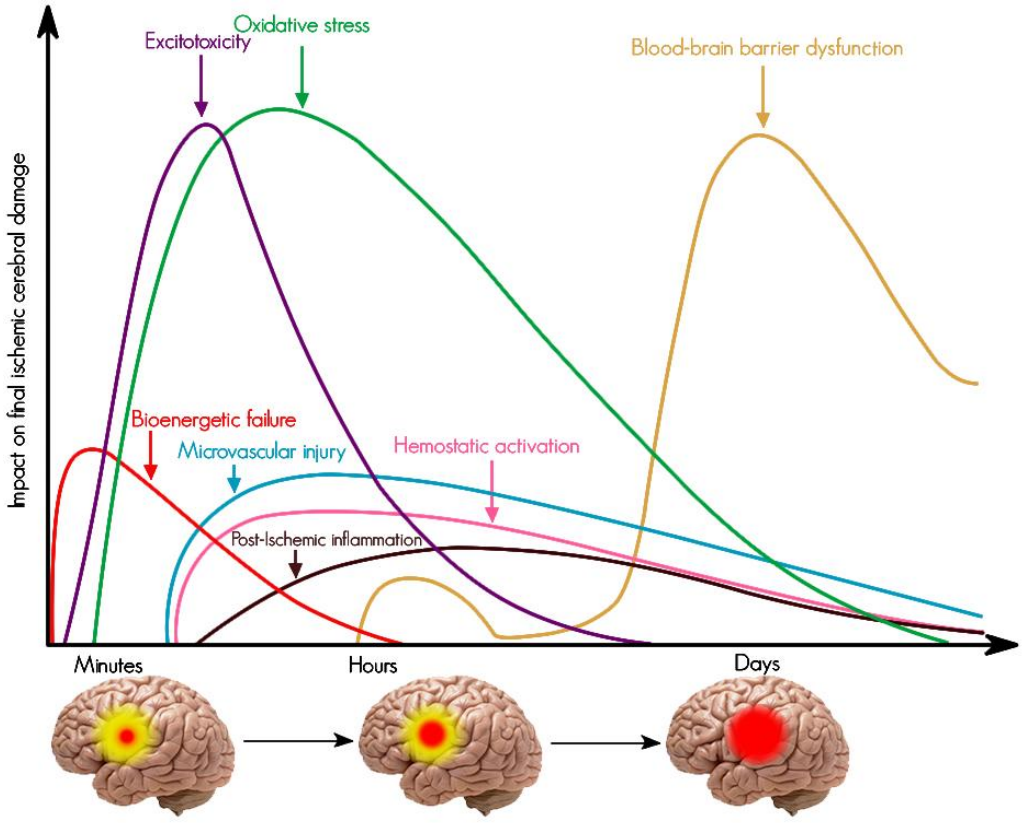

Fig. 14
Potential therapeutic targets to manage ischemia pathophysiology.
The graph represents the temporal profile of the main pathophysiological mechanisms underlying acute focal cerebral ischemia and their impact on the final ischemic damage. In the absence of early reperfusion or appropriate treatment, neurons in the ischemic *penumbra* (yellow brain areas) subside due to ongoing injury, resulting in expansion of the infarcted core (red brain areas). *Excitotoxicity*, inflammation, oxidative stress, bioenergetics failure and BBB and microvasculature injury are promising targets to address for effective therapeutic approaches. (Adapted from Brouns and De Smedt, 2012).

3.1 NMDARs and glutamate-driven *excitotoxicity* as therapeutic targets

The prevention of glutamate-mediated neurotoxicity has been a central therapeutic target in numerous RCTs (Randomized Clinical Trials). Nevertheless, a long list of drugs with assorted mechanisms of action addressing glutamatergic pathways sadly failed when assessed in clinical trials (Chamorro et al., 2016).

Given that glutamate receptor activation and Ca^{2+} influx promptly occur at the very onset of the ischemic cascade, the therapeutic time window for intervention is supposed to be in this case extremely narrow. Consequently, neither AMPA receptor antagonists (*i.e.* YM872, MPQX), nor NMDA receptor antagonists (*i.e.* MK-801, Selfotel®) met their clinical targets (Lee et al., 2000; Yam et al., 2000), not unexpectedly leading to side effects respectively embracing sedation or alterations in motor and cognitive functions.

Ifenprodil®, a NR2B subunit-selective antagonist of NMDARs mostly expressed in forebrain compared to hindbrain offered modest neuroprotection along with less interference with motor function compared to subtype-unselective NMDAR antagonists (Doğgan et al., 1997; Tadano et al., 1995).

On the same line, memantine (1-amino-3,5-dimethyladamantane), an uncompetitive open-channel NMDAR blocker with fast on/off kinetics and low-moderate receptor affinity, was able to block the deleterious effects of excessive glutamate release without interfering with the physiologic activation of NMDA receptors (Johnson and Kotermanski, 2006).

Since 2002 memantine has been approved for the treatment of moderate to severe Alzheimer's disease (Allgaier and Allgaier, 2014), also demonstrating some additional benefits for pathologies like vascular dementia (Orgogozo et al., 2002). Recent evidence from *in vitro* and *in vivo* studies underlined memantine as an attractive candidate for clinical translation also in stroke therapy, due to good biological availability and tolerability profile. The restoration of brain functionality provided by memantine occurs indeed in a dose-dependent manner, with low memantine concentrations significantly rescuing neurons and glia via *excitotoxic* cascade interruption, while high concentrations significantly enhanced cell death (Trotman et al., 2015). In particular, memantine apparently acts via non-neuroprotective mechanisms, but rather involving increased BDNF/TrkB signaling, reduced reactive astrogliosis and improved vascularization, associated with better recovery of sensory and motor cortical function after MCAo (Lopez-Valdes et al., 2014). To date, a deeper evaluation of memantine in the clinical setting is warranted, particularly concerning the prophylactic administration in those patients identified as being at risk of ischemic stroke.

Overall, in spite of initial tiny but encouraging results, glutamate receptor antagonists as well as postsynaptic Ca^{2+} channel blockers (*i.e.* nimodipine, ziconotide), Na^{+} channel blockers (*i.e.* sipatrigine, fosphenytoin), or GABA mimetics (*i.e.* clomethiazole) were all rejected because of toxic drawbacks, including nausea, vomiting, and severe psychotomimetic side effects (Gladstone et al., 2002; Lai et al., 2014).

Some other relevant clinical attempts to target *excitotoxicity* are summarized below.

- *Magnesium sulfate:*

Magnesium is an endogenous calcium channel antagonist, and its putative neuroprotective properties have been variously ascribed to NMDA receptor uncompetitive blockade, calcium channel blockade, excitatory neurotransmitter release inhibition, and smooth muscle vasodilation (Ginsberg, 2008).

The FAST-MAG randomized double-blind trial was run as a pre-hospital therapy initiated in the ambulance as an IV bolus of magnesium sulfate followed by 24 h infusion. Not surprisingly, lack of clinical benefit resulted (Saver et al., 2015).

- *PSD-95:*

Intravenous NA-1 (Tat-NR2B9c), an inhibitor of postsynaptic density-95 (PSD95) protein that links NMDA receptors to neurotoxic signaling in neurons, proved to halt glutamate *excitotoxicity* and reduce infarct volume in non-human primates after transient or permanent brain ischemia (Cook et al., 2012; Sattler et al., 1999). In the ENACT trial, NA-1 showed to be safe, although no difference was noted by MRI analysis with respect to placebo concerning the volume of lesions (Hill et al., 2012). Further studies are currently ongoing.

- *Ca^{2+} channel antagonists:*

Calcium influx is a downstream event into the signaling pathway of glutamate. Therefore, receptor-operated calcium channel antagonists have been targeted as well.

The calcium channel antagonist Ginsenoside-Rd has been for instance assessed in a Chinese RCT on patients with acute ischemic stroke treated within 72 h (Liu et al., 2012). Ginsenoside-Rd displayed no substantial adverse effects and showed better functional recovery in the treated group, although many previous trials indicated no clinical benefits. Further confirmation is warranted.

- *Peritoneal dialysis:*

In order to reduce blood glutamate concentrations without further affecting normal brain neurophysiology, peritoneal dialysis has been shown to efficiently reduce hematic glutamate levels in a rat model of cerebral ischemia (Godino et al., 2013), consequently the EUDRA clinical trial is ongoing on patients with acute ischemic stroke.

3.2 Oxidative stress as therapeutic target

The neutralization of oxidative and nitrosative stresses is undoubtedly a potential therapeutic strategy to attempt, due to the brain high susceptibility to oxidative damage, its rich content of iron and unsaturated lipids, and its relatively low endogenous antioxidant capacity.

As a consequence, the prevention of ROS and RNS (reactive nitrogen species) generation at *penumbra* sites proved to be an effective measure to limit the expansion of the ischemic lesion in preclinical stroke models (Fukuyama et al., 1998).

- *NXY-059:*

Peroxynitrite among other RNS gained particular interest due to its harmful activity on lipid peroxidation, mitochondrial damage, protein nitration and oxidation, depletion of antioxidant reserves, and breakdown of the BBB (Beckman, 1996). Peroxynitrite scavengers such as the nitrone disufenton sodium (NXY-059), the disulfonyl derivative of the radical-scavenging phenylbutylnitrone, provided controversial results, resulting efficiently neuroprotective from one large-scale trial (*i.e.* SAINT I) (Lees et al., 2006) but lacking reproducibility in a second trial (*i.e.* SAINT II) (Shuaib et al., 2007).

- *Edaravone:*

Edaravone is an antioxidant able to scavenge hydroxyl, peroxyl, and superoxide radicals. In both *in vitro* and *in vivo* assays, this drug inhibited a plethora of pathogenic mechanisms associated with ischemic cell death including microglia-induced neurotoxicity, chronic inflammation, oxidation of low-density lipoproteins, and altered expression of endothelial and neuronal proteins (Lapchak, 2010). Several trials on edaravone, however, reported no conclusive evidence for its therapeutic efficacy in stroke patients, although marked neurological improvement was more recently obtained when given in combination with standard therapy (Feng et al., 2011).

Since 2001 edaravone has been approved in Japan for patients with acute stroke.

- *Melatonin:*

Melatonin is a neurohormone produced by the pineal gland, known to exert a wide variety of biological actions besides the control of circadian rhythms. So far, the neurotherapeutic potential of melatonin in brain ischemia has emerged thank to the success of its use in animal

stroke models, exhibiting a reduction in infarct volume by 40% and significantly improving neurologic deficits (De Butte et al., 2002).

Melatonin was indeed demonstrated to possess a plethora of functions, ranging from direct free radical scavenger activity against ROS/RNS, indirect antioxidant properties via increased expression of antioxidant enzymes and NO synthesis suppression (Liu et al., 2015; Manchester et al., 2015; Reiter et al., 2009), up to anti-inflammatory, neuromodulatory, anti-apoptotic and anti-*excitotoxic* effects, also via prevention of Ca^{2+} dyshomeostasis (Ramos et al., 2017). Additionally, melatonin is worth to note as a versatile modulator of multiple signaling pathways involved in neuronal tissue damage, promoting cell proliferation and neurogenesis, maintaining the integrity and permeability of BBB, as well as improving electrophysiological recovery, either alone or in combination therapy with thrombolytic agents (Ramos et al., 2017).

Considering the low toxicity even in very high doses and the good efficacy in spite of low bioavailability, these beneficial properties makes melatonin a suitable option for potential treatment against brain ischemia (Andersen et al., 2016; Harpsøe et al., 2015).

- *Citicoline:*

Citicoline, a phosphatidylcholine precursor, may stabilize neuronal cell membrane due to its scavenging activity and brain bioenergetics modulation. Given the favourable outcomes observed in rat models of ischemic stroke, citicoline has been also tested in humans in several trials (Clark et al., 2001; Dávalos et al., 2002). Unfortunately, the benefits observed in previous meta-analyses were not confirmed in a conclusive prospective trial (Dávalos et al., 2012).

- *Uric acid:*

Uric acid represents the endogenous final oxidation product from purine catabolism and accounts for roughly two-thirds of the whole plasmatic antioxidant capacity (Squadrito et al., 2000). As such, uric acid prevented glutamate-induced cell death and suppressed ROS and RNS generation, conclusively improving the functional outcome in rats with hyperemia following focal ischemia (Onetti et al., 2015). Additionally, a synergistic neuroprotection when combined with alteplase® was exhibited in a thromboembolic rodent model of stroke (Romanos et al., 2007).

The URICO-ICTUS phase III clinical trial tried to assess the effect of uric acid combined with IV rt-PA within 4.5 h from stroke onset. No supplemental benefits over rt-PA alone have been obtained (Chamorro et al., 2014), although a *post-hoc* analysis reported some improved outcome in the female subgroup (Llull et al., 2015).

3.3 Inflammation as therapeutic target

The immune-mediated inflammatory response that follows acute ischemic stroke has also provided promising therapeutic targets. Several RCTs have been therefore conducted or proceed under current investigation.

- *Fingolimod:*

Fingolimod is a high-affinity agonist of the sphingosine-1-phosphate receptor, able to prevent lymphocytes egress from lymph nodes, thereby limiting their infiltration into the brain. Moreover, fingolimod inhibits local activation of microglia and macrophages, reducing number of dying cells, infarcted area, neurological deficits, and edema in several rodent models of brain ischemia (Liu et al., 2013; Wei et al., 2011).

The efficacy of oral fingolimod in improving functional outcome in stroke patients has been assessed in a small open-label pilot study (Fu et al., 2014). Administration within 72 h from stroke onset exhibited no severe adverse effects together with decreased microvascular permeability and attenuated neurological deficits. Additionally, the combination of fingolimod with alteplase® given within 4.5 h after stroke onset presented synergistically improved clinical results, according to the National Institutes of Health Stroke Scale (Zhu et al., 2015).

- *Natalizumab:*

Natalizumab is a humanized CD49d antibody that blocks α4-integrin, attenuating leukocytes infiltration into the brain. Preclinical studies investigating natalizumab on brain ischemia led to contrasting results (Langhauser et al., 2014; Liesz et al., 2011; Llovera et al., 2015), therefore research efforts still have to be paid before landing onto the clinic.

A related compound, Rovelizumab (LeukArrest®) is a monoclonal antibody against CD11/CD18 neutrophil CAM designed to prevent neutrophil invasion of the ischemic bed and subsequent inflammatory injury (Rhee et al., 2000). After establishing safety in humans, a

phase III trial (HALT) on acute ischemic stroke patients was run, but no suggestion of benefit has been cited.

- *Anakinra:*

Interleukin-1 receptor antagonist (IL-1ra) is a naturally occurring competitive antagonist of the proinflammatory cytokine IL-1 (Allan et al., 2005). Anakinra, the recombinant form of IL-1ra, has been so far widely used in chronic inflammatory disorders due to its powerful antiphlogistic activity associated with good safety profile (Dinarello and van der Meer, 2013). Treatment with recombinant IL-1ra already showed neuroprotective effects in rodent models of stroke (Mulcahy et al., 2003). An ongoing phase II study will soon unveil any potential therapeutic action in stroke patients as well, in spite of the increased risk of infection manifested so far (Becker et al., 2014).

- *Minocycline:*

Minocycline, a tetracycline derivative, proved to attenuate apoptosis and inhibit metalloproteases expression following focal cerebral ischemia in animal models of stroke (Murata et al., 2008). The acceptable safety profile observed in an open-label, dose-escalation study together with the wider therapeutic window and the inhibition of matrix metalloproteases-driven inflammatory response offered by the combination with alteplase® (up to 6 h) have strongly encouraged on the potentialities of this drug (Fagan et al., 2010; Kohler et al., 2013). The results of a further RCT on minocycline with thrombolytic treatment are awaited.

- *Miscellaneous strategies:*

Ultimately, the exogenous administration of growth factors including nerve growth factor (NGF), brain-derived neurotrophic factor (BDNF), neurotrophins 4/5 (NT-4/5), basic fibroblast growth factor (FGF-β), and insulin-like growth factor 1 (IGF-1) accomplished some beneficial effects in the functional recovery of rats subjected to cerebral ischemia (Lee et al., 2000), however a clear-cut evidence for satisfying therapeutic outcomes is still missing.
Some of the principal randomized trials run so far have been summarized in **Tab. 1**.

TRIAL NAME	COMPOUND	PHARMACOLOGY	SAMPLE SIZE	TRIAL FEATURES	STATE OF TRIAL	OUTCOME
FAST-MAG (*NCT00059332*)	Magnesium sulfate	Anti-*excitotoxic* (endogenous Ca^{2+} channel antagonist)	1700	Randomized double-blind trial	Completed in 2013	Treatment within 12 h of acute stroke failed to improve mortality and morbidity; no shift in mRS distribution by treatment (p = 0.28) (Saver et al., 2015).
ENACT (*NCT00728182*)	NA-1 (Tat-NR2B9c)	Anti-*excitotoxic* (inhibitor of PSD95)	185	Randomized, double-blind, placebo-controlled trial	Phase II	Treatment initiated after the completion of endovascular aneurysm repair surgery resulted in significantly fewer ischemic infarction. The treatment was well tolerated, with no serious side effects (Hill et al., 2012).
Traxoprodil (*CP-101,606*)	Traxoprodil	Anti-*excitotoxic* (NMDAR NR2B-subunit antagonist)	53 + 30 + 404	Open-label and double-blind trials	Phase II	Open-label: treatment within 12 h of hemorrhagic stroke showed above-average outcome (Bullok et al., 1999). Double-blind: treatment within 8 h of traumatic brain injury improved mortality and morbidity at 6 months (Yurkewicz et al., 2005).
Ginsenoside-Rd (*NCT00815763*)	Ginsenoside- Rd	Anti-*excitotoxic* (Ca^{2+} channel antagonist)	390	Randomized, double-blind trial	Completed in 2008	Improved functional recovery in the treated group and overall mRS score- distribution (OR 1.74, CI1.08-2.78, p =0.02). Results not confirmed (Liu et al., 2012).
SAINT I (*NCT00119626*) **and SAINT II** (*NCT00061022*)	NXY-059 nitrone disufenton sodium	Antioxidant (Peroxynitrite scavenger)	1722 + 3306	Randomized, double-blind trial	Respectively completed in 2005 and 2006	SAINT I: improvement on mRS but not on NIHSS score from baseline (p = 0.86) (Lees et al., 2006). SAINT II: no difference by treatment in mRS distribution (OR 0.94, p = 0.33) (Shuaib et al., 2007).
Edaravone	Edaravone	Antioxidant (ROS scavenger)	1200	Randomized, double-blind trial	Completed in late 2016	Under revision
ICTUS (*NCT00331890*)	Citicoline	Antioxidant (neurovascular repair)	2078	Randomized, double-blind trial	Terminated prematurely in 2012	Global recovery was similar in treated and control subjects (OR 1.03, CI 0.86-1.25, p = 0.364). Not consistent results (Dávalos et al., 2012).
URICO-ICTUS (*NCT00860366*)	Uric acid (combined with IV rt-PA)	Antioxidant (ROS scavenger)	421	Randomized, double-blind trial	Completed in 2013	Difference in outcome (39% uric acid vs. 33% control) not significant (Chamorro et al., 2014). *Post-hoc* analysis showed excellent outcome in women (42% vs. 29%; p = 0.036) (Llull et al., 2015).
Natalizumab (*ISRCTN7423629*)	Natalizumab	Anti-inflammatory (humanized CD49d Ab)	Not known	Randomized, double-blind trial	Completed in late 2016	Under revision
NeuMAST (*NCT00930020*) **and PIMMS**	Minocycline	Anti-inflammatory (reduction of microglia activation and MMP-9)	139 + 95	Randomized, double-blind trial	To be completed	---

Tab. 1
Main randomized controlled trials assessing neuroprotective strategies to manage ischemia pathophysiology. mRS: modified Rankin Scale; OD: Odd Ratio; CI: Confidence Interval.

3.4 Non-pharmacological approaches

Various non-pharmacological strategies have been approached.

In a subset of patients, angioplasty and stenting could be surgical viable options in the treatment of acute ischemic stroke. The rate of technical success for intra-cranial stenting ranged around 90-98% in relieving symptomatic intracranial arterial stenosis. The rates of re-stenosis and recurrent strokes following the treatment were also favourable (Ansari et al., 2011; Derdeyn and Chimowitz, 2007; Francoeur and Mayer, 2016) but further data are still required. Hyperbaric oxygen therapy has been studied as a possible protective measure, since multiple putative clinical benefits could be attained, including mitochondrial rescue, attenuation of cortical spreading depression, and salutary effects on endothelial-leukocyte interactions (Kumaria and Tolias, 2009). A recent meta-analysis of animal studies suggested that hyperoxia may reduce infarct size and improve neurological function, particularly when administered promptly following MCA occlusion (Xu et al., 2016), although additional studies haven't been undertaken so far.

Conclusively, the targeted temperature management has gained increasing momentum for clinical translation to stroke intervention (Chamorro et al., 2016; Lee et al., 2017). Compelling evidence from preclinical research in animal models demonstrated marked protective effects of mild to moderate therapeutic hypothermia in ameliorating functional outcomes via the downregulation of multiple pathogenic pathways including oxidative stress, inflammatory responses, metabolic disruption, and cell death signaling (Choi et al., 2012; Lee et al., 2014). Indeed, therapeutic hypothermia provided promising options for neuroprotection, correlating with diminished free radicals production (Hall, 1997), impaired neuronal apoptosis via modulation of p53 and Bcl-2, shutdown of matrix metalloproteases and cytochrome c pathways (Lee et al., 2014), decreased expressions of proinflammatory mediators such as TNF-α, NF-κB and IL-1β (Lee et al., 2016).

Notably, glutamate release proved to be temperature-dependent (Campos et al., 2012; Yenari and Han, 2012), possibly due to a plethora of underlying mechanisms such as modulation of the GluR2 subunit of AMPA receptors (Colbourne et al., 2003), reduction of the number of

AMPA and NMDA receptors expressed (Friedman et al., 2001), decreased calcium influx and brain glycine levels (Hall, 1997; Kvrivishvili, 2002).

In spite of all these obvious beneficial effects of therapeutic hypothermia, its clinical application is still limited due to multiple shortcomings. For instance, current hypothermia protocols contemplate procedures both slow and impractical (ice cooling may require up to 8 hours) or invasive in the case of endovascular cooling, eventually providing tremendous need for optimization. On this line, the pharmacologically induced hypothermia can directly target the peripheral or central thermoregulatory mechanisms and is currently emerging as a more efficient and safer treatment (Cao et al., 2014; Wei et al., 2013).

Several pilot studies have clearly indicated the clinical benefits offered by pharmacological thermoregulatory agents like neurotensin, transient receptor potential vanilloid 1 (TRPV1), cannabinoids and opioids, thyroxine derivatives, dopamine, gases, and adenosine derivatives (Feigin et al., 2002; Muzzi et al., 2012), although more incisive results are still needed.

3.5 The translational roadblock

Overall, cytoprotective strategies including anti-*excitotoxic* drugs, free radical scavengers, anti-inflammatory or anti-apoptotic agents as well as non-pharmacological approaches did not show the expected beneficial results (Chamorro et al., 2016).

A plausible explanation for these discrepancies of translatability from bench to bedside in ischemic stroke could been ascribed to the difficulty of conducting clinical trials with stroke patients, due to the lack of a fitting linearity between lesion size and clinical deficits assessed by clinical scales, as well as to shortcoming in proper patients randomization to afford heterogeneity of study populations in relation to duration and severity of ischemia, gender differences, age and underlying or co-morbid diseases. Likewise, timing of drug administration, drug dosage, pharmacokinetics and bioavailability in the target area, concealed side effects, suitable therapeutic window for effective neuroprotection and clinical trials design itself might be sharply taken into consideration and, implemented, where needed, in order to avoid bias or contrived outcomes (Grupke et al., 2015; Howells et al., 2013; Landis et al., 2012). Increased awareness of the relevance of rigorous testing and appropriate selection for clinical inclusion criteria seem to offer the key for the search of safer and more effective treatment strategies (**Fig. 15**).

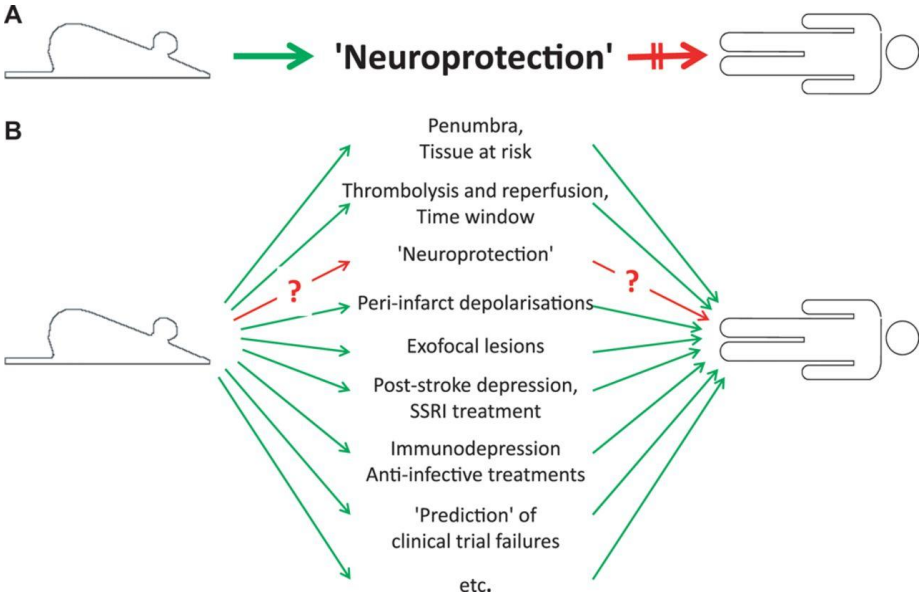

Fig. 15
Stroke: a global problem with unmet medical needs.
A) Translational roadblock: the focus of basic stroke researchers, clinicians, and pharmaceutical industry is on the failure to translate purportedly neuroprotective preclinical therapies into improved treatment of patients with stroke.
B) A more comprehensive strategy toward ischemia clinical management may include several successful bench-to-bedside translations in neuroprotection and stroke pathophysiology.
(Adapted from Dirnagl and Endres, 2014).

Among the several therapeutic options tried over the past three decades, strategies directly targeting *excitotoxic* mechanisms rather than collateral signaling including inflammation and oxidative stress have received great scientific concern.

In particular, NMDAR antagonism, whether competitive, uncompetitive or occurring via inhibition of the glutamate-binding site, the glycine-binding site, or the channel pore, exhibited effective therapeutic potential in the treatment of ischemic stroke damage, although without any drug succeeding the approval in trials.

The reason for this lack of clinical success is likely multifactorial. NMDAR blockers merely have a short therapeutic window, resulting effective only if administered before or immediately following stroke.

Moreover, due to the involvement in neurophysiological functions, unselective NMDAR blockade may obviously produce multifarious unwanted effects as well as neuronal pathomorphological changes, as reported already from preclinical testing.

Due to such concerns, a great number of NMDAR antagonists under clinical evaluation have been painfully discontinued from further human clinical studies.

3.6 Animal models for ischemic stroke: potentialities, capstones and issues

The use of pertinent animal models for cerebral ischemia is currently matter of vibrant debate, being animal models strong predictors of clinical value, drug tolerance and side effects for translational therapeutic approaches in human subjects.

The main aim of cerebral ischemia models is the induction of hypoxia and hypoglycemia to the brain, in order to recapitulate that variety of cellular and molecular mechanisms that impair neuronal energetics and lead to cerebral infarction, as observed in humans.

Thereby, most focal cerebral ischemia models have been produced since early ‘60s, conveniently focusing on both large and small animals depending on the respective advantages regarding affinity with the human brain in terms of anatomic structure and function, financial costs, public animal welfare concerns, transgenic manipulation reproducibility, and compatibility with imaging techniques, physiological monitoring, behavioural assessments, and surgical procedures (reviewed in Sommer, 2017 and Traystman, 2003).

Experimental models for ischemia may be global, focal, or multifocal, depending on the pattern and severity of reduction in cerebral blood flow.

To fit the purposes of this dissertation, only mice models of focal transient cerebral ischemia will be taken into account among the huge variety of possible experimental animals.

Focal cerebral ischemia is widely achieved by clogging a major cerebral blood vessel like the middle cerebral artery (MCA), by means of intraluminal filament suture (Engel et al., 2011), electrocoagulation (Llovera et al., 2014) or photochemical approaches (Sugimori et al., 2004). MCA occlusion (MCAo) results in the absolute shutdown of oxygen and glucose supply in the very central infarcted area, while peripheral areas may be still sustained by collateral circulation from the circle of Willis and/or from leptomeningeal anastomoses.

This procedure mostly induces injury at striatal and cortical level in the ischemic core, whereas shades of severity in the *penumbra* depend on the duration and site of occlusion along the artery, as well as on subsequent potential reperfusion and adequate systemic blood pressure.

So far, both transient and permanent MCAo models have been involved in the majority of studies investigating pathophysiological processes and potential novel neuroprotective agents, due to their close emulation of human ischemic stroke, and to reliability and reproducibility of generated infarcts.

A wealth of fruitful insights later recognized also in the setting of human stroke have been unveiled from those experimental models, including the concept of *penumbra*, the identification of spreading cortical depolarization, the detection of post-stroke neurogenesis and the phenomenon of preconditioning (Dirnagl and Endres, 2014).

Nevertheless, it appears immediately obvious how such experimental models can cover only individual specific aspects of this multifaceted disease, due to man/mouse discrepancies in molecular pathogenic mechanisms, genetics and epigenetics, brain anatomy and functional organization, vascular anatomy, immune system, behavioural and psychiatric outcomes, features of populations analysed (Sommer, 2017) (**Fig. 16**).

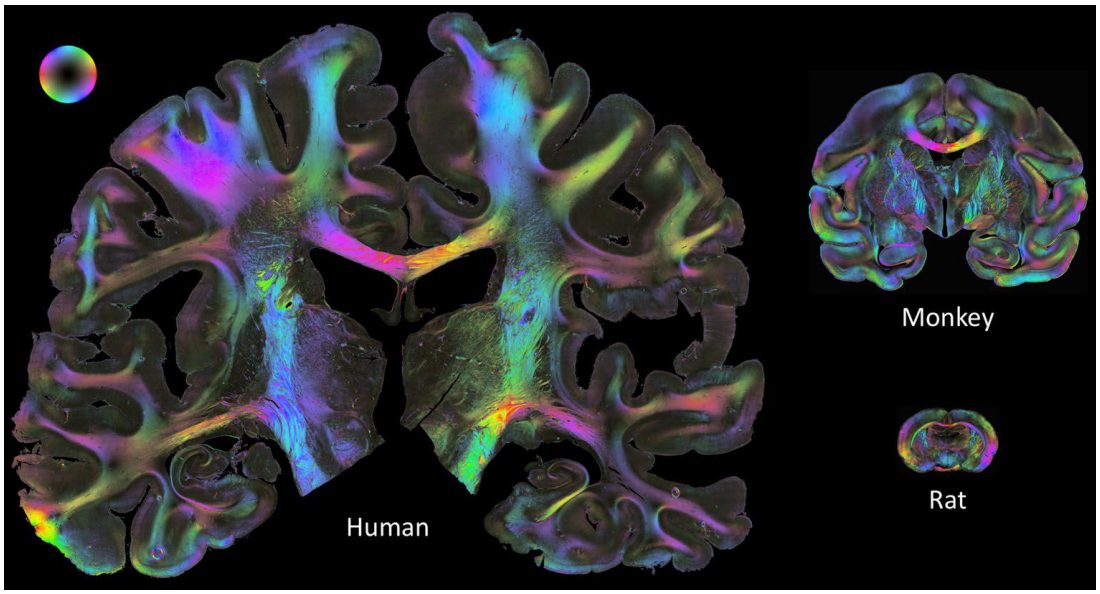

Fig. 16
Anatomy of brain across species.
Illustration of connectivity as obtained by 3D-polarized light imaging (3D-PLI). Coronal sections from a human brain, a vervet and a rat brain. The *colour sphere* indicates the direction of fibers; *black* corresponds to a steep course of fibers in the third dimension, within the physical section. The comparison illustrates that not only the absolute volume of brains differs among the three species, but also the relative amount with a much higher proportion of white matter in human brains as compared to vervet and rodent brains.
(Adapted from Sommer, 2017).

In addition, target endpoints in animal models generally account for infarct volume rather than long-term functional outcome which is instead the most relevant parameter in human patients, with special concern for the *penumbral* salvageable areas (Gladstone et al., 2002). Consequently, the deep gap between ischemic stroke in experimental models and the reality of stroke in human patients is sadly illustrated by the resoundingly failure that followed the moment of translation into human trials, with recanalization of occluded vessels being the only successful exception (Jickling and Sharp, 2015).

Besides the issues of internal validity, external validity of preclinical stroke research has also been burdened by insufficient methodological zeal. Many drugs, for instance, have been tested in inbred adolescent healthy male mice with no co-morbidity or co-medication, rather fed on a diet high in antioxidants and housed under optimal pathogen-free conditions.

This situation is in stark contrast to human reality where stroke patients are often old, with co-morbidities, and under poly-pharmacology treatments (Dirnagl and Endres, 2014; Sena et al., 2010).

This poor translational power of preclinical stroke models has led to the establishment of the *Stroke Therapy Academic Industry Roundtable* (STAIR) that brought together basic and clinical science researchers, industry, regulators and NIH representatives with the goal of predispose landmarks and recommendations to optimize the quality of preclinical stroke research and the design of trials for neuroprotective drugs before moving to clinical trials. Moreover the STAIR aims at providing appropriate stroke models in the experimental setting for a future more incisive translatability, and to discourage overstated preclinical evidence of efficacy (Fisher et al., 2009; Stroke Therapy Academic Industry Roundtable (STAIR), 1999).

Among the items listed in the guidelines, emphasis should be put on age, gender, co-morbidities, replication in gyrencephalic non-human primates, drug pharmacokinetics and pharmacodynamics, acute and long-term histological and functional outcomes, sample size calculation, random and blinded animal allocation (Moretti et al., 2015).

4. Looking for novel therapeutic molecular targets

Due to such resoundingly discouraging scenario, further approaches pursued a dual line of neuroprotective strategies, focusing at extending the therapeutic time window for pharmacological intervention on one hand, while simultaneously targeting the signaling

events further downstream in the *excitotoxic* cascade, with the aim of being more selective and allow even delayed therapeutic operations to be effective.

In an effort to circumvent the limitations reported above, recent studies have attempted to target the highly conserved intracellular signaling of mitogen-activated protein kinases (MAPK), including JNKs, p38 and ERKs kinases, so far mentioned among the biochemical pathways critically contributing to neuronal death following the ischemic induction.

MAPKs are activated via the dual phosphorylation of a tripeptide motif (*Thr-X -Tyr*) located in the activation loop. These phosphorylations are mediated by a MAPK kinase (MAPKK) that is in turn activated via phosphorylation by another MAPKK kinase (MAPKKK) in the context of a kinases signaling cascade (Davis, 2000).

Treatment with the selective p38 inhibitor *SB203580* or ERK inhibitor *PD98059* demonstrated to reduce neuronal demise respectively after transient global and focal ischemia (Alessandrini et al., 1999; Sugino et al., 2000).

Current work is emphasizing the utmost relevant role of the JNKs (c-Jun *N*-terminal kinases), also known as SAPK (stress-activated MAP kinases), in mediating neurotransmission in both physiological and, upon further activation, pathological conditions.

4.1 JNK signaling pathway

Three mammalian genes are known to encode the JNK isoforms, namely JNK1 and JNK2 that present ubiquitous patterns of expression, and JNK3 mostly restricted at neuronal, cardiac and testis level, with an activity up to 30 folds higher in the brain with respect to other tissues (Davis, 2000; Gupta et al., 1996). Those genes are additionally subjected to alternative mRNA splicing to yield ten isoforms which nearly all fall into two molecular weight categories of 54 and 46 kDa, characterized by distinct repertoires of brain expression (Coffey, 2014).

The very first studies coming from ‘90s identified JNK as a “p54 microtubule-associated kinase”, activated upon cytokines input (TNF and IL-1) or environmental stressors (hypoxia, redox stress, heat shock, UV irradiation, inflammation, Aβ toxicity) via MKK4 or MKK7-mediated phosphorylation within the *Thr-Pro-Tyr* motif (Centeno et al., 2007; Mukherjee et al., 1999; Nisticò et al., 2015; Sclip et al., 2014). To date, MAP kinases MKK4 and MKK7 are the only known JNK activators, although their contribution in neuronal *excitotoxicity* has not yet been fully elucidated (Centeno et al., 2007). In turn, activated JNK may bind to and phosphorylate the c-Jun target, starting its downstream signaling (Pulverer et al., 1991).

Conversely, JNK inactivation is mediated by a group of phosphatases that determine the magnitude and duration of this MAPK activity, including *Ser/Thr* and *Tyr* phosphatases like PP2Cα and MKP-1 (Davis, 2000; Kondoh and Nishida, 2007) (**Fig . 17**).

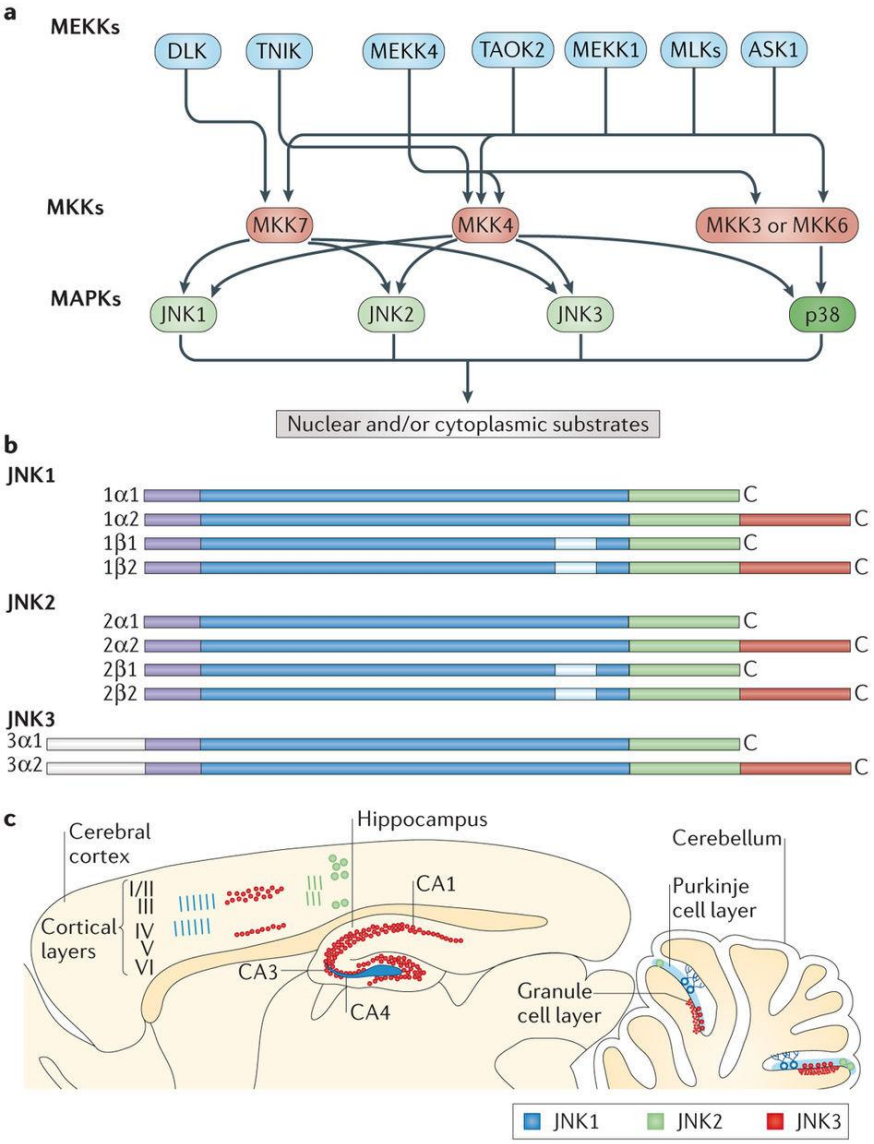

Fig. 17
MAP kinases cascade and JNK isoforms splicing and distribution into the brain.
A) JNK proteins belong to a classical MAPK signaling cascade. JNKs are activated by dual phosphorylation of the *T-P-Y* motif within their activation loop by two MAPK kinases MKK4 and MKK7. Upstream, various MKK kinases (MEKKs, ASK1, TAOK2, TRAF2, DLK, TNIK) phosphorylate and thereby activate MKK7 and/or MKK4.
B) In the brain, *JNK1*, *JNK2* and *JNK3* are alternatively spliced to yield ten proteins, which nearly all fall into two molecular weight categories of 54 and 46 kDa, depending on the variants formed at the *C*-terminal.

C) An overview of JNKs subcellular distribution in the mouse brain. In the cortex and hippocampus, JNK1 expression is largely cytosolic and found in the neuropile, whereas JNK3 expression is predominantly nuclear and found in approximately 30% of cells in layers III and V. Of note, JNK3 is the dominant JNK isoform expressed throughout the hippocampus. In the cerebellum, JNK3 is found in nuclei of Purkinje cells and cerebellar granule neurons, whereas JNK1 expression is prominent in Purkinje cell dendrites. JNK2 expression is similar to JNK1 and JNK3 expression in the cortex, although this isoform is found in both nuclei and soma of neurons in the hippocampus and cerebellum.
(Adapted from Coffey, 2014).

JNKs tuned expression and subsequent substrate phosphorylation is essential to govern brain morphogenesis and axodendritic architecture during development (*i.e.* neuronal migration, axonal sprouting, spines elongation and maintenance), as well as to regulate important neuronal specific functions (*i.e.* synaptic plasticity, memory formation) (Coffey, 2014; Weston and Davis, 2007; Yamasaki et al., 2012). Coherently, mutations in *JNK1* and *JNK2* genes, as well as MKK4 and MKK7 knock-out mice are not viable or associated with exencephaly, indicating the crucial role of activated phospho-JNK for nervous system development.

Furthermore, although very few is known about JNKs specific involvement in cognitive and behavioural functions, the pronounced basal expression, the regulation of gross and fine brain architecture and the central control of gene expression and metabolic homeostasis strongly suggest a relevant role for JNKs in higher brain functions (Reinecke et al., 2013).

A recent study analysed the effects of single JNK deficient mice, reporting that the constitutive genetic deletion of JNK isoforms does not substantially affect memory consolidation but does elicit different phenotypic explorative behaviours, with JNK1 knock-out mice displaying a stronger explorative behaviour whereas JNK2 or JNK3 knock-out showed opposite tendencies (Reinecke et al., 2013).

On the other hand, JNKs signaling has been strongly correlated to several types of injurious processes, with particular concern upon neurodegenerative diseases (Sclip et al., 2014, 2011), psychiatric disorders (Coffey, 2014), cerebral ischemia (Borsello et al., 2003a; Repici et al., 2007) and traumatic brain injury (Tran et al., 2012), possibly mediated by transcription-dependent apoptotic pathways involving p53 and c-Myc as JNK targets (Davis, 2000).

JNK has also been proposed to be required for stress-induced release of mitochondrial cytochrome c via Bcl2 inactivation, via phosphorylation and consequent caspase-driven

apoptotic death (Tournier et al., 2000; Wei et al., 2008), strengthening the hypothesis of a JNK-mediated neuronal demise following ischemia.

4.2 JNK role in ischemia

In response to the *excitotoxic* paradigm, JNK is known to be activated after focal or global ischemia during both permanent and transient events (Borsello et al., 2003a), with the phosphorylated fraction increasing 3 hours after the occlusion and peaking at 6 hours. This trend correlates well with c-Jun and caspase-3 time course in the ischemic core but not in the *penumbra*, emphasizing an interesting correlation with ischemia-induced apoptotic neuronal death (Repici et al., 2007).

Given the relevant association between JNK and NMDARs at postsynaptic sites, NMDA-induced *excitotoxicity* has been classically entailed as a potent JNKs signaling activator, operated through the rapid and selective phosphorylation carried by MAP kinases, although divergent results have not identified whether MKK7 or MKK4 contributes the most (Centeno et al., 2007; Repici et al., 2007).

Moving beyond this evidence, several studies have been conducted in order to thoroughly unveil the involvement of JNK in ischemic *excitotoxicity*, looking at feasible therapeutic avenues. Coherently, JNK inhibition was shown to prevent NMDAR-mediated neuronal death in both cortical neurons and organotypic hippocampal slice cultures (Borsello et al., 2003a, 2003b; Centeno et al., 2007). In particular, JNK3 is currently associated with protection from *excitotoxicity* and hypoxia since adult JNK3-deficient mice exhibit reduced seizure outbreak and apoptotic avoidance (Kuan et al., 2003; Yang et al., 1997). JNK1 and JNK2 seem instead to be important for apoptosis during brain development (Kuan et al., 1999). Mice lacking *c-Jun* gene are also less prone to the *excitotoxic* insult, overall raising JNK signaling pathway blockade as a promising target for neuroprotection.

Notably, as previously reported, addressing to this delayed downstream pathway may crucially extend the therapeutic window for intervention, allowing a more opportune chance for ischemic patients reaching the emergency room later than 3 h after stroke onset, *i.e.* beyond the effective temporal range for thrombolysis.

On this line, *D-JNKI1*, a *D*-retro-inverse cell-penetrating peptide able to block JNK access to its phosphorylatable substrates was the first drug to achieve remarkable reduction in infarct

volume and neuroprotection even when administered 6 to 12 h after both transient and permanent cerebral artery occlusion in MCAo models (Borsello et al., 2003a).

Recent evidences are furthermore shedding new light on the biological involvement of JNK and its scaffold proteins JIP (JNK interacting protein) (Kennedy et al., 2007) also at presynaptic sites (Biggi et al., 2017; Nisticò et al., 2015), and particularly under the perspective of their potential association with presynaptic NMDARs (Corlew et al., 2007). Indeed, JIP proteins have been implicated in the assembly and coordination of JNK signaling partners, and mice lacking JIP expression were found to exhibit severe defects in NMDAR function, including decreased NMDA-evoked current amplitude, aberrant regulatory phosphorylation of NR1 and NR2 subunits, impaired cytoplasmic Ca^{2+} homeostasis, and altered gene expression (Kennedy et al., 2007).

Contextually, JIP1 was also required for JNK activation and neuronal death in response to ischemia in *in vitro* and *in vivo* stroke models (Whitmarsh et al., 2001).

Concurrently, presynaptic NMDARs have been newly characterized as important key players implicated in brain development, neurotransmitter release, synaptic strength modulation, and memory consolidation (Banerjee et al., 2016; Larsen et al., 2014), but also in pathologies including ischemia and Alzheimer's disease (Biggi et al., 2017; Frasca et al., 2011).

As a matter of fact, the existence of glutamate receptors at presynaptic terminals has been suggested by immunochemical localization experiments, functional studies, ultrastructural fractionation and receptor subunit trafficking analyses, bridging a gap on the lack of evidence for NMDARs and JNK implication in glutamate release at this synaptic compartment in both physiological and pathological settings (Biggi et al., 2017; Feligioni et al., 2006; Grilli et al., 2012; Nisticò et al., 2015).

In a recent work, our group employed transgenic knock-out mice for single JNK isoforms, underlining a unique and specific contribution of the JNK2 subtype in mediating such presynaptic events at cortical nerve endings (Nisticò et al., 2015).

Indeed, JNK2 knock-out mice displayed a dramatic reduction of NMDA-evoked glutamate release as direct consequence of the decreased NMDA-elicited JNK activation, thereby suggesting a striking mechanism by which glutamate overflow might be controlled via the upstream presynaptic interaction among NMDAR, JNK2, JIP1 and other protein partners of the release machinery.

4.3 Presynaptic JNK modulates glutamate release

Protein–protein interactions and formation of protein complexes are thought to be critical for the normal function of the JNK signaling pathway. Thereby, our research effort is exploring the role of JNK in the presynaptic modulation of vesicle release, focusing on the interaction between JNK and SNARE proteins.

A work by Biggi and coworkers (Biggi et al., 2017) just confirmed JNK localization at presynaptic compartments, as well as its activation upon presynaptic NMDARs stimulation. Additionally, the presence of putative JNK-binding domains (JBDs) in some proteins belonging to the presynaptic release machinery let authors hypothesize a possible physical interaction of those proteins with JNK. Basically, a JNK-dependent phosphorylation of t-SNARE proteins may be involved in neurotransmitter release at presynaptic sites, with potential application in both synaptic plasticity and ischemic events.

On purpose, we examined whether JNK may act as an effector for the SNARE complex formation, in order to regulate glutamate vesicle release.

4.4 SNARE complex assembly in the synaptic vesicles machinery

In the central nervous system, neurotransmitter release in both physiological and pathological conditions is mediated by exocytosis of synaptic vesicles from electron-dense regions called *active zones* in the presynaptic plasma membrane of nerve terminals. These specialized biochemically insoluble, disk-like structures are embedded with multidomain proteins that provide a scaffold for synaptic vesicles, *i.e.* 40–100 nm spherical lipid-bilayer organelles generated from the endoplasmic reticulum or presynaptic plasma membrane, filled with molecules of neurotransmitter via a vacuolar proton pump and transported by cellular trafficking toward the presynaptic active zone (Ramakrishnan et al., 2012; Südhof, 2004).

Exocytosis at fast synapses is a calcium-dependent event that occurs on a millisecond timescale (0.5 ms or less) following transient calcium current into nerve terminals during incoming action potentials (Jahn and Fasshauer, 2012). Under resting conditions, synaptic vesicles are referred to as "*readily-releasable pool"* and get tethered in the nerve terminal in close proximity to the voltage-gated calcium channels that cluster around the active zone to regulate exocytosis and endocytosis in the frame of rapid and repeated rounds of transmitter release.

When action potentials induce the opening of Ca^{2+} channels (mostly *CaV2.1 P/Q*- or *CaV2.2 N*-type Ca^{2+} channels), the resulting Ca^{2+} influx effectively triggers exocytosis.

For the sake of clarity, it appears obvious that these fine-tuned mechanisms may deregulate and exacerbate during the spreading depolarizing waves characterizing the ischemic progression and culminating into *excitotoxic* demise.

Presynaptic neurosecretion is traditionally divided into three stages preceding vesicles endocytosis and recycling, namely:

- *docking* at the active zone, as morphologically observed by electron microscopy;
- *priming* of vesicles to become electrophysiologically Ca^{2+} responsive and competent for fusion;
- *fusion* of vesicular-presynaptic bilayers and opening of an aqueous channel termed fusion pore to release ready vesicles into the synaptic cleft (Acuna et al., 2014).

A major goal in structural and functional neurobiology studies during the past two decades has been to gain insight into the molecular machinery that mediates neurotransmitter release, in order to yield a unified picture for the key players crowding at the presynapse.

Several genes and protein families have been so far identified and likely targeted to modulate the dynamics of neuronal exocytosis, and particularly upon pathologic conditions such as cerebral ischemia. Many of them belong to an array of structurally conserved proteins, collectively called SNARE (*Soluble-N-ethylmaleimide-sensitive factor Attachment protein REceptors*) and SM (*Sec1/Munc18 like*) proteins (Südhof, 2012).

SNARE proteins are defined by an extended homologous 70-residue coiled-coil stretch, referred to as a SNARE motif, and include the vesicular *v*-SNARE protein synaptobrevin/VAMP (vesicle-associated membrane protein) and the target *t*-SNARE proteins Syntaxin and SNAP25 (synaptosomal-associated protein 25) on neuronal presynaptic membrane. On the other hand, SM proteins Munc18 and Munc13 are generally clustered with the assembling complexes via the interaction with Syntaxin, bearing a fundamental role in orientation and localization of the vesicles at the active zone (Dawidowski and Cafiso, 2016; Südhof, 2013a). Indeed, deletion of either Munc18 or Munc13 completely inhibits neuronal exocytosis (Jahn and Fasshauer, 2012).

The first step in neurotransmitter exocytosis is the tethering of vesicles at the presynaptic membrane via the formation of protein complexes (Whyte and Munro, 2002). In the active zone, Syntaxin is generally found strongly attached to Munc18 in a close conformation in

which its H_{abc}-domain folds against the *N*-terminal part of the SNARE motif, mutually excluding further interaction with other SNARE proteins (Smyth et al., 2010) (**Fig. 18**).

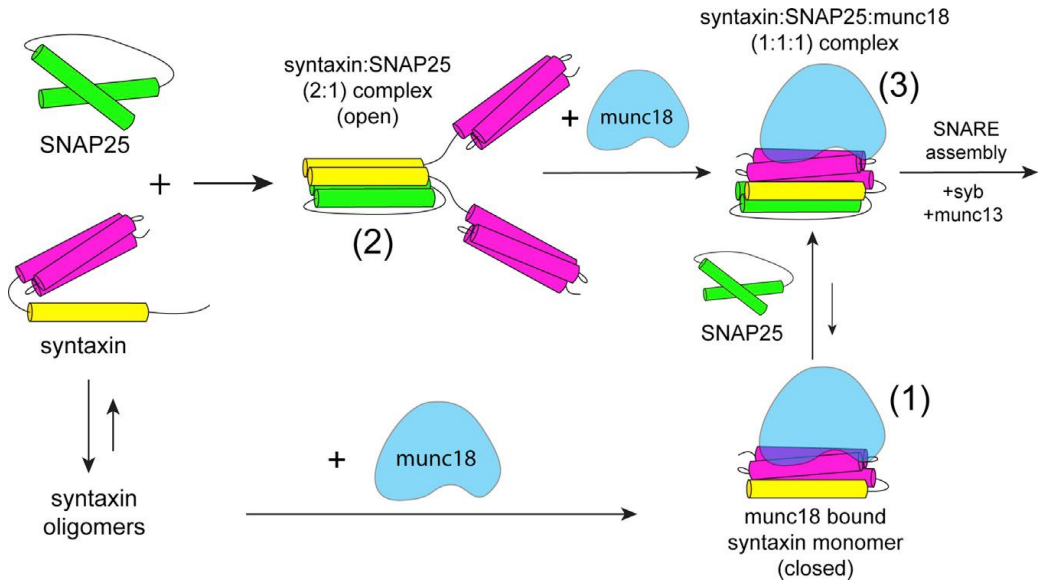

Fig. 18
Open/closed state of Syntaxin in presence of SNAP25 and Munc18.
Syntaxin readily forms oligomers in solution that dissociate to form a 1:1 complex in a closed configuration with Munc18 (form 1). Conversely, Syntaxin preferentially forms a 2:1 Syntaxin/SNAP25 complex (form 2) with excess of SNAP in solution, switching to the open conformation. Further addition of Munc18 dissociates this 2:1 complex, yielding a 1:1:1 Syntaxin/SNAP25/Munc18 complex where Syntaxin goes back to the closed configuration (form 3). The equilibrium between complexes (1) and (3) favours form (3) that is supposed to be the starting point for SNARE assembly.
(Adapted from Dawidowski and Cafiso, 2016).
.

The regulatory interaction between Syntaxin and Munc18 has been intensely debated due to controversial findings. So far it is recognized a dual mechanism to explain the distinct fates of this protein interplay. As said above, in the inhibitory mode Munc18 envelopes Syntaxin, sequestering it from SNARE protein interactions. On the other hand, the direct binding of Munc18 to the evolutionarily conserved *N*-terminal domain of Syntaxin has been proposed to promote the priming in the fusion reaction, ultimately fostering transmitter release (Deák et al., 2009; Rickman and Duncan, 2010; Rickman et al., 2007). In parallel, also Munc13 might

switch Syntaxin into the open conformation, unmasking its SNARE motif and making it competent for SNARE-complex assembly (Dawidowski and Cafiso, 2016).

Interestingly, transgenic mice modified for constitutively open Syntaxin are viable but succumb to generalized seizures in young age, due to impaired binding to Munc18 and dramatically enhanced rate of synaptic vesicle fusion (Gerber et al., 2008), as a proof of the inevitably supervised switch between closed/open state for the normal SNARE assembly.

The *"SNARE hypothesis"* describes a mechanistic model for priming and fusion based on the specific and high-affinity interactions between the highly conserved SNARE domains present in *v*- and *t*-SNAREs proteins. The leucine-zipper-like assembly of the SNARE motifs consists of a highly twisted and parallel four-helical trans bundle wherein Synaptobrevin and Syntaxin respectively share two individual helices while SNAP25 contributes with other two helices, as seen by high-resolution analysis (Brunger et al., 1998; Li et al., 2007). The resulting *SNAREpin* is a competent and thermodynamically stable core fusion machinery that bridges and spans through vesicle/target bilayers, catalyses the steps involved in the release by reducing the energy barrier, and ultimately drives to membranes fusion (Acuna et al., 2014; Li et al., 2007).

The number of assembled SNARE complexes per vesicle during fusion determines the presynaptic discharge probability and the fusion kinetics, with only 1 to 3 SNARE complexes supposed to be minimally required for a fusion reaction (Acuna et al., 2014).

Following transmitter release, vesicles detache from the presynaptic membrane by dissociation of the SNARE complex in an ATP-dependent process and recycle to the reserve pool, which serves to replenish the readily releasable pool upon its depletion.

Besides forcing membranes close together, SNARE nucleation importantly ensures the spatial and temporal specificity of fusion reactions, in a tightly coordinated and finely regulated process.

However, this unique orchestra of calcium-triggered exocytosis is not mediated by the direct binding of Ca^{2+} to the SNARE engine, but rather primarily encoded by calcium-binding proteins located near active zones. Among these, Synaptotagmins are specialized vesicle-bound proteins that constitute the dominant calcium sensors at synaptic terminals (Südhof, 2013a; Südhof, 2013b) and whose deletion results in a complete loss of fast, synchronous calcium-triggered exocytosis (Kochubey et al., 2011). In parallel, Complexins are small calcium-dependent neuronal regulators of exocytosis that facilitate synchronized vesicle fusion via their interaction with SNARE proteins (Giraudo et al., 2006) (**Fig. 19**).

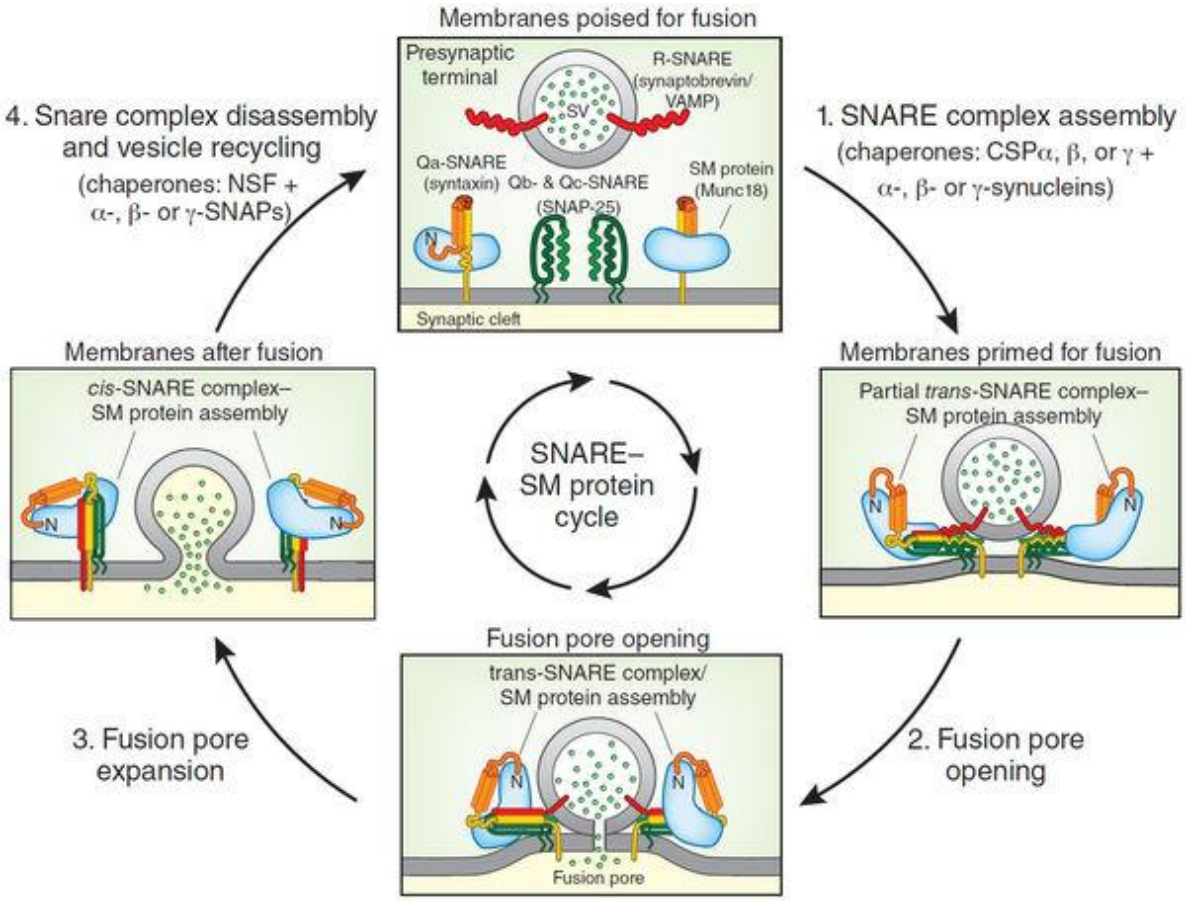

Fig. 19
Paradigmatic diagram of the SNARE–SM protein cycle during synaptic vesicle fusion and neurotransmitter release.
Synaptic vesicles are primed for fusion via a switch of the Munc18-binding mode on Syntaxin from the closed to the open conformation (step 1). This partial assembly of *trans*-SNARE complexes is facilitated by recently discovered chaperones CSPs and synucleins.
The fusion pore opens following a full *trans*-SNARE complex assembly (step 2) and expands converting *trans*-SNARE into *cis*-SNARE complexes (step 3), permitting neurotransmitter release. Ultimately, NSF and SNAPs mediate the disassembly of the SNARE complex, leading to vesicle recycling (step 4).
(Adapted from Südhof, 2013b).

Several other proteins actually contribute to the engine of membrane fusion, representing potential targets for the machinery manipulation. Indeed, many forms of neurodegeneration initiate presynaptically, where nerve endings release neurotransmitters thousands of times per minute. During each release event, SNARE-complex assembly and disassembly may render the terminals potentially vulnerable to activity-dependent degeneration, especially in cases of

disproportionate neurotransmitter overflow, as seen with glutamate-based *excitotoxicity* in cerebral ischemia. A deeper knowledge of the individual players belonging to the release machinery may thereby provide useful insights in the search for novel therapeutic strategies.

4.5 Syntaxin involvement in neurotransmitter vesicle release

Syntaxins are *t*-SNARE transmembrane proteins that play a central role in synaptic vesicle exocytosis.

16 members are known to characterize this protein family in mammalian cells. Among them, Syntaxins 1–4 are localized into the plasma membrane, although Syntaxin-1a and -1b are the major variants expressed in the brain.

Hereby, Syntaxin-1a is the isoform taken into consideration, due to its pivotal contribution in neurotransmitter release at presynaptic terminals (Südhof, 2004).

Different Syntaxin functional domains are known take part to different steps during calcium-triggered membrane fusion. The amino-terminal regulatory domain consists of an antiparallel three-helix bundle termed the H_{abc} domain, connected to the SNARE motif (H_3) by a flexible linker (Jahn and Fasshauer, 2012). The H_{abc} domain may fold to form a closed configuration or unfold to expose the H_3 SNARE motif for interaction during vesicle fusion, thereby regulating, as previously seen, Syntaxin pertinence to the SNARE complex nucleation (**Fig. 20**).

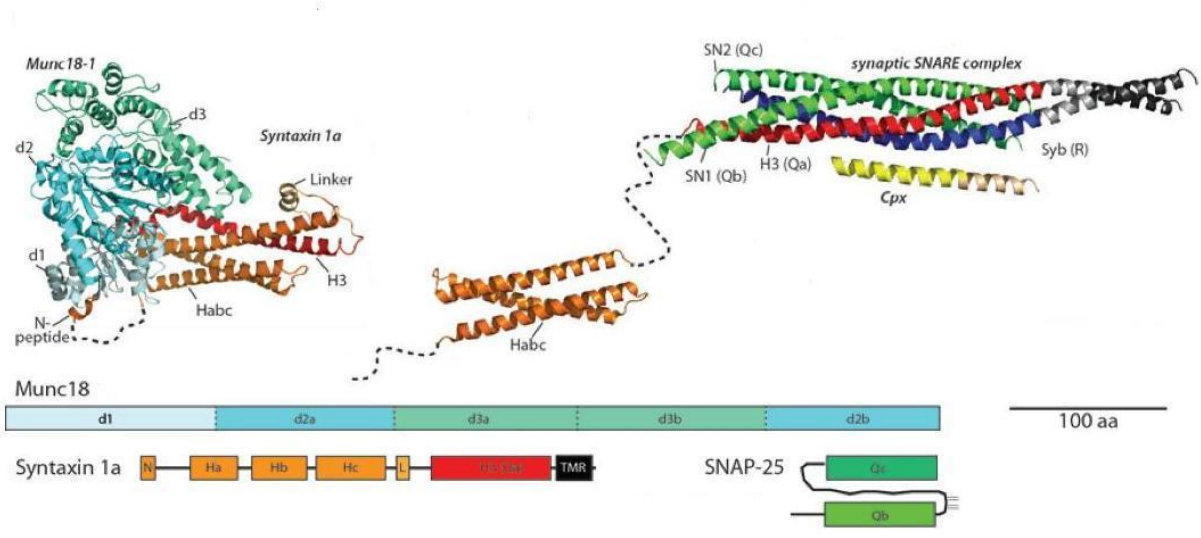

Fig. 20

Schematic representation of domain and crystal structures of core proteins of the neuronal fusion machine.

Domain structures of Syntaxin-1a, Munc18 and SNAP25 are here depicted.

The dashed lines between the *N*-peptide and H_{abc} domain represent flexible regions in Syntaxin-1a.

Syntaxin-1a is shown assembled with Mun18 (left) and in the SNARE complex (right) with SNAP25, Complexin (Cpx) and Synaptobrevin (Syb).

(Adapted from Jahn and Fasshauer, 2012).

Besides assembling with Synaptobrevin and SNAP25 for the indisputable role in synaptic transmission, Syntaxin also interacts with a number of regulatory proteins such as Munc18, Synaptotagmin, and calcium channels, providing essential additional cues to that fine-tuning of the fusion process discussed above.

In the engine of the exocytotic apparatus, it is reasonable to speculate that the phosphorylation/dephosphorylation state of synaptic proteins may be another critical mechanism accounting for the regulation of the biochemical pathways leading from vesicle docking to neurotransmitter release, in the context of either normal synaptic plasticity or possible disease conditions (Südhof, 1995). Obviously, the time course between action potential arrival at nerve terminal and the consequent vesicle fusion is roughly too short for protein phosphorylation to exert a direct and acute effect upon a single exocytotic event. Nevertheless, both protein kinases and phosphatases deserve influential roles on subsequent neurotransmitter release events.

The *N*-terminal of Syntaxin-1a contains, for instance, a highly conserved consensus site for the ubiquitous *Ser/Thr* casein kinase II (CKII). Serine 14 has been observed to be the target for *in vivo* phosphorylation (Foletti et al., 2000; Risinger and Bennett, 1999), and mutagenesis assays also proved that this residue is the sole CKII phosphorilatable site for Syntaxin-1a. Notably, this phosphorylation is rather specific for Syntaxin-1a and poorly conserved in other mammalian Syntaxin paralogs, suggesting a patterning for specific differential modulation of downstream functions.

Previous studies underlined that the amount of phospho-Syntaxin in the rat brain increases during development from 4% in embryos to 40% in adult animals, bearing a potential regulatory implication in development, in parallel with synapse development and maturation. Immunoprecipitation assays have also shown that phosphorylated Syntaxin can form complexes with SNAP25, VAMP and Synaptotagmin, although it results mostly enriched in

complexes with SNAP25 and localizes into discrete domains of the axonal plasma membrane that do not necessarily colocalize with pools of synaptic vesicles, rather defining fusion sites outside classical active zones (Foletti et al., 2000).

A more recent study pointed out the key regulatory role of phosphorylation at serine 14 for *priming*–based interaction between Syntaxin-1a and Munc18 at the plasma membrane, evidencing the utmost relevance of this phosphorylation for downstream vesicle motion and efficacy of the fusion apparatus (Rickman and Duncan, 2010).

On the other hand, the Ca^{2+}-dependent phosphorylation by DAP (death-associated protein) kinase at serine 188 in the *C*-terminal domain significantly decreases Syntaxin-1a binding to Munc18, providing and additional mechanism for the modulation of Syntaxin binding properties in response to elevated intracellular Ca^{2+} concentrations and synaptic activity (Tian et al., 2003).

4.6 Beyond molecular biology: clinical implications for Syntaxin1a

Neurotransmitter release is irreproachably recognized as the milestone for synaptic communication. Consequently, impairment engaging any of the proteins involved in any release step may lay the foundation for an array of pathologies, including neurodegenerative (Alzheimer's and Parkinson's diseases), neurodevelopmental (autism), neurovascular (migraine, ischemia) and psychiatric (schizophrenia, depression) disorders (Cao et al., 2009; Castillo et al., 2010; Corominas et al., 2009; Durdiaková et al., 2014; Nakamura et al., 2008).

Besides the well documented involvement in the SNARE complex-mediated exocytosis, Syntaxin has been found to directly impact on mental well-being, due to its variegated implication in pathways underlying functional/behavioural entailment.

Consequently, the analysis of the human genome has been prompted, looking for possible associations between Syntaxin and genetic-based disorders.

The genomic structure of *STX1A* is based on the UCSC May 2004 draft assembly of the human genome (*OMIM 186590*) (*www.genome.ucsc.edu*). The gene *STX1A* consists of 10 exons spanning a 20.42 kb region (mRNA 2064 bases) and lies at 7q11.23, a locus found to be duplicated in some individuals with autism, and associated with delayed speech and autistic behaviour (Berg et al., 2007) (**Fig. 21**).

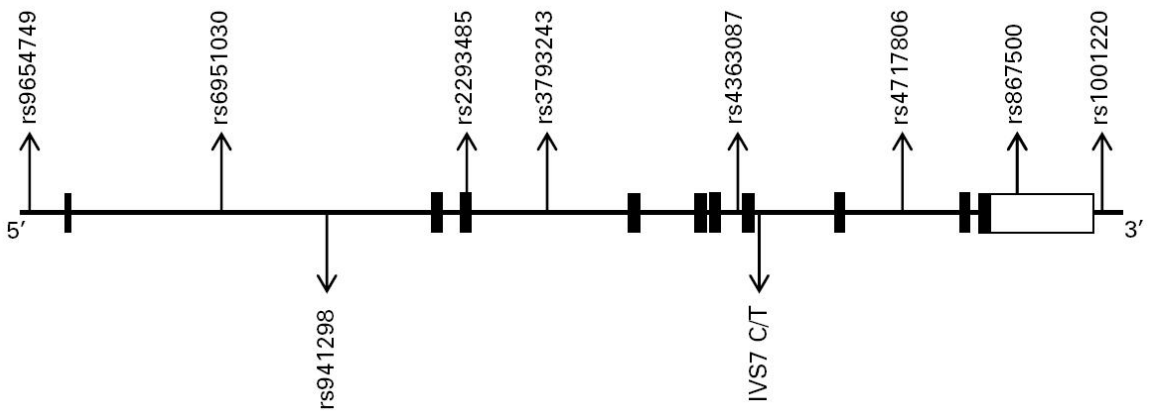

Fig. 21
Genomic structure of *STX1A* and location of SNPs.
Exons are indicated by boxes, with translated regions in closed boxes, and untranslated regions in open boxes. Introns are indicated by lines. SNP positions are denoted by arrows (from *http://www.genome.ucsc.edu*).

Overexpression of Syntaxin-1a has been indeed implicated in Asperger syndrome, a high-functioning form of autism characterized by pervasive difficulties in social interaction and impaired communication, alongside unusually narrow interests and repetitive, stereotyped behaviour, although lacking delay in language and cognitive development (Kanner, 1968; McPartland and Klin, 2006).

Abnormalities in serotoninergic neurotransmission have extensively been reported in autism (Betancur et al., 2002; McDougle et al., 2005) and, in parallel, Syntaxin regulates subcellular localization and expression of the serotonin transporter 5-HTT, which in turn modulates serotonin brain levels, particularly during neurodevelopment (Quick, 2002). Furthermore, Syntaxin-1a has been thought to interact with the glutamatergic system, via promotion of the endocytic sorting of the glutamate transporter EAAC1, leading to deregulation of glutamate transport (Yu et al., 2006), already associated with the pathophysiology of autism (McDougle et al., 2005). Finally, Syntaxin-1a is an important component of the GABAergic system, due to its involvement in the transport of glutamate and its conversion to GABA (gamma-aminobutyric acid) (Yu et al., 2006), another targeted network in autism (Coghlan et al., 2012). The rational for a potential correlation between Syntaxin and autism, as well as other neurological disorders, is thereby justified. Consistently, in transmission disequilibrium test analyses, two Single Nucleotide Polymorphisms (SNPs) for *STX1A* (*i.e. rs2293485* and

rs4717806) showed nominal association with Asperger syndrome and were therefore related to the pathogenesis of early developmental abnormalities in the Caucasian population (Nakamura et al., 2008). In a similar vein, a more recent study restricted to the Japanese population showed the nominal association of the *rs69510130* SNP with autism. In addition, authors further evidenced in *post-mortem* specimens from autistic patients compared to non-autistic controls a significantly lower Syntaxin-1a expression in the anterior cingulate gyrus, a region of the brain associated with rational function and social cognition, suggesting another hint to the possible role of Syntaxin-1a in the pathogenesis of autism (Nakamura et al., 2011).

rs941298 is another intronic SNP that showed significant association with Asperger syndrome, confirming the role of Syntaxin-1a as an important candidate gene in autism spectrum disorders (Durdiaková et al., 2014). Interestingly, it is likely that the expression of *STX1A* may be putatively regulated by these SNPs via alteration of transcription factor binding sites both directly or through other variants in high linkage disequilibrium (Durdiaková et al., 2014).

The latter polymorphisms, *rs6951030* and *rs941298*, are also susceptibility factors associated with increased risk of migraine, a common neurological disorder with a complex inheritance pattern, characterized by recurrent episodes of invalidating headache, that affects more than 15% of the European population (Corominas et al., 2009; Lemos et al., 2010; Stovner et al., 2006). Besides the presynaptic reduction of serotonin and GABA reuptake, there is some evidence suggesting that ion channel subunits might also be involved in the more common forms of migraine, and Syntaxin-1a is known to physically interacts with the α1A and α1B subunits of the voltage-dependent calcium channel, enabling the rapid glutamatergic secretory response to cortical spreading membrane depolarization, incriminated as the underlying mechanism for visual, sensory, or motor aura in migraine pathophysiology (Zamponi, 2003).

A significant genetic association has also been reported between an intron 7 SNP in the *STX1A* gene and schizophrenia, a psychiatric disorder described as a “disease of the synapse” (Mirnics et al., 2001; Wong et al., 2004). *Post-mortem* studies provided evidence for increased Syntaxin immunoreactivity in the cingulate cortex, but not in other brain regions of schizophrenic subjects when compared with controls (Gabriel et al., 1997; Honer et al., 1997). Interestingly, the altered phosphorylation of this key presynaptic protein has been related to the pathophysiology of schizophrenia. Previous studies reported a significant reduction in the levels and activity of CKII in the brain of patients with schizophrenia, with no apparent correlation with any antipsychotic drug treatment (Aksenova et al., 1991). This deficit

correlates with the 25% decrease in CKII-mediated phosphorylation of Syntaxin-1a observed in schizophrenia, and potentially affects Syntaxin-1a binding to the protein partners for the SNARE complex assembly, ultimately wrecking synaptic transmission (Castillo et al., 2010).

Given the pivotal functional role fulfilled by Syntaxin-1a at neuronal level, and moreover considering its prominent implication in neurotransmitter exocytosis, we wonder how and to what extent this protein could be involved in the presynaptic *excitotoxic* glutamate release defining neuronal cell death after ischemia, aiming at the precise molecular mechanisms governing this unknown signaling.

Evidence from previous studies in permanent focal ischemia rat models already revealed a significant acute up-regulation of Syntaxin-1a immunoreactivity, but not synaptotagmin, in the core cortex and peri-ischemic cortex at 1 day after infarction (Cao et al., 2009). Authors hypothesized a possible protective contribution of Syntaxin-1a to neuronal demise via inhibition of the *Kv2.1* potassium channel, leading to a reduced K^+ efflux-induced apoptotic death after cerebral ischemia.

However, a concretely compelling evidence for Syntaxin-1a involvement in ischemia pathogenesis would be the demonstration of a pathophysiologic mechanism in addition to the prominent association between the gene and the disease. By this approach, as science progresses in the understanding of biochemical mechanisms and potential genetic predisposition at the basis of certain illnesses, the possibility for convenient chances of therapeutic intervention, in turn, increases.

This is what our work yearns for.

AIM OF THE WORK

In the frame of the discouraging scenario concerning the clinical failure of almost every therapeutic avenue approached so far, our purpose was to provide a novel tool to be efficiently exploited in the clinical setting of the ischemic pathology.

To date, besides rt-PAs, the most promising therapeutics have pointed to the inhibition of NMDA receptors, with more or less subunits specificity, thereby directly targeting the upstream culprit in *excitotoxicity*. The major drawback undermining these disappointing attempts is the limited time to opportune intervention, as well as a plethora of unwanted side effects deriving from the multifarious involvement of the glutamatergic receptors in normal neurophysiology, together with the trivial pathological implications.

On the other hand, a new direction for therapeutic possibilities has been the pursuit of downstream signaling in order to permit delayed intervention and to dam off-target undesired outcomes.

In this context, we aimed at identifying potential yet undisclosed molecular mechanisms involved in the *excitotoxic* cascade following ischemia.

Our investigation contribution so far evidenced the role of JNK proteins also at presynaptic sites, besides their well-known role in the postsynapse. In particular, we unveiled a JNK2 specifically mediated role in NMDA-evoked glutamate release during *excitotoxic* conditions (Nisticò et al., 2015).

Considering this new subset of data deriving from our previous work, we hereby present an interesting molecular interplay between the JNK2 isoform and STX1a, a key player in the SNARE complex assembly and neurotransmitter vesicular release. We hypothesized that this interaction should support an essential role in synaptic transmission in times of excessive glutamatergic storm, given the deep involvement at presynaptic sites of these two proteins.

In order to verify and subsequently counteract the occurrence of this sordid partnership, we took advantage of bioinformatics analyses to identify the protein regions physically contacting and, on the basis of this knowledge, to design the appropriate sequence of a novel peptide able to competitively disrupt this contact. We additionally provided the peptide with the HIV-Tat portion in order to let it pass through membranes, according to our experimental objectives.

Following several experiments ranging from biochemistry to molecular biology, from electrophysiology, to *in vivo* manipulation and human genotyping, we collected a bulk of data emphasizing that:

- a physical interaction between JNK2 and STX1a does occur, and is more robust during *excitotoxicity*;
- this interaction is causally implicated in the presynaptic release of glutamate during ischemic injury and, more in general, in the context of *excitotoxicity*;
- this interaction can be itemized as novel molecular pathway to target, in order to specifically inhibit the presynaptic NMDA receptor overactivation;
- our cell-permeable Tat-linked peptide resembling the *N*-terminal portion of STX1a proved to be able to disrupt JNK2/STX1a interplay with high selectivity of action in several experimental paradigms, proving to be a suitable neuroprotective drug;
- genetic studies focusing on the SNPs of *STX1A* gene from human blood samples of stroke patients demonstrated the occurrence of a haplotype significantly associated with increased susceptibility to stroke.

Future perspectives:

Encouraged by the therapeutic neuroprotective potential of our peptide, we are currently planning further sets of experiments with the aim of deepening the findings already obtained and, at the same time, widening the translational possibilities of *JGRi1*.

On purpose, we would like to broaden the number of ischemia animal models employed for the experiments, as well as the samples genotyped from stroke patients, in order to rely on a still more consistent statistics.

We are additionally interested in evaluating our peptide efficacy upon several paradigms and time windows of reperfusion, being reperfusion injury an important issue to consider in the context of neuroprotection.

Under a more clinical perspective, behavioural tests will be also taken into consideration to assess the rescue from neurotoxicity provided by *JGRi1* concerning functional sensorimotor and cognitive outcomes. Among the most plausible, rotarod, pole, wire-hanging, corner, open field, Morris water maze and radial arm maze tests will be worth of attention.

Functional testing is indeed a crucial achievement for cutting-edge evaluation of experimental procedures in animal stroke models in that it provides an alternative analysis of the

therapeutic intervention, particularly in the direction of bridging the gap between the evaluation criteria used in animal studies with respect to human clinical trials.

The difficulty in translating preclinical findings to humans, conventionally referred to as the *translational roadblock,* still represents a major challenge in cerebrovascular research. The importance of this issue resides in the fact that many pathologies associated with *excitotoxicity* still lie under the burden of the lack of innovative medicaments to tackle brain damage.

In the context of the double-edged sword represented by glutamatergic neurotransmission, the pressing need to find new pharmacological targets to be more specifically and convincingly addresses is of utmost urgency. We are consequently moving at dissecting the role of *JGRi1* in the wide universe of the *excitotoxicity*-mediated pathologies, including traumatic brain injury, epilepsy, perinatal asphyxia, diabetic retinopathy and glaucoma.

In addition, the neurotoxicity of glutamate can also be involved, at least partially, in the pathogenesis of various late-onset and chronic diseases that are classified in the context of neurodegeneration and neuroinflammation such as Alzheimer's and Parkinson's diseases, amyotrophic lateral sclerosis, multiple sclerosis, Huntington's disease, as well as various psychiatric disturbances (*i.e.* major depressive disorder, schizophrenia, anxiety disorders), migraine, autism, chronic neuropathic pain.

By blocking the NMDA glutamate receptor, the drugs on the market today may be initially effective on one hand, but on the long-term produce side effects that may even be severe.

Our preclinical research on the intracellular partners of the NMDA receptor brought about a new druggable tool to overcome these limitations and fulfil the medical and human longing of novel specific and less toxic therapeutics.

Gazing to this overflowing medical crossroads, we wish to make clear that we are not yet holding the keystone for neuroprotection. Nevertheless, we are working hard to empower our ambitious future research with the best direction for best scientific achievements.

MATERIALS AND METHODS

Animal handling, brain tissue preparation and drug administration

Two and three months old C57BL/6 mice (Charles River Laboratories, Calco, Italy) weighting 20-25 g and pregnant Wistar rats (Charles River Laboratories, Calco, Italy) at gestational age 17-18 (E17-18) were used for the experiments, kept with standard food and water *ad libitum*, on a 12 hours light/dark cycle, under environmentally monitored conditions (room temperature set at 22 ± 1 °C; relative humidity 40 ± 5%).

Animal care procedures and testing have been disciplined by the guidelines established by the European Communities Council Directive (Directive 2010/63/EU of 22/09/2010), and accepted by the Italian Ministry of Health (D.L. 26/2014 of 04/03/2014). According to the ethical care and handling of animals, all experiments were performed in conformity with the *"International Guiding Principles for Biomedical Research involving animals"* (Council for the International Organizations of Medical Sciences, Geneva, CH) and approved by the Ethical Committee on animal experiments of EBRI (*European Brain Research Institute* - "Rita Levi-Montalcini" Foundation, Rome, Italy).

All adequate measures were taken to minimize animal suffering or discomfort, and to reduce the number of animals used to obtain statistically trustworthy results.

Mice were anesthetized with proper drugs and killed by decapitation. Brains were rapidly dissected out on ice in order to collect the tissues to use in the various experiments. All the procedures necessary to prepare the brain fractions were done at 0–4 °C.

Systemic intraperitoneal and intracerebroventricular injections were performed to administer *JGRi1* peptide variants for subsequent analysis. Surgery for transient MCAo induction was performed under 5% isoflurane anaesthesia and maintained on 1.5% isoflurane.

Synaptosomes preparation

Synaptosomes are artificial, membranous sacs of purified intact nerve endings, firstly prepared in the late 1950s by Whittaker and colleagues to define the functional components of the synapse and to study the synaptic signaling (Gray and Whittaker, 1962).

Synaptosomes are generated by the subcellular fractionation of homogenized nerve tissue and contain the complete presynaptic terminal enriched with mitochondria and synaptic vesicles,

along with a portion of the postsynaptic membrane, as observed through electron microscopy. This "pinched-off nerve endings" preparation is currently established as an amenable and elegant *in vitro* model system to analyse the molecular mechanisms that coordinate the temporal and spatial synaptic activity in the brain. Indeed synaptosomes maintain intact membrane potential and metabolic activity, contain the molecular machinery of presynaptic proteins, and, upon convenient exogenous stimulation, may release neurotransmitters including glutamate in a Ca^{2+}-dependent manner (Evans, 2015). Synaptosomes purification is additionally an essential tool to study synaptic proteomics and phospho-proteomics and to finely dissect the networks of synaptic protein–protein interactions in either normal or disease conditions (Munton et al., 2007; Wilhelm et al., 2014).

The basis of synaptosomal preparations is the starting homogenization of fresh cerebral tissue under isotonic conditions to generate shear forces that physically detach nerve terminals from the axons, but still allow the lipid bilayers to naturally reseal together in closed synaptosomes (**Fig. 22**).

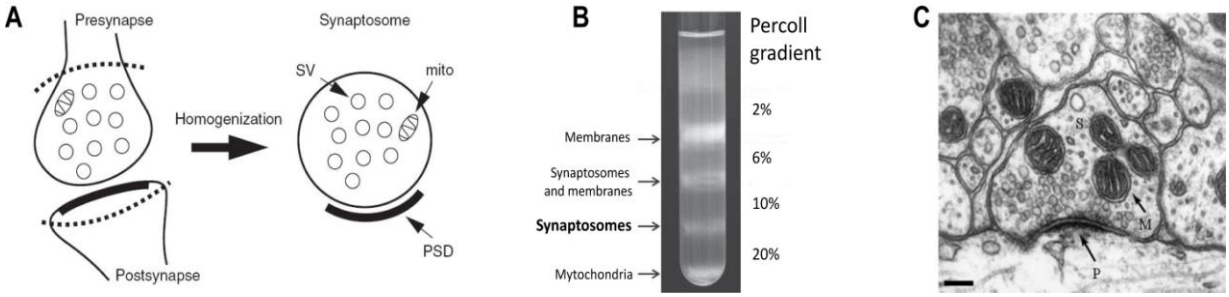

Fig. 22
Preparation and composition of synaptosomes.
A) Schematic representation of a synaptic cleft, comprehending the presynaptic nerve terminal (upper dotted line) and the attached postsynaptic density (lower dotted line) that result pinched off following homogenization of brain tissue.
B) Representation of the typical appearance of a centrifuge tube at the end of the centrifugation step of the Percoll density gradient. The synaptosomal fraction is isolated between 10 and 20% Percoll layers (see below).
C) Electron micrograph of a mouse brain synaptosome, illustrating a synaptic vesicle (S), mitochondria (M), and the postsynaptic density (P). Scale bar = 100 nm.
(Adapted from Bai and Witzmann, 2007; Dunkley et al., 2008; Evans, 2015).

The protocol used in the present work has already been described in Marcelli et al., 2016. Briefly, dissected C57BL/6 mice cortices were homogenized at 4 °C using a glass/Teflon

grinder (clearance 0.25 mm) in 10 volumes of a preservative solution containing 0.32 M sucrose, buffered to pH 7.4 with 1 mM Tris-(hydroxymethyl)-amino methane. The homogenate was centrifuged 5 min at 1000 xg to remove nuclei and cellular debris and the supernatant was gently stratified on a discontinuous Percoll gradient (Sigma-Aldrich, USA) composed of 4 layers (2, 6, 10, 20% v/v in Tris-buffered glucose), then centrifuged 5 min at 33500 xg to obtain a purer preparation (Dunkley et al., 2008; Nakamura et al., 1993). The synaptosomal fraction was isolated between 10 and 20% Percoll layers, washed by centrifugation and collected by centrifugation. The pellet was then resuspended in a physiological solution (saline buffer) pH 7.2-7.4 constituted by NaCl 140 mM, KCl 3 mM, $MgSO_4$ 1.2 mM, $CaCl_2$ 1.2 mM, $NaHPO_4$ 1.2 mM, $NaHCO_3$ 5 mM, HEPES 10 mM, glucose 10 mM and used for subsequent biochemical and confocal analyses.

Synaptosomal stimulation in biochemical studies

Stimulation of synaptosomes was performed in batch, as previously reported (Nisticò et al., 2015).

Resuspended synaptosomes were divided into 0.2 ml aliquots and gently agitated at 37 °C for 10 min to allow full restoration of the enzymatic machinery. Synaptosomal suspensions were subjected to differential stimulation with either NMDA (100 μM) + glycine (1 μM) or KCl (8 mM), respectively for 10 min or 90 seconds at 37 °C.

0.2 ml of warm saline buffer containing proteases and phosphatases inhibitors was added at the end to stop the stimulation. *JGRi1* (1 μM) was added, where needed, and left for 30 min at 37 °C before the NMDA stimulus and till the end of the experiments. The experiments were terminated by immediate centrifugation at 12000 ×*g* to pellet the synaptosomes. In NMDA stimulation experiments, external Mg^{2+} ions were omitted from the resuspension buffer to avoid the functional inactivation of the receptor.

The final pellets were lysed in ~100 μl of Lysis Buffer solution (LB) made up of 1% Triton X-100 (Serva, Germany), complete proteases inhibitor cocktail solution (Serva, Germany), phosphatases inhibitor cocktail solution (Serva, Germany) and the following components (mM): TRIS acetate, 20; sucrose, 0.27; EDTA, 1; EGTA, 1; NaF, 50; Na Orthovanadate, 1; Na Pyrophosphate, 5; Na β-glycerophosphate, 10; DTT, 1.

Protein concentration was ultimately quantified by Bradford assay and samples directly analysed by Western blot, following 5 min heating at 95 °C upon resuspension in Laemmli Sample Buffer 2x containing 10% β-mercaptoethanol.

Immunoprecipitation experiments

In order to study JNK2/STX1a interaction and *JGRi1* activity on that, cortical synaptosomes were stimulated and treated as previously described, and samples quantified for protein content via Bradford assay.

Magnetic beads (Protein G Mag Sepharose™, GE Healthcare, UK) were washed three times in Binding Buffer (Tris Base 50 mM, NaCl 150 mM) and 15 µl were added to each sample tube, composed of 350 µg of protein extract from synaptosome lysate diluted in Lysis Buffer. This pre-clearing step was performed over 30 min at 4 °C upon gentle agitation.

The supernatant was then collected by means of a rack that allows easy beads separation via magnetic holding. p-JNK antibody (1:200, rabbit Cell Signaling, USA) was added in each sample, excluding the one for the 'Input' total synaptosomes lysate and the 'Beads' alone, before leaving them at 4 °C overnight.

The day after, 25 µl of freshly washed beads were added to each sample and left for 3 h at 4 °C in mild agitation. After the indicated time, the supernatant was removed and the beads were washed four times in Binding Buffer enriched with phosphatases and proteases inhibitors (Serva, Germany). The immunoprecipitated complexes were resuspended in Sample Buffer 1x, incubated 30 min at 50 °C and loaded on gels for immunoblot analysis.

Western Blot

10% SDS polyacrylamide gels were used to resolve 15 µg of proteins (equal amount in each condition) and then blotted onto PVDF membranes (Amersham Hybond 0.2 µm; GE Healthcare, UK) previously activated in methanol. The resulting membranes were incubated 1 h at room temperature in blocking buffer (5% skim milk diluted in tween-Tris-buffered saline (t-TBS) (M) Tris, 0.02; NaCl, 0.15; Tween 20, 0.1%). After several washes in t-TBS, membranes were incubated overnight at 4 °C with specific primary antibodies: rabbit anti STX1a 1:1000 (Synaptic System, Germany), rabbit anti p-STX1a 1:1000 (AbCam, USA), rabbit anti JNK 1:1000 (Cell Signaling, USA), rabbit anti p-JNK 1:1000 (Cell Signaling, USA), rabbit anti JNK2 1:1000 (AbCam, USA), mouse anti SNAP25 1:1000 (BioLegend, USA), rabbit anti Munc18 1:1000 (Cell Signaling, USA), mouse anti Actin 1:1000 (Sigma-Aldrich, USA), and mouse anti HA 1:1000 (Sigma-Aldrich, USA).

Membranes were washed for 50 min in t-TBS before incubation with peroxidase-conjugated goat anti-rabbit or anti-mouse IgG secondary antibodies (UCS Diagnostic) 1:3000 for 1 h at room temperature. Several washes with t-TBS for 50 min were performed again before the

membranes were exposed to chemiluminescence reagents (ECL; WESTAR, Cyanagen, Italy) and the resulting signals acquired on blue X-Ray films (Aurogene, Italy).

Bioinformatics analysis and computational details

Coordinates and structures for JNK2 and the *N*-terminal domain of Syntaxin-1a were obtained from Protein Data Bank (PDB) with ID(s) accession number respectively 3NPC (Kuglstatter et al., 2010) and 1BR0 (Fernandez et al., 1998). Docking simulations were performed using the *Rosetta 3.4* software (Sircar et al., 2010), allowing backbone movements and side-chain optimization. One hundred thousand docking decoys were generated and ranked according to the total score, taking into account the contributions from Van der Waals interactions, solvation, hydrogen bonds, electrostatic interactions, probability of side-chain rotamers, and interface score (*i.e.* the difference between the total score of the complex and the total score of isolated protomers). Three top structures were selected according to higher scores and considered for further analysis. Buried surface area upon complex formation for each structure has been evaluated with *NACCESS* (*NACCESS* Computer Program http://www.bioinf.manchester.ac.uk/naccess), a stand-alone program that calculates the atomic and residue accessibility area for proteins in PDB format file.

Multiple sequence alignment for JNK1, JNK2 and JNK3 was virtually performed with *Clustal Omega* (Sievers et al., 2011) using default options. Buried surface and sequence alignment data outlined that one among the selected structures exhibited peculiar features, making it the most plausible for protein-protein interaction.

Indeed, although the three JNK isoforms on their whole display high sequence identity, the sole JNK2 domain binding to Syntaxin-1a showed a unique distinctiveness with respect to analogue domains in JNK1 and JNK3, also accompanied by the highest buried surface upon complex formation. The good shape complementarity between the two binding partners sustained the hypothesis of a possible interaction linking JNK2/STX1a.

***JGRi1* peptides synthesis**

In order to selectively disrupt the possible JNK2/STX1a interaction, *JGRi1*, a novel cell permeable peptide, has been designed and synthetized on the basis of the above presented computational data.

Therapeutic approaches involving the administration of proteins as druggable agents is actually gaining increasing momentum for the management of disorders ranging from single

enzyme deficiencies to cancer. In this frame, protein transduction via peptides able to ubiquitously cross both cellular membranes and BBB launched a novel field in molecular delivery based on non-invasive small vectors generally referred to as *cell-penetrating peptides* (CPPs) (Dinca et al., 2016; Guidotti et al., 2017).

Over the past twenty years, CPPs showed to efficiently transport various biologically active cargoes with valuable results in both *in vitro* and *in vivo* experimental systems, being therefore established as feasible and promising devices for medical and biotechnological drug development (Bechara and Sagan, 2013; Dinca et al., 2016) (**Fig. 23**).

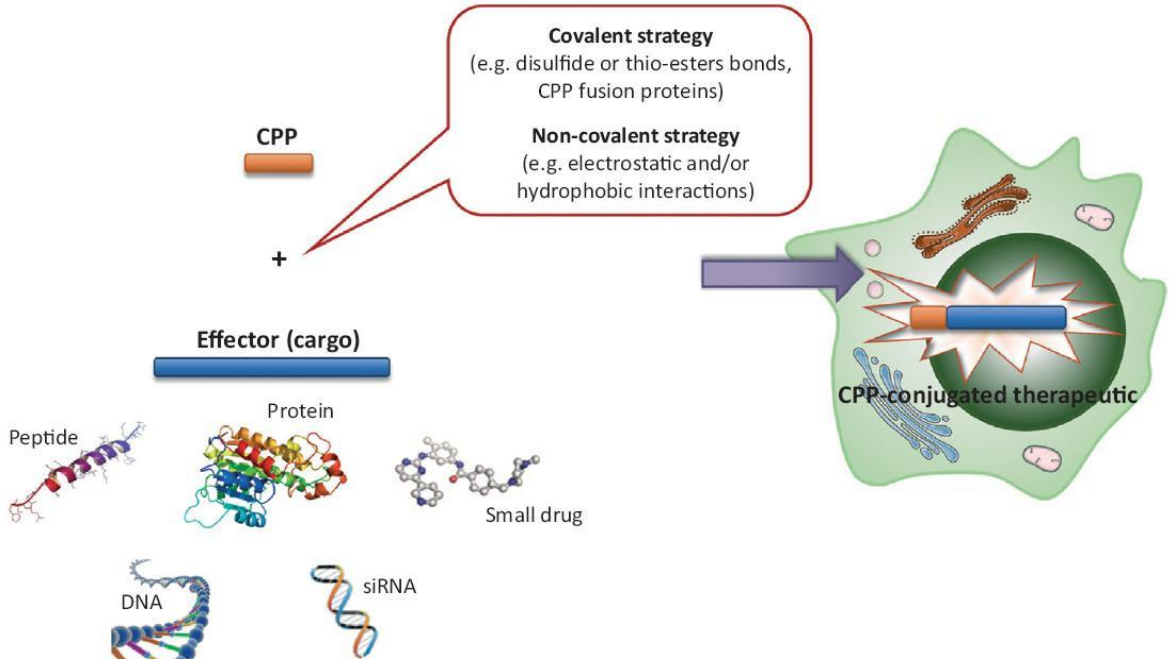

Fig. 23
Schematic representation of Cell-Penetrating Peptide (CPP)-based technologies.
Due to their hydrophilic nature, cargoes (blue) including peptides, proteins, nucleic acids, or small drugs cannot generally be uptaken by the cell to reach eventual intracellular targets. Conjugation to a CPP (orange) by covalent bond or non-covalent complex formation enables the CPP–effector conjugate to cross the cell membrane and reach the intracellular milieu, providing an enhancement of the therapeutic effectiveness.
(Adapted from Guidotti et al., 2017).

The first CPP discovered serendipitously in the late 1980s is the *trans-activator of transcription protein* (Tat), belonging to the human immunodeficiency virus (HIV) (Green et al., 1989).

Tat sequence generally consists of a basic domain coding region of 9-11 amino acids from residue 48 to 56 within the first exon (Choi et al., 2002). The variants mostly used are the cationic Tat_{48-60} (sequence: GRKKRRQRRRPPQ) and the Tat_{49-57} (sequence: RKKRRQRRR).

Several others CPPs have been lately identified, like the Antennapedia homeodomain from *Drosophila melanogaster*, providing new appeal in the cellular uptake of exogenously delivered active conjugates, including proteins as large as 110 kDa that would have been otherwise hampered without cellular entry.

To date, no CPP-tagged protein has yet succeeded in clinical trials. Nevertheless, several evidences are underlining the extensive use of CPPs in experimental diseases. In a recent work, for instance, delivery via the Tat-linked $A\beta 1\text{-}6_{A2V}(D)$ was able to confer neuroprotection against both *in vitro* and *in vivo* TgCNRD8 Alzheimer disease synaptopathy models, suggesting that the abovementioned CPP-conjugated peptide can cross the BBB, penetrate the brain parenchyma, and finally reach its therapeutic target (Cimini et al., 2016). Data from another group also reported the impact of *D-JNKI1*, a CPP acting as JNK inhibitor in MCAo animal models. This Tat-linked peptide has emerged as a potent *in vivo* neuroprotectant, with a remarkably long therapeutic window and a strong effect on both functional outcome and ischemic lesion size (Borsello et al., 2003a).

In a parallel vein, we have produced our 26 amino acids long *JGRi1*, composed by 12 amino residues (*GRKKRRQRRRPP*) belonging to the HIV-1 Tat_{48-59} protein in order to provide cell permeability (Chauhan et al., 2007). This arginine rich domain has been covalently linked to the effector sequence (*IEQSIEQEEGLNRS*) able to competitively induce JNK2/STX1a unbinding.

The exact sequence was assessed by HPLC chromatographic analysis.

For peptide synthesis, pre-loaded Wang resin, Fmoc-protected amino acids, 2-(1*H*-benzotriazol-1-yl)-1,1,3,3-tetramethyluronium hexafluorophosphate (HBTU), 1-hydroxybenzotriazole (HOBt) and Diisopropylethylamine (DIEA) were purchased from Iris Biotech Gmbh (Germany). Solvents, piperidine and other reagents were purchased from Sigma-Aldrich (USA). All peptides were synthesized using a CEM Liberty peptide synthesizer and purified using RP-HPLC with a Jasco BS-997-01 instrument and a DENALI C-18 column from GRACE VYDAC (10 μm, 250 × 22 mm). ESI mass spectra were recorded on an LCQ Advantage spectrometer from Thermo Finnigan.

Overall, several structures of the peptide have been synthetized for the experimental purposes of the present work, including full-length effector and scrambled *JGRi1* sequences, a Tat-*JGRi1*-FITC peptide (able to penetrate through membranes) and a ΔTat-*JGRi1*-FITC form (unable to penetrate through membranes due to the lack of Tat). In particular, the FITC peptides have been covalently coupled to a fluorophore that enables the indirect detection through the fluorescein fluorescent label. Due to the fact that, in general, fluorimetry detection does not allow defining if the peptide is still linked to the fluorescent probe once inside cells, we designed the peptide in the sequence Tat-cargo-FITC, so that the fluorescence detection should represent only internalized integral entities.

- *Solid phase peptide synthesis:*

JGRi1 peptides were prepared by microwave-assisted solid phase synthesis (Pellegrino et al., 2012), based on 9-Fluorenylmethyloxycarbonyl (Fmoc) chemistry on pre-loaded Wang resin (0.4 meq/g substitution), choosing a five-fold molar excess of 0.2 M Fmoc-protected amino acids dissolved in *N*-methyl pyrrolidinone, and using HOBt/HBTU/DIEA (5 : 5 : 10 eq) as activators. Coupling reactions were performed for 5 min at 40 W with a maximum temperature of 75 °C. Deprotection was performed in two stages using 20% piperidine in dimethylformamide (5 and 10 min each).

Cleavage from the resin was performed using 10 ml of Reagent K (trifluoroacetic acid/phenol/water/thioanisole/ 1,2-ethanedithiol; 82.5 : 5 : 5 : 5 : 2.5) for 180 min. Following cleavage, labeled peptides were precipitated and washed using ice-cold anhydrous ethyl ether. The peptides were therefore purified by RP-HPLC (Reversed phase High-performance liquid chromatography) using a gradient elution of 5–70% solvent A-B (solvent A: water/acetonitrile/trifluoroacetic acid 95 : 5 : 0.1; solvent B: water/acetonitrile/trifluoroacetic acid 5 : 95 : 0.1) over 20 min at a flow rate of 20 ml/min. The purified peptide was freeze-dried and stored at 0 °C.

- *N-terminal labeling with FITC:*

FITC (Fluorescein isothiocyanate) labeling at the *N*-terminal of *JGRi1* was performed on resin, before the cleavage, using 10 eq of 5(6)-carboxyfluorescein and HOBt/DIC (10 eq) as activators. The coupling reaction was performed twice for 1 h each, in the dark under vigorous shaking. 20% piperidine in dimethylformamide was then added and the mixture was shaken for 1 h.

- *C-terminal labeling with FITC:*

C-terminal labeling of *JGRi1* was done by addition of an orthogonal protected lysine residue at the *C*-terminal of the peptide sequence. The peptide was synthesized as above described. Lysine side chain deprotection was performed on resin. FITC was linked to the side chain lysine amino group as described for the *N*-terminal.

HEK-293 cell cultures and transfection

Human embryonic kidney cells (HEK) -293 were seeded into 6-well plates with a density of 4×10^5 the day before treatments and maintained in complete medium with the following composition: DMEM (LONZA Group LTD, Switzerland) 4.5 g/l glucose, 10% fetal bovine serum (LONZA Group LTD, Switzerland), 1% L-glutamine (Gibco, Invitrogen, USA), 1% penicillin/streptomycin antibiotics (Gibco, Invitrogen, USA), 1% MEM non-essential amino acids solution 100× (Sigma-Aldrich, USA). Cells were incubated at 37 °C under 5% CO_2.
Transfections were performed in serum-free culture medium using 2 µl/sample Lipofectamine® 2000 (Invitrogen, USA) as transfection reagent. Cells were co-transfected with 1 µg/sample of full length non-tagged STX1a plasmid (pCMV5 backbone) and one of the following plasmid DNAs: HA-JNK1, HA-JNK2, or HA-JNK3. Incubation with exogenous DNAs was maintained over 3 h, then the medium was replaced with fresh complete DMEM, and cells incubated overnight to let DNAs to be expressed. The following day, treatment with *JGRi1* (40 µM) was performed during 1 h 30 min. Cells were then scraped in Lysis Buffer solution, harvested in test tubes, sonicated and quantified via Bradford assay. 350 µg of protein extract from each sample was immunoprecipitated for anti-HA (mouse 1:1000; Sigma-Aldrich, USA), following the protocol previously reported.

SNARE complex assay

The SNARE complex is a detergent resistant clustering that can be analysed by Western blotting on unboiled non-denatured samples (Burré et al., 2010). The modulation of the complex assembly upon NMDA (100 µM) + glycine (1 µM) or *JGRi1* (1 µM) stimulation has been tested on cortical synaptosomes and evaluated via Western blotting, comparing unboiled with boiled (5 min, 95 °C) samples. The immunoreactive bands identified by anti STX1a primary antibody (1:1000; Synaptic System, Germany) at approximately 50–100 kDa were quantified as an indicator of the SNARE complex assembly upon treatment. The band at 33 kDa indicates instead free unassembled STX1a.

Measurements of synaptic release

Synaptogreen (Sigma-Aldrich, USA), also known as FM1-43, is a green fluorescent dye widely used to track synaptic release activity by synaptic vesicles staining. Due to the two peculiar cationic charges located in their headgroup, the styryl dye molecules are able to partition into the outer leaflet of surface membranes without permeating. Upon a proper stimulus, FM1-43 molecules are internalized so that newly formed synaptic vesicles become stained with the dye. By evoking exocytosis, FM1-43 molecules ultimately dissociate from the membranes and lose fluorescence following the concentration gradient, with the destaining being directly proportional to the exocytosis rate (Amaral et al., 2011).

We used here a protocol already reported in Marcelli et al., 2016.

Cortical synaptosomes (0.3 mg/ml) obtained from mice following 2 or 24 h *JGRi1* (20 mg/kg) intraperitoneal (Ip) injection were incubated in 2 ml of Saline Buffer for 2 min at 37 °C in mild agitation. Synaptogreen (50 μM) was added 1 min after stimulation with NMDA (100 μM) and glycine (1 μM) to load the fluorescent dye. After 3 min of stimulation, synaptosomes were washed twice to remove non-internalized Synaptogreen in a Saline Buffer containing BSA 1 mg/ml. Synaptosomes (200 μg of proteins) were then seeded on poly-L-lysine (50 ug/ml) treated coverslips and let sediment over 40 min in the dark. Two washes were then performed to remove not seeded synaptosomes. The coverslips were placed on a time-lapse system mounted on an inverted fluorescence microscope (TiE; Nikon, Japan), equipped with an incubation chamber (Okolab), a cooled CCD camera (Clara; Andor), Perfect Focus System to avoid z-axis focus fluctuations and a Niss Elements imaging software (Nikon). Video recordings were performed with a 40× oil objective (N.A 1.4) for 6 min (upon 30 mM KCl stimulation) or 30 min (upon NMDA 100 μM + glycine 1 μM stimulation), by taking 14 bit images every 2 s at room temperature (25 °C). Fluorescence was recorded and video images were analysed by using the Spot module of the Imaris® Suite 7.6 software (Bitplane A.G., Zurich, Switzerland) by selecting a 1.5 μm radius diameter of fluorescent puncta. Fluorescence intensity was measured in 15–20 randomly selected synaptosomes within the microscopic field. The criteria for fluorescence *puncta* inclusion in the data analysis were the spherical shape ranging between 0.5-1.5 μm and the stimulation-dependent destaining response. Destaining time-courses were generated by normalization of each fluorescence spot trace. Quantification of FM1-43 responses was accomplished by calculating the average percentage of fluorescence loss. A group of control experiments was run to test the specificity of Synaptogreen loading and destaining. Ca^{2+} free medium drastically reduced the dye loading

and inhibited the stimulus-induced dye release. The Synaptogreen photobleaching rate was also measured in absence of the stimulus and compared to the stimulated Synaptogreen destaining traces for each experimental group.

Glutamate release experiments

Release experiments were performed on synaptosomes in a superfusion system (Pittaluga et al., 2006) where each event affecting glutamate release is attributable only to the functional presynaptic compartment.

Cortical synaptosomes were incubated for 45 min at 37 °C in a rotary water bath in the presence of the radioactive tracer [^{3}H]D-aspartate ([^{3}H]D-Asp, final concentration 50 nM). *JGRi1* was added at different concentrations (2, 5, 10 μM) in the incubation medium for 30 min. After the labeling period, synaptosomes were maintained and superfused with physiological solution at 37 °C, layered in the superfusion system (Ugo Basile, Comerio, Varese, Italy) for 48 min. After 36 min of re-equilibration period, four consecutive 3 min fractions (termed b1 to b4) were collected. *N*-methyl-D-aspartic acid (NMDA) (100 μM) plus glycine (1 μM), or (*S*)-α-Amino-3-hydroxy-5-methyl-4-isoxazolepropionic acid (AMPA) (50 μM) were applied at the end of the first fraction collected (b1) and maintained in the superfusion medium till the end of the superfusion period. In NMDA experiments the medium was replaced, at t= 20 min, with a Mg^{2+} ion-free solution to permit NMDAR activation.

In KCl experiments synaptosomes were transiently (90 s) exposed, at t= 39 min, to high K^+ containing medium (8 mM). In these experiments, fractions were collected according to the following scheme: two 3 min fractions (basal release), one before (t= 36–39 min) and one after (t= 45–48 min) the 6 min fraction stimulation (t= 39–45 min; evoked release). Fractions collected and superfused synaptosomes were counted for radioactivity. The amount of radioactivity released by each superfusate fraction was expressed as a percentage on the total synaptosomal tritium content at the start of the fraction collected (fractional efflux). Agonists and K^+-induced effects were estimated by subtracting the neurotransmitter content into the fractions corresponding to the basal release from those corresponding to the evoked release.

Electrophysiology

The effect of *JGRi1* on NMDA receptor-dependent presynaptic glutamate release was evaluated by measuring miniature Excitatory Postsynaptic Currents (mEPSCs), according to a protocol previously described (Nisticò et al., 2015).

mEPSCs are small currents deriving from the vesicular release of neurotransmitter that represents the presynaptic terminal activity reaching the patched postsynaptic neuron. The higher the frequency of mEPSCs, the stronger the connectivity of the cell tested. Conversely, mEPSCs amplitude relies on the amount of neurotransmitter filling the vesicles.

For the experiments, two months old C57BL/6 mice were anesthetized with halothane and killed by decapitation. The brain was rapidly removed from the skull and combined entorhinal-hippocampal slices were cut (250 μm) using a vibratome (Leica) in cold artificial cerebrospinal fluid (aCSF) consisting of (mM) NaCl, 124; KCl, 3.0; $MgCl_2$, 1.0; $CaCl_2$, 2.0; NaH_2PO_4, 1.25; $NaHCO_3$, 26; glucose, 10, saturated with 95% O_2 and 5% CO_2 (pH 7.4) (Jones and Heinemann, 1988; Nisticò et al., 2015).

After an incubation period of 1 h in saturated aCSF at 33.5 °C, slices were maintained at room temperature or transferred to a submerged recording chamber (2.5–3 ml min^{-1}, 33.5 °C) on the stage of an upright microscope (Eclipse FN1, Nikon, Italy), equipped for infrared video microscopy (Hamamatsu, Japan).

Layer II neurons of the entorhinal cortex were recorded in whole-cell patch-clamp configuration using 1.5 mm borosilicate glass electrodes (3–4 mOhm) pulled with a vertical puller (PP-83 Narishige, Japan) in voltage-clamp mode, filled with (mM) $CsMeSO_4$, 130; HEPES, 5; EGTA, 0.5; $MgCl_2$, 1; NaCl, 1; $CaCl_2$, 0.34; QX-314, 5 and MK-801, 1; adjusted to pH 7.3 with CsOH. QX-314 is a Na^+ channel blocker used to block action potentials in the patched neurons, whereas the antagonist MK-801 was used to prevent NMDAR activation.

Neurons were held in hyperpolarized voltage-clamp conditions, at -70 mV. Current signals were filtered at 2 kHz and digitized at 10 kHz using a Multiclamp 700 B differential amplifier linked to a Digidata 1440A, operated by the pClamp10 software (Molecular Devices, USA).

No series resistance compensation was implemented, in order to keep a low signal-to-noise ratio, however, series resistance and whole-cell capacitance were monitored continuously during the experiment and recordings were discarded if series resistance changed by more than 15% from control conditions. Spontaneous synaptic events were analysed offline using the pClamp10 software package (Molecular Devices, USA). The spontaneous events were detected from 3 min trace records, through an algorithm based on the minimization of the sum of squared errors between data and a template function. Single template waveforms were created by averaging a number of spontaneous events following a visual inspection of a representative trace in each cell. The template-matching threshold was set between 5 and 5.5, providing a good balance to avoid detection of false events.

Rat neuronal cultures and assessment of cell viability

Cortical primary neurons were obtained from E17-18 rat embryos, dissociated in trypsin, and seeded into 24-well poly-L-lysine-coated plates with a density of 1.5×10^6. Neurons were maintained in complete medium containing Neurobasal (Gibco, Invitrogen, USA), 2% B-27 supplement (Gibco, Invitrogen, USA), 1% penicillin/streptomycin antibiotics (Gibco, Invitrogen, USA), incubated at 37 °C under 5% CO_2 and maintained for ten days before further use.

NMDA stimulus (100 µM) was applied over 3 h, preceded, where needed, by 1 h pretreatment with *JGRi1* at increasing concentrations (0.1, 0.5 and 1 µM). Cellular viability was assessed following 24 h from drugs administration, by counting the number of intact nuclei upon neuronal lysis in a detergent-containing solution (Esposito et al., 2012). The culture medium was removed and replaced over 2 min with 0.5 ml of a lysing solution (0.5% ethylhexadecyldimethylammonium bromide, 0.28% acetic acid, 0.5% Triton X-100, 3 mM NaCl, 2 mM $MgCl_2$ in PBS pH 7.4 diluted 1/10). The resulting uniform suspension of single, intact, viable cells was then collected and nuclei counted and quantified in a hemocytometer. Nuclei from viable cells appeared as phase-bright intact circles surrounded by a dark ring. Broken or damaged nuclei could not be included in the count since the detergent solution selectively dissolves nuclei of broken or dying cells (Pieri et al., 2010).

Confocal images

Among *JGRi1* peptide variants, one was designed and synthetized to contain a FITC tag, *i.e.* a green fluorescent dye with excitation wavelength at 495 nm and emission wavelength at 519 nm. Contextually, it was possible to evaluate whether and to what extent the FITC-peptides could reach brain regions driven by their HIV-Tat domain, without requirement of any antibody.

Mice treated with Ip and ICV injection were sacrificed after 1, 3, 6, 24 h and cortex slices were analysed.

ICV injections were performed at hippocampal level; the site of infusion was located 1 mm mediolateral, 0.2 mm anteroposterior and 2 mm dorsoventral with respect to the Bregma.

Animals were deeply anesthetized with tribromoethanol (Avertin®) and perfused through the aorta with ice-cold 4% paraformaldehyde. Brains were post-fixed for at least 4 h at 4 °C and equilibrated with 30% sucrose overnight. 30 µm thick sections were permeabilized in PBS

with Triton-X 0.25% (t-PBS) and preincubated with 10% normal donkey serum solution for 1 h at room temperature containing DAPI 0.01 mg/ml.

Sections were mounted with Vectashield (Vector Labs, USA) on poly-L-lysine coated slides, air-dried and coverslipped.

Slides were examined under a confocal laser scanning microscope (Leica SP5, Leica Microsystems, Wetzlar, Germany) equipped with 4 laser lines and a transmitted light detector for differential interference contrast (DIC; Nomarski) imaging. Confocal acquisition setting was kept identical among the slides and throughout the whole acquisition.

Organotypic slice preparation and oxygen/glucose deprivation

Brain slice models are an *ex vivo* system that extensively replicates several aspects of the *in vivo* biology, offering unique advantages over *in vitro* platforms. Slices indeed preserve brain tissue architecture and functional local synaptic circuitry, additionally providing surrogate screening systems for pharmacological agents, without recourse to whole animal studies (Cho et al., 2007).

Oxygen/glucose deprivation (OGD) is a simple yet highly useful technique chiefly validated as an *in vitro* model for ischemia. By mimicking the key pathophysiological events occurring in *in vivo* stroke (Cimarosti and Henley, 2008; Dennis et al., 2011), OGD provides a chance to dissect those cellular and molecular pathways, besides offering a useful setting for development and testing of novel neuroprotective strategies, as is the case.

OGD can be experimentally obtained by exposing brain slices to simultaneous anoxic and aglycemic conditions (Cimarosti et al., 2001; Frantseva et al., 1999) in order to recapitulate the interruption of oxygen and nutrients supply to cerebral parenchyma, as well as the stroke-like energy failure. Importantly, the insult achieved via OGD proved to be consistent and largely reproducible to be so far the most widely used method to simulate the *in vivo* injury.

For our experimental purposes, acute cortical slices were obtained from 3 months old C57BL/6 mice, killed by decapitation under anaesthesia with halothane. The brains were rapidly removed and placed in an ice-cold, oxygenated (95% O_2 and 5% CO_2) artificial cerebral spinal fluid (aCSF) composed by (mM): NaCl, 126; KCl, 2.5; $MgCl_2$, 1.2; $CaCl_2$, 2.4; NaH_2PO_4, 1.2; $NaHCO_3$, 24; glucose, 10 (pH 7.4). Coronal slices (300 µm thickness) were cut in the same conditions using a vibratome (Leica). Cortices were microdissected (~2 mm from bregma) and then kept in oxygenated aCSF for 1 h at room temperature to restore synaptic circuitry.

In vitro oxygen/glucose deprivation (OGD) was obtained by switching the slices into a hypoglycemic solution obtained by omitting glucose from standard aCSF, bubbled with nitrogen (95% N_2 and 5% CO_2) for 15 min at room temperature (Nisticò et al., 2008). For slice treatment, *JGRi1* (10 µM) was added in the incubation plate 1 h before the OGD and maintained until the end of the experiment. At the end of the ischemic induction, the slices were not reperfused but immediately collected in Lysis buffer solution, and homogenized at 4 °C using a glass/Teflon grinder. The protein fraction was obtained upon centrifugation and quantified by Bradford assay. Samples were directly analysed by Western blot, or used for immunoprecipitation, as explained above.

Transient MCAo induction and ischemic damage evaluation

Since its inception in the late 1980s, MCA occlusion (MCAo) by means of the intraluminal filament has become an established, quite simple and relatively non-invasive technique to produce either permanent or transient ischemic animal models.

Proximal focal vessel closure is generally obtained by inserting a 4-0 nylon surgical suture with an acryl-thickened tip into the internal carotid artery of murine models, and advancing orthogradely toward the cranium to occlude both the MCA and the collateral circulation from the anterior communicating arteries. In this way, cerebral blood flow may be reduced up to 80% in the cortex, as confirmed by Laser-Doppler flowmetry (Ansari et al., 2011; Engel et al., 2011). In this way it is possible to closely simulate the real *in vivo* infarction occurrence, also thanks to the fact that most thromboembolic events in humans occur in the territory of the MCA.

Reperfusion may easily follow by thread withdrawal after a specified period of time (generally 30 to 90 min for transient models), permitting animal survival and enabling further functional outcome measurements (Traystman, 2003) (**Fig. 24**).

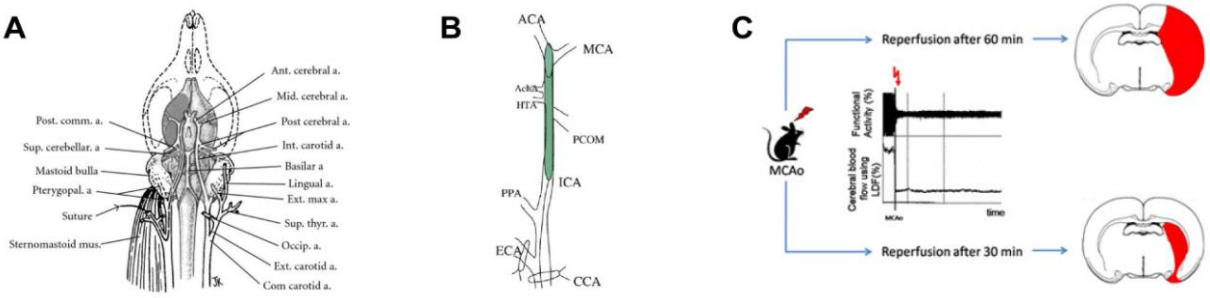

Fig. 24
Middle cerebral artery occlusion in animal models.
A) Vascular brain anatomy of the rat.
B) Induction of middle cerebral artery occlusion (MCAo) by insertion of a filament into the common carotid artery, as reported in Koizumi's method. (ACA = anterior carotid artery; AchA = anterior choroidal artery; CCA = common carotid artery; ECA = external carotid artery; ICA = internal carotid artery; HTA = hypothalamic artery; PPA = pterygopalatine artery; PCOM = posterior communicating artery).
C) Schematic illustration of typical cerebral lesion and relative size insult following different time points of reperfusion in the proximal MCAo mouse model. The graph in the middle illustrates a representing time-course of functional activity and cerebral blood flow after MCAo (LDF = Laser-Doppler flowmetry).
(Adapted from Canazza et al., 2014; Engel et al., 2011).

Avoiding craniectomy is a great advantage of this technique that eliminates possible influences of surgical manipulation on blood brain barrier permeability and intracranial pressure. On the other hand, many other factors can lead to inconsistency in this model, including strain-related differences, housing conditions, size of suture tip, duration of occlusion, body temperature, anaesthesia (Ansari et al., 2011).

For the sake of our experimental protocol, C57BL/6 mice were anesthetized with 5% isoflurane and maintained on 1.5% isoflurane in 70% nitrous oxide and 30% oxygen. Regional cerebral blood flow was measured by Laser-Doppler flowmetry (PF2B; Perimed, Stockholm, Sweden), using a flexible skull probe. In randomly selected animals, the left femoral artery was cannulated with a PE-10 polyethylene tube for blood gas determination and arterial blood pressure measurement. Rectal temperature was maintained between 36.5 and 37.5 °C with a homeothermic blanket (Frederick Haer and Co., Brunswick, Maine, USA). Mice were randomized and Middle Cerebral Artery (MCA) was occluded proximally for 1 h using the classical intraluminal filament technique (Muzzi et al., 2012).

JGRi1 was injected intracerebroventricularly (ICV) at the dose of 16ng/5µl 30 min before artery occlusion, to determine eventual prophylactic therapeutic efficacy. Animals were sacrificed after 24 h of MCA reperfusion and the brains snap frozen in N_2 vapour for cryostat sectioning. Infarction areas were quantified by a blind evaluator by means of MCID M4 image analysis software (Imaging Research Inc., St. Catharine's, Ontario, Canada) on toluidine blue stained sections. In order to account for and eliminate swelling/edema alterations, infarction volume was calculated using an indirect measurement, summing the area of each section using the following formula: Corrected Infarct Volume (CIV) = contralateral hemisphere volume (mm^3) – undamaged ipsilateral hemisphere volume (mm^3).

Human experiments: patients and controls

Eight patients (5 females and 3 males, mean age 69.66 years; SD= 12.71 years) from the Department of NeuroRehabilitation at "*Casa di Cura Privata del Policlinico*" (Milan, Italy) were included in this study in order to take part to the Biobank project, after subscribing a written consent approved by the Ethic Committee.

All patients are Caucasian with a clinical diagnosis of Acute Ischemic Stroke (AIS), previously tested for neurological scales, including the National Institute of Health and Stroke scale (NIHSS), Mini-Mental State Examination (MMSE), Cumulative Illness Rating Scale (CIRS) and Barthel Index (BI). The only inclusion criterion was a CIRS severity index < 2.

In addition, seventeen Caucasian healthy controls (HC) (10 females and 7 males, mean age 69.66 years; SD= 7.67 years) age- and gender-matched with patients, were enrolled in this study. Notably, also their cognitive status was assessed by MMSE.

SNP typing on human blood samples

Human blood samples of a group of stroke patients were analysed in a pilot study in order to assess the eventual implications of *STX1A* SNPs on ischemia susceptibility.

Due to the reliable correlation with the functions of central nervous system, lymphocytes are considered as convenient neural probes and easily accessible alternative to brain samples for biochemical and genetic investigations (Gladkevich et al., 2004). Genomic DNA was therefore isolated from peripheral blood lymphocytes of patients and healthy controls using Chemagic blood 10k (Perkin-Elmer, GmbH) following the manufacturer instructions.

SNPs *rs4717806* and *rs6951030* respectively located in intron 9 and intron 2 of *STX1A*, and SNP *rs2293489* located in *WBSCR22* gene, ~6 kbp upstream to 5' UTR *STX1A* gene (**Fig. 40A**) were typed using the Taqman SNP Genotyping Assays (Applied Biosystems Inc., CA, USA) on Bio-Rad CFX96™ Real-Time PCR system.

For *rs2293489*, *rs4717806* and *rs6951030* respectively the C__15971044_10, C__27872627_10 and C__29194787_10 Human Pre-Designed Assays (Applied Biosystems) were used.

Statistical Analysis

- *Biochemical and animal experiments:*

ANOVA was used to carry out variance analysis together with Newman-Keuls multiple-comparison test in the experiments for neurotransmitter release. A Student's two-tailed *t*-test

was chosen when it was about to compare a single treatment group. A value of *$p < 0.05$ was the minimum accounted to validate our data. Appropriate controls were always run in parallel with enzyme inhibitors. GraphPad PRISM 4 (GraphPad software, USA) was used to analyse all biochemical experiments. Values shown represent the mean ± SEM of a different number of separated experiments (as indicated in figure legends). In case of intergroup comparisons, one-way or two-ways ANOVA were used, followed by Newman-Keuls test.

- *Human experiments:*

Chi-squared (χ^2) analysis was used to exclude any deviation of SNPs genotype distribution from Hardy-Weinberg equilibrium (HWE); p value was > 0.05 both in cases and in controls. χ^2 statistics or Pearson's exact test, appropriately needed, were applied to 2XN table to compare case-control differences of SNPs distributions. p value was considered significant after Bonferroni correction for multiple SNPs testing (p_c). The Kolmogorov-Smirnov (K-S) test was applied to verify normal distribution of numerical variable scores.

MMSE, a cognitive score which resulted normally distributed, was shown as mean and standard deviation (SD) and analysis of variance ANOVA was calculated in relationship with SNPs distribution.

Statistical analysis was performed using commercial software (IBM SPSS Statistics 23.0, IBM Inc., Chicago, IL, USA). Haplotype analyses were performed using the SHEsis software freely available at *http://analysis.bio-x.cn* (Li et al., 2009; Yong and He, 2005). Haplotype association analysis was performed using PLINK software (Purcell et al., 2007) by logistic regression analysis. Age, sex and pathology were incorporated as covariates in the regression model which estimated the Beta value associated with MMSE.

RESULTS

Modulation of presynaptic JNK isoforms and STX1a activity by NMDA or KCl stimuli

It is widely recognized that the apoptotic cascade following *excitotoxicity* is transmitted through postsynaptic NMDA receptors, via the intracellular activation of JNK protein-mediated signaling in both brain (Centeno et al., 2007) and spinal cord (Guo et al., 2009). This postsynaptic interaction between NMDA receptors and JNK proteins is ensured by the JNK scaffolding protein JIP (Kennedy et al., 2007).

We recently showed that, also in the presynaptic side, the *excitotoxic* input induced by NMDA stimulation provokes the phosphorylation of JNK proteins and that, interestingly, JNK2 is the isoform preferentially implicated in this mechanism (Nisticò et al., 2015).

As already reported (Dong et al., 1998; Nisticò et al., 2015), JNK proteins are present as double isoforms with different molecular weights, *i.e.* JNK1 46 kDa and JNK2 54 kDa, respectively.

It is therefore possible to estimate their specific isoform phosphorylation by measuring the relative band densitometry at the corresponding molecular weight.

In cortical synaptosomes under NMDA (100 μM) + glycine (1 μM) or KCl (8 mM) stimulus, JNK1 phosphorylation (Thr183/Tyr185 p-JNK) was not changed while JNK2 phosphorylation, as expected, was augmented only by the NMDA stimulus (1.58 ± 0.12 vs. control, ***$p < 0.001$) and not by KCl (**Fig. 25A**).

As previously said, the phosphorylation of STX1a (Ser14 p-STX1a) is a fundamental step toward the SNARE complex assembly leading to neurotransmitter release (Ramakrishnan et al., 2012; Südhof, 2004).

Accordingly, both NMDA (1.38 ± 0.07 vs. control =1, **$p < 0.01$) and KCl (1.22 ± 0.11 vs. control =1, *$p < 0.05$) stimuli increased the levels of phosphorylated STX1a (p-STX1a) in mouse cortical synaptosomes (**Fig. 25B**).

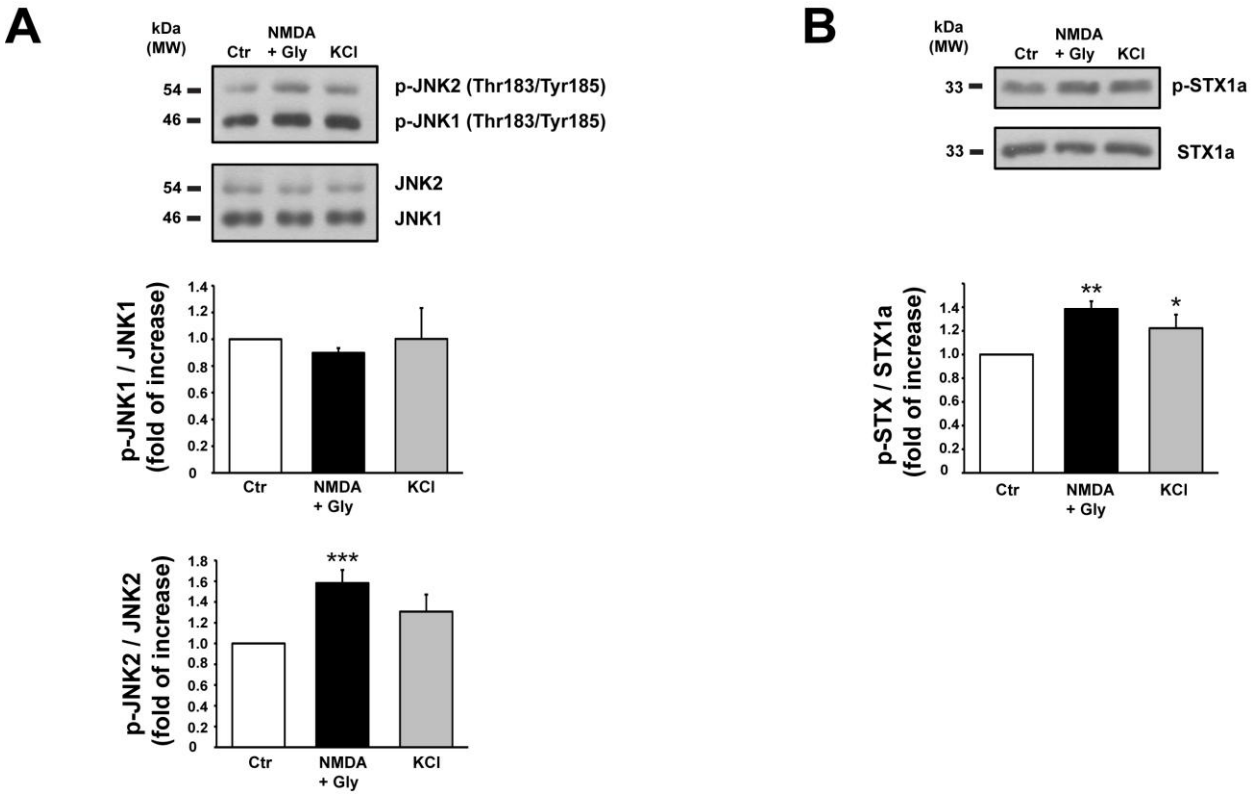

Fig. 25

Presynaptic JNKs and STX1a activity by NMDA or KCl stimuli.

A) Cortical synaptosomes prepared from 3 months old wild-type mice have been stimulated either with NMDA (100 µM) + glycine (1 µM) for 10 min or with KCl (8 mM) for 90 seconds, and subsequently lysed. Quantification of the phosphorylation state for both JNK1 and JNK2 isoforms has been separately evaluated. The top histogram shows that JNK1 phosphorylation was not affected by both stimuli. The lower histogram shows instead an increased and significant phosphorylation of JNK2 corresponding to NMDA stimulus (n= 6, ***$p < 0.001$ vs. control, Newman-Keuls multiple-comparison test).

B) The same cortical synaptosome preparation has been used for the quantification of STX1a phosphorylation. Ser14 phosphorylation of STX1a was increased from both NMDA (n= 6, **$p < 0.01$ vs. control, Newman-Keuls multiple-comparison test) and KCl stimuli (*$p < 0.05$ vs. control, Newman-Keuls multiple-comparison test).

JNK interacts with STX1a

To test whether the presynaptic STX1a physically interacts with JNK, mouse cortical synaptosomes previously stimulated with NMDA (100 µM) to induce JNK phosphorylation, were immunoprecipitated (IP) by using a specific p-JNK antibody (Thr183/Tyr185 p-JNK). The IP experiment demonstrated that JNK and STX1a actually interact, since p-JNK pulled down STX1a already in basal conditions. Noteworthy, the NMDA stimulus increased the level of p-JNK level without significant modifications of total JNK level. This finding was

moreover accompanied by an augmented level of p-STX1a, thereby suggesting that upon *excitotoxic* stimuli the release of glutamate is likely controlled by the interaction between the phosphorylated forms of JNK and STX1a (**Fig. 26 left panel**).

IP performed with a specific JNK2 antibody confirmed the increased p-JNK levels under the NMDA stimulus (**Fig. 26 right panel**).

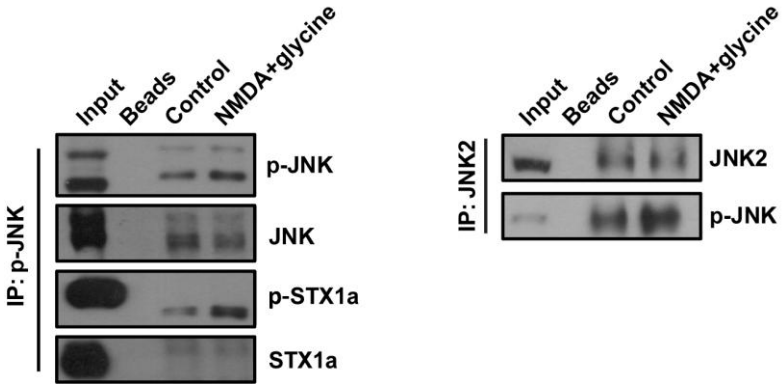

Fig. 26
IP after stimulus.
Cortical synaptosomes underwent NMDA (100 µM) + glycine (1 µM) stimulus for 10 min and, together with respective controls, were IP either for p-JNK (left panel) or JNK2 (right panel). p-JNK resulted to be augmented by NMDA stimulus and beside the interaction with STX1a. On the other hand, the phosphorylation of STX1a was also increased by NMDA with respect to control.
'Input' lane corresponds to the total lysate from untreated synaptosomes. 'Beads' lane shows the quality of the IP procedure, since no unspecific immunoreactivity was detected.

Docking results for JNK isoforms and JNKs alignment

A JNK2-STX1a complex model has been built *in silico* using the protein-protein docking software Rosetta 3.4 (Sircar et al., 2010) (**Fig. 27A-1**) (see computational details). STX1a binds to JNK2 through the groove formed by two of the three alpha helices that form its structure, namely helix B and helix C, which have been therefore proposed as the most plausible binding site for Syntaxin-1a partners (Fernandez et al., 1998). The contact surface between the two proteins comprehends an area of 2680 Å highlighted in red (**Fig. 27A-2**). The sequence alignment of the three known JNK isoforms shows that although the JNK isoforms (-1, -2, -3) present a high sequence homology among them, the amino acid sequence at the interface between JNK2 and STX1a (in red) clearly differs from both JNK1 and JNK3,

making it a potential specific site for STX1a interaction (**Fig. 27B**). This finding may therefore explain the high specificity of STX1a binding with JNK2 when compared to other JNK isoforms.

In order to selectively disrupt JNK2/STX1a interaction, *JGRi1*, a novel cell permeable peptide long 26 amino acids has been designed, based on these computational data. The 12 amino residues (*GRKKRRQRRRPP*) of the HIV-1 Tat_{48-59} protein that confer cell permeability (Chauhan et al., 2007) have been linked to the effector portion (*IEQSIEQEEGLNRS*).

Several peptide variants have been designed and produced in order to be used in the experiments (**Fig. 27C**).

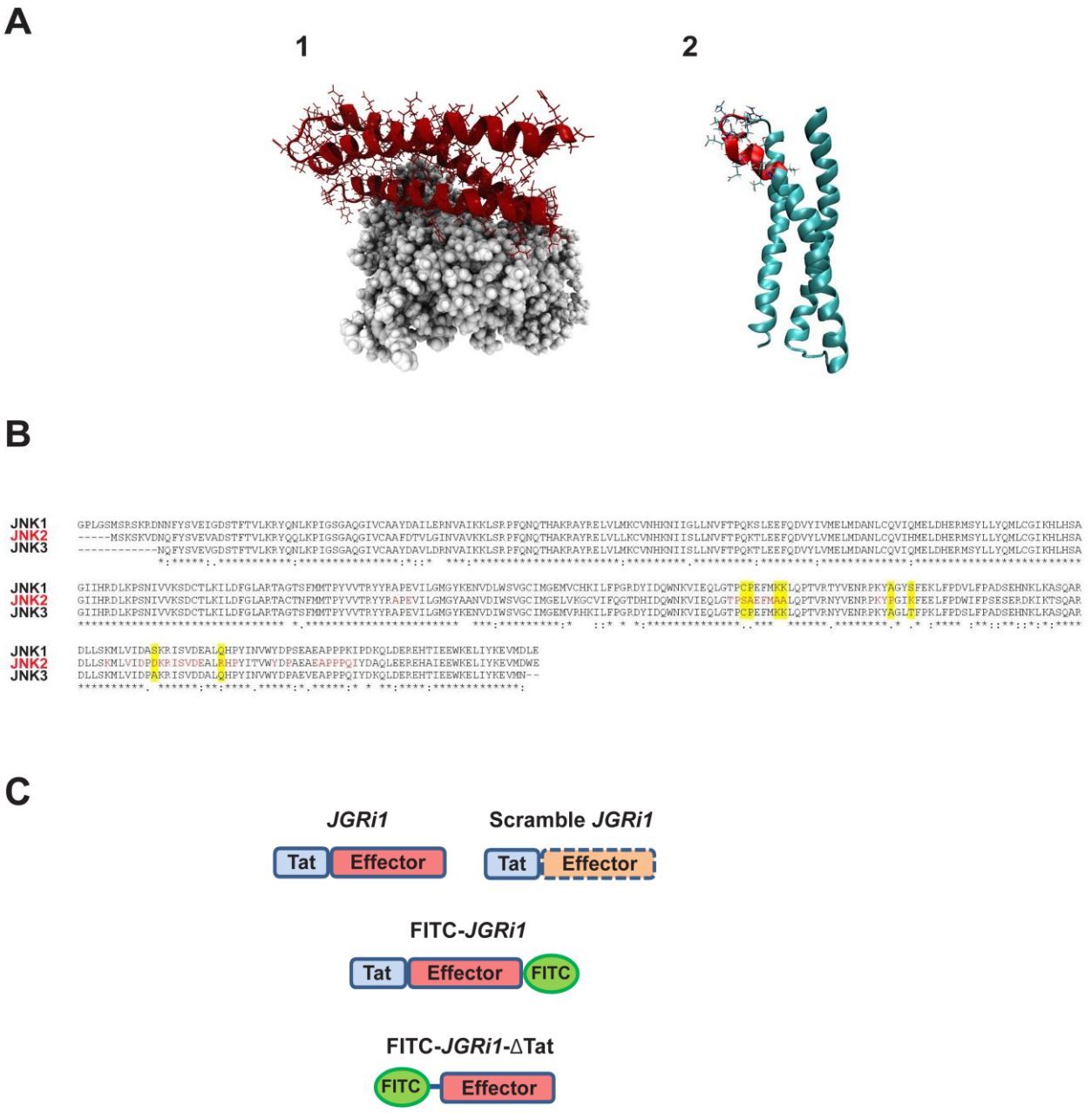

Fig. 27
Bioinformatics and docking experiments.
A) 3D structures of the molecular docking resolving the possible interaction between JNK2 (grey) and the *N*-terminal portion of STX1a (red) (1). The image originates from a computational analysis that allowed the determination of the minimum region of contact between the two proteins. The portion of STX1a that has been used to design *JGRi1* has been coloured in red (2).
B) Amino acid sequences corresponding to the region of contact between JNK and STX1a have been aligned for all 3 JNK isoforms. In the emphasized contact region, JNK2 has several distinguishing amino acids while JNK1 and JNK3 are mostly equal among them.
C) Figurative cartoon that summarizes the peptides variants that have been synthesized and used for the experiments.

JGRi1 is able to specifically disrupt JNK2/STX1a interaction

To verify the actual occurrence of the interaction between JNK2 and STX1a, we exploited HEK-293 cell cultures, an *in vitro* system useful for our purposes since it lacks of endogenous expression of STX1a (Toonen et al., 2005). HEK-293 cells have been transfected with HA-tagged JNK1, JNK2 or JNK3 plasmids together with full length STX1a (non-tagged) plasmid. In the total lysate from cells harvested, endogenous JNK2 and exogenous STX1a levels were present in all the lanes while HA-JNK2 was present only in the JNK2 lane (**Fig. 28 left blots**). HEK-293 cells overexpressing HA-tagged JNK1, JNK2 or JNK3 proteins and STX1a further underwent treatment with *JGRi1* 40 µM and were subsequently immunoprecipitated (IP) with HA antibody. Beside the presence of all HA-JNKs protein, as expected, the treatment with *JGRi1* prevented the interaction of STX1a with HA-JNK2 but not with HA-JNK1 and HA-JNK3 (**Fig. 28 right blots**), confirming that this protein interplay does exist and that our peptide effectively disrupts it.

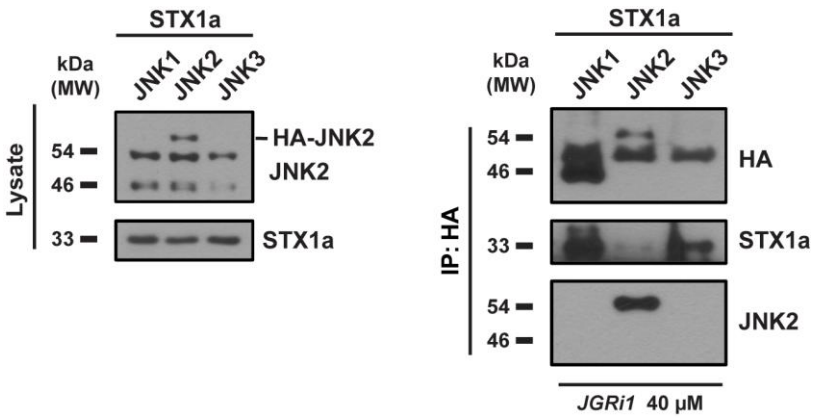

Fig. 28
***JGRi1* specifically interferes with JNK2/STX1a interaction.**
HEK-293 cells co-transfected with STX1a plus HA-JNK1, -JNK2, or -JNK3 were IP for HA and probed for HA and STX1a. Upon treatment with *JGRi1*, STX1a was pulled down in correspondence of JNK1 and JNK3 but not JNK2, as expected, confirming the specificity of action of our peptide.

JGRi1 disrupts JNK/STX1a interaction in mouse cortical synaptosomes

The JNK2/STX1a interaction has been evaluated also in cortical synaptosomes that were previously stimulated with NMDA (100 µM) + glycine (1 µM) and then immunoprecipitated for p-JNK. The treatment increased the phosphorylation of JNK, accompanied by an augmented interaction between p-JNK and STX1a, p-STX1a and Munc18. Interestingly, pretreatment with *JGRi1* reduced p-JNK levels probably because a 30 min administration of the peptide given before NMDA stimulus was sufficient to induce the blockade of the NMDA receptor activity. Moreover, as expected, pretreatment with *JGRi1* also reduced the interaction of p-JNK with SNARE complex proteins, like Munc18 (Südhof, 2004; Wan et al., 2010) and STX1a (Südhof, 2004). On the other hand, SNAP25 was not pulled down by p-JNK (data not shown), coherently with the observation that the assembly of SNAP25 intervenes in a second step with respect to Munc18-STX1a interaction (Cheng et al., 2013; Südhof, 2004).
Presynaptic JNK2 presence in the p-JNK IP was confirmed by the JNK2 specific antibody (**Fig. 29**).

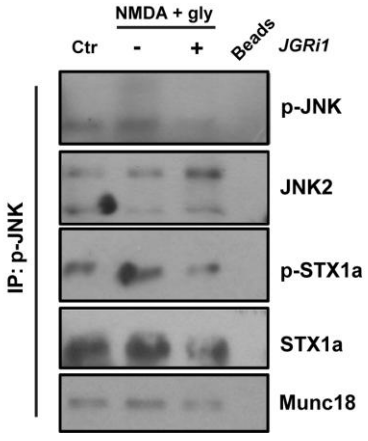

Fig. 29
p-JNK IP experiment.
p-JNK was augmented by 10 min NMDA (100 µM) + glycine (1 µM) NMDA stimulus while it was reduced by 30 min pretreatment with *JGRi1* (1 µM). p-STX1a as well resulted increased under NMDA. In all conditions JNK2 was present. *JGRi1* reduced both STX1a and p-STX1a level, as well as Munc18.

JGRi1 does not impair JNK phosphorylation but affects STX1a activation

The differential activation of the various JNK isoforms has been evaluated in cortical synaptosomes that underwent NMDA stimulation. An increased level of JNK2 phosphorylation was detected after NMDA treatment alone (1.58 ± 0.12 vs. control =1, ***p < 0.001). Interestingly, *JGRi1* administered before the NMDA insult prevented the abrupt increase in JNK2 phosphorylation (1.40 ± 0.20 vs. control = 1, *p < 0.05), with a decrease of about 20% with respect to NMDA alone. Pretreatment with *JGRi1* alone or the scrambled version *sJGRi1* did not determine any change in p-JNK2 levels. On the other hand, JNK1 phosphorylation level was not affected in any case (**Fig. 30A**).

Conversely, NMDA increased STX1a phosphorylation (1.38 ± 0.07 vs. control = 1, *p < 0.05) while, as expected, *JGRi1* prevented it. Scrambled *JGRi1* and *JGRi1* applied alone did not evoke STX1a phosphorylation (**Fig. 30B**).

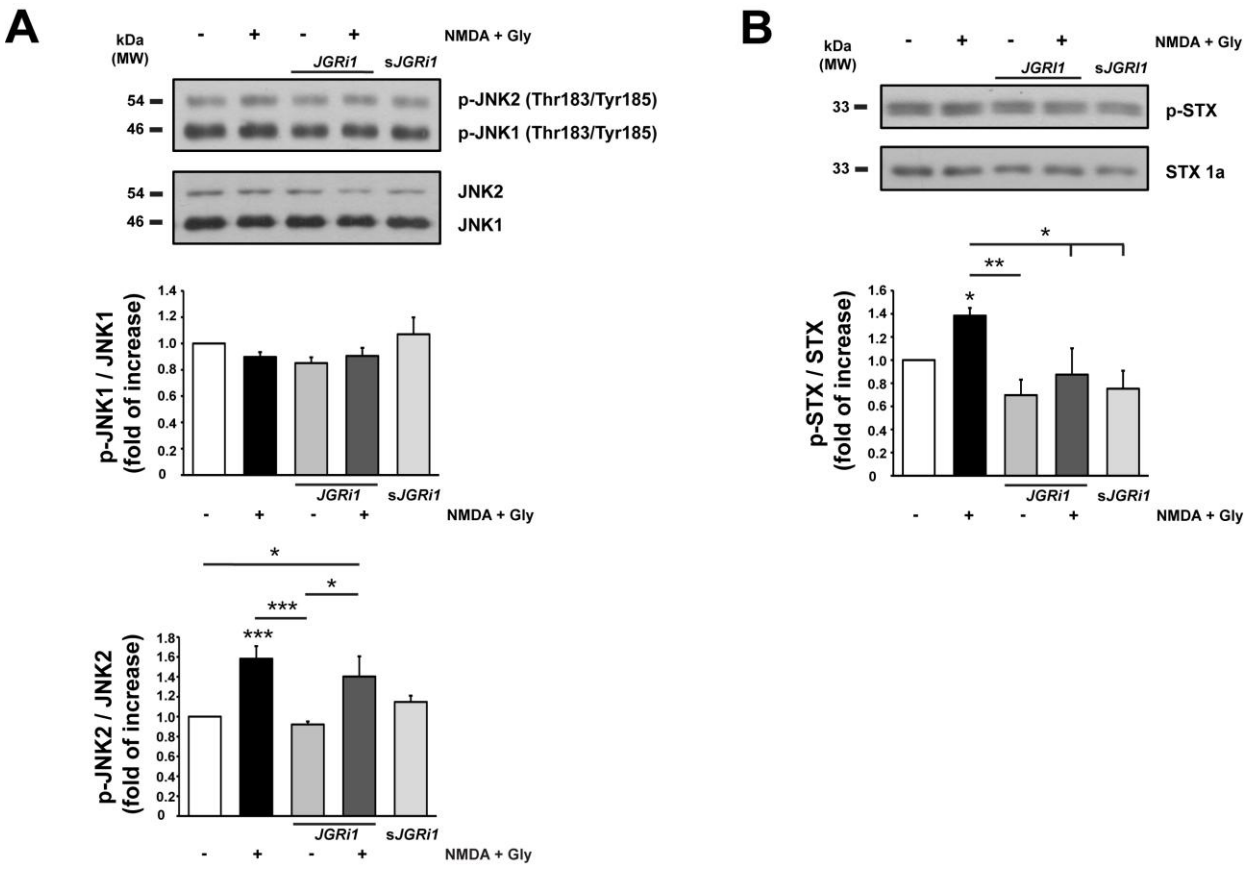

Fig. 30

***JGRi1* modulates JNK phosphorylation and STX1a activation.**

A) p-JNK1 was not affected by treatments while p-JNK2 was increased after 10 min NMDA (100 µM) + glycine (1 µM) alone or pretreated with *JGRi1* (1 µM). *JGRi1* (1 µM) or *sJGRi1* (1 µM) alone did not affect the

phosphorylation state of JNK2 (n = 5, ***p < 0.001 NMDA stimulus vs. control, ***p < 0.001 *JGRi1* alone vs. NMDA, *p < 0.05 NMDA + *JGRi1* vs. *JGRi1* alone, *p < 0.05 NMDA + *JGRi1* vs. control, Newman-Keuls multiple-comparison test).
B) NMDA stimulus increased STX1a phosphorylation that was in turn prevented by pretreatment with *JGRi1* (n= 5, *p < 0.05 NMDA stimulus vs. control, **p < 0.01 *JGRi1* alone vs. NMDA, *p < 0.05 s*JGRi1* alone vs. NMDA, Newman-Keuls multiple-comparison test).

JGRi1 prevents the formation of the SNARE complex

The biochemical evidence of the inhibitory effect of *JGRi1* upon the release of glutamate was evaluated by performing a SNARE complex formation assay, being SNARE complex assembly a crucial step for the release of neurotransmitters (Jahn and Fasshauer, 2012). Indeed, by probing unboiled samples from cortical synaptosomes for STX1a it is possible to evaluate the formation of the SNARE complex, measuring the non-resolved higher molecular weight complexes that are evident in the smear from Western blot (Biggi et al., 2017; Burré et al., 2010).

As expected, NMDA stimulus was able to increase the formation of the SNARE complex while *JGRi1* prevented it. The higher levels of free STX1a in the boiled samples compared to the unboiled ones indicate the quality of the procedure, being STX1a no more engaged in the SNARE complex in boiled samples (**Fig. 31**).

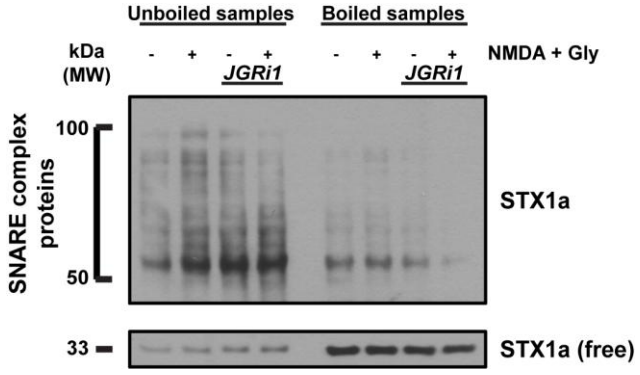

Fig. 31
SNARE complex assay.
JGRi1 (1 µM) was applied, as indicated, to cortical synaptosomes 30 min before 10 min NMDA (100 µM) + glycine (1 µM) stimulus. SNARE complex formation was evaluated by probing STX1a in unboiled samples comparing STX1a lanes smearing (from 50 to 100 kDa) with free STX1a. NMDA increased SNARE complex formation while *JGRi1* prevented it.

JGRi1 reduces presynaptic NMDA-evoked neurotransmitter release

Vesicular release has been tested by means of Synaptogreen destaining assay in cortical synaptosomal preparations, as previously described (Nisticò et al., 2015).

Interestingly, NMDA-evoked vesicle release in basal experimental conditions (68% ± 10) was reduced by pretreatment with *JGRi1* in a dose dependent manner (*JGRi1* 5 µM: 27% ± 8 vs. 0 µM, **p < 0.01; *JGRi1* 10 µM: 18% ± 4 vs. 0 µM, **p < 0.01). On the other hand, KCl-evoked release was not affected by *JGRi1*, overall indicating that *JGRi1*-mediated release inhibition is specific for NMDA receptors (**Fig. 32A**).

The specific release evoked by tritiated aspartic acid ([^{3}H]D-Asp) was also studied (**Fig. 32B**). In this experimental conditions *JGRi1* reduced again the NMDA-evoked release in a dose dependent manner (2 µM: 41% ± 5 vs. 0 µM, **p < 0.01; 5 µM: 34% ± 4 vs. 0 µM, **p < 0.01; 10 µM: 18% ± 4 vs. 0 µM, **p < 0.01), while KCl and AMPA-evoked release were not affected.

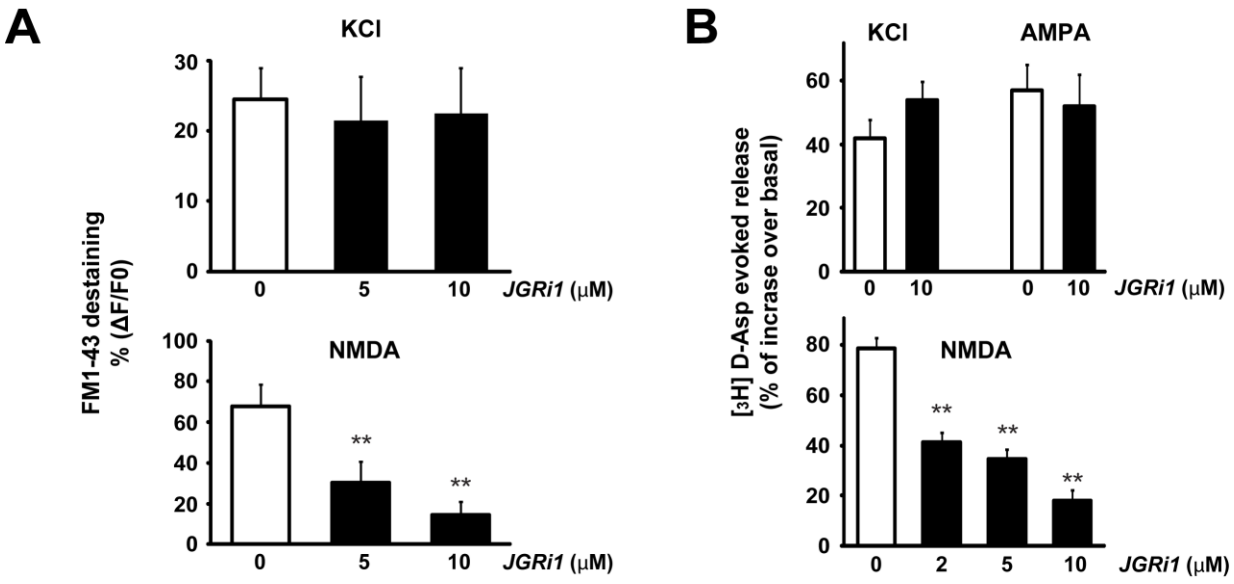

Fig. 32

Glutamate release experiments.

A) Exocytosis evoked by KCl (8 mM) or NMDA (100 µM) + glycine (1 µM) stimulus has been evaluated in cortical synaptosomes as a measure of FM1-43 destaining in a time-lapse image setting. Pretreatment with *JGRi1* at different concentrations given 30 min before the registration specifically reduced NMDA-evoked exocytosis. Average percentage of fluorescence loss has been reported in the histograms (n= 5, **p < 0.01 vs. control, Newman-Keuls test). In each experiment three coverslips for each experimental group were analysed.

B) Wild-type mice cortical synaptosomes preloaded with radioactive tracer were incubated with several stimuli in absence or presence of *JGRi1*, as indicated. The experiment demonstrated that, among the applied stimuli, *JGRi1* was able to specifically inhibit the sole NMDA-evoked glutamate release in a dose dependent manner. Means ± SEM n= 3 experiments run in triplicate (three superfusion chambers for each experimental condition), (**p < 0.01 vs. basal release, Newman-Keuls test).

JGRi1 blocks spontaneous presynaptic NMDA currents in patch-clamp experiments

The effect of *JGRi1* on NMDA receptor-dependent presynaptic glutamate release was evaluated by measuring mEPSCs, as already reported (Nisticò et al., 2015).

In basal conditions, the tiny and rapid mEPSCs on the field are inward currents corresponding to depolarizing events linked to glutamatergic signaling through AMPA/Kainate receptor. Possibly, each spike observed corresponds to a single presynaptic vesicle released.

Postsynaptic NMDARs in the recorded neurons were blocked by MK-801 (10 μM) in the patch-pipette, in the presence of extracellular tetrodotoxin (1 μM) and picrotoxin (100 μM). Application of the selective NMDA receptor antagonist D-AP5 in the same experimental conditions induced an increase of the inter-event interval (*iei*) (**p < 0.01, *t*-test, vehicle vs. D-AP5, n= 8; **Fig. 33**), whilst the amplitude of the same events was unaffected (*p > 0.05, Student *t*-test, vehicle vs. D-AP5, n= 8; **Fig. 33**).

Inter-event interval can be considered an indirect measure of mEPSCs frequency. Consequently, the increase of *iei* indicates a decrease in NMDARs firing, confirming that NMDARs clearly contribute to the depolarization of the presynaptic terminal.

Perfusion with D-AP5 did not lead to significant changes of *iei* in slices preincubated with *JGRi1* for 30 min at 5 μM and 10 μM (*p > 0.05, *t*-test, *JGRi1* 5 μM vs. D-AP5, n = 7; *p > 0.05, *t*-test, *JGRi1* 10 μM vs. D-AP5, n = 9; **Fig. 33**), indicating that presynaptic NMDAR inhibition has been effectively accomplished by *JGRi1*, since the pharmacological inhibition by D-AP5 did not further reduce the *iei*.

On the other hand, no changes were observed in the amplitude of mEPSCs under the same conditions, suggesting that *JGRi1* does not influence the biochemistry of glutamate release (*i.e.* neurotransmitter metabolism, vesicular filling).

Overall these electrophysiological results indicate that *JGRi1* specifically reduces glutamate release mediated by presynaptic NMDA receptors.

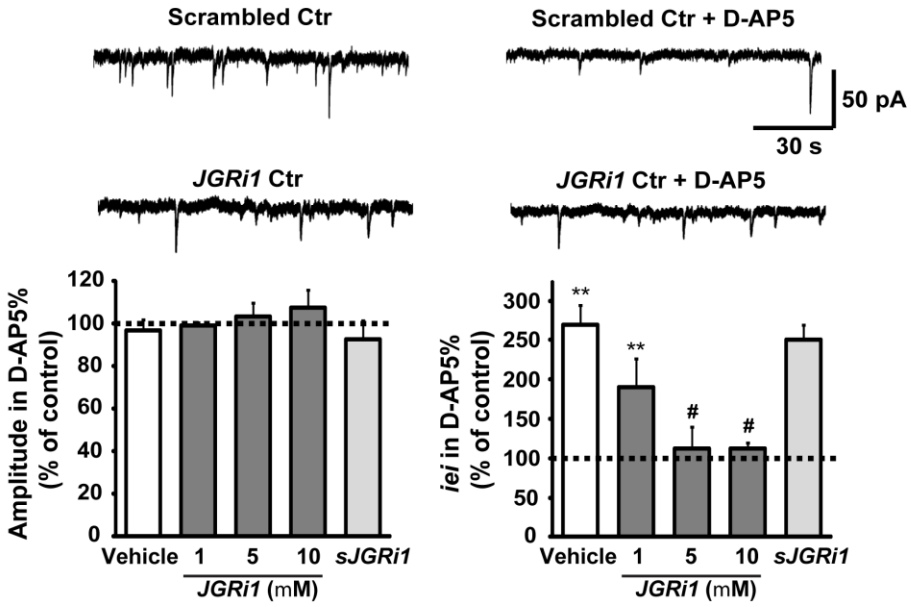

Fig. 33

***JGRi1* prevents spontaneous NMDA currents in the presynaptic site.**

Histograms show the median values expressed as percentage versus control (100%) of mEPSC amplitude (left) and *iei* (right) recorded in vehicle, *JGRi1* (1-10 μM) or scrambled condition, in response to D-AP5. (**p < 0.01 vs. ctrl, #p<0.05 vs. *JGRi1* (1 μM) (*t*-test).

NMDA-mediated neuronal death is prevented by *JGRi1*

Rat cortical primary neurons pretreated with *JGRi1* for 1 h were subjected to further NMDA *excitotoxic* stimulation (100 μM) for 3 h, in order to activate the cell death machinery. Neuronal viability was assessed 24 h after the drug treatment, by counting the number of nuclei non permeable to DAPI coloration (**Fig. 34**). Pretreatment of neuronal cells with *JGRi1* showed a neuroprotective effect, strongly reducing NMDA-driven cell death in a concentration-dependent manner. *JGRi1* was efficacious at 1 μM (43.5 ± 1.62 vs. 0 μM, ***p < 0.001) or 0.5 μM (38 ± 0.98 vs. 0 μM, **p < 0.01) but not at 0.1 μM (28.4 ± 1.68 vs. 0 μM).

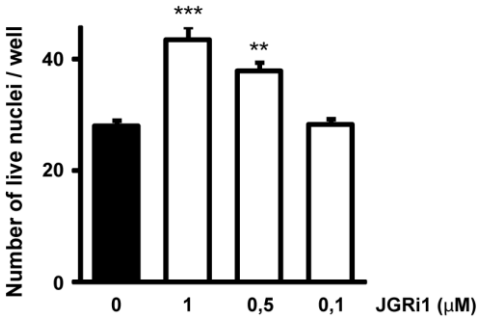

Fig. 34
Neuronal cell cultures were pretreated 1 h with *JGRi1* at different concentrations before 3 h NMDA stimulation (100 µM). Following 24 h from the applied stimulus, neuronal cells nuclei have been counted to evaluate the degree of cell death. *JGRi1* was able to protect from cell death in a dose dependent manner.
Histograms show the number of cells alive in each well. A number of 3 triplicates per well has been counted for each experiments. (n= 6, ***p < 0.001 and **p < 0.01 vs. control, Newman-Keuls multiple-comparison test).

JGRi1 brain distribution following *in vivo* administration

Peptides containing HIV-Tat sequences (generally 47-57) are able to cross the BBB within 1 h after injection (Bechara and Sagan, 2013; Stalmans et al., 2015).

In addition, fluorescence-based protocols are the most common methods used to allow indirect quantification and localization of these probes inside living cells by observation of fluorimetry at confocal microscopy.

On purpose, the fluorescent tag on the FITC-linked peptide variants was exploited to determine the cerebral distribution of *JGRi1* upon administration through differential routes.

As expected, FITC-*JGRi1* was detectable in the cortex (**Fig. 35A**) from 1 h till 24 h post intra-peritoneal (Ip) injection as well as in hippocampus (**Fig. 35B**). Since the fluorescein (FITC) tag is linked at the *C*-term of the Tat-peptide (**Fig. 27C**) we could rely on the belief that the whole peptide should be intact when it reaches the brain, in order to fluoresce. Coherently, the variant version lacking the Tat portion (FITC-*JGRi1*-ΔTat, **Fig. 27C**) did not show any green fluorescence under the same conditions of administration, indicating that it is definitely not able to cross the BBB and distribute within cortical tissues (**Fig. 35C**).

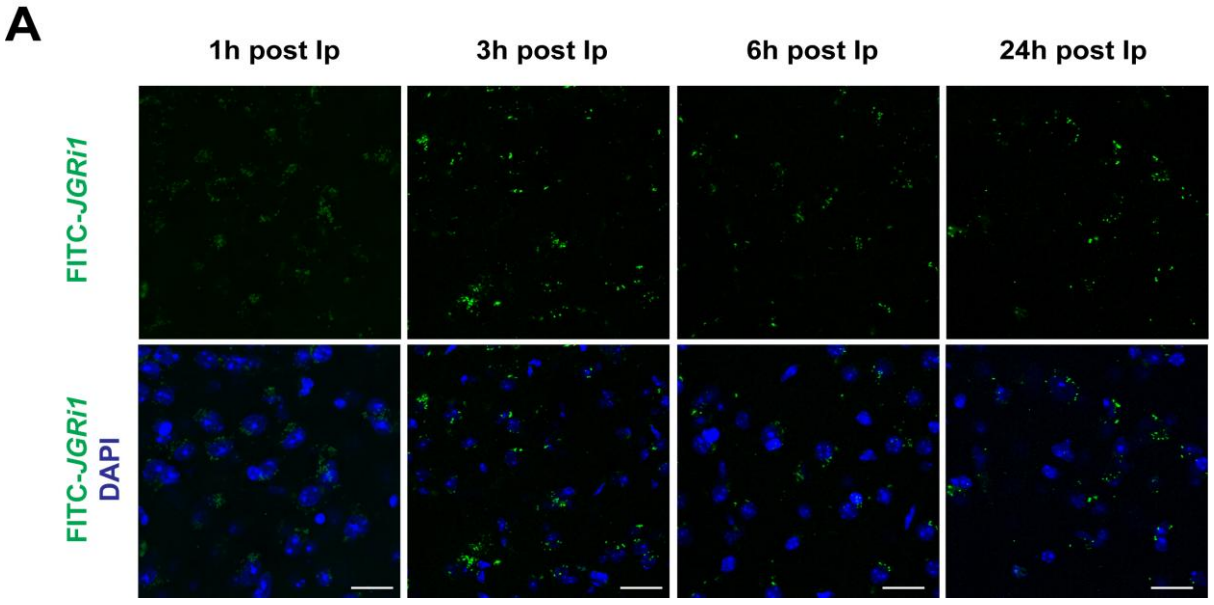

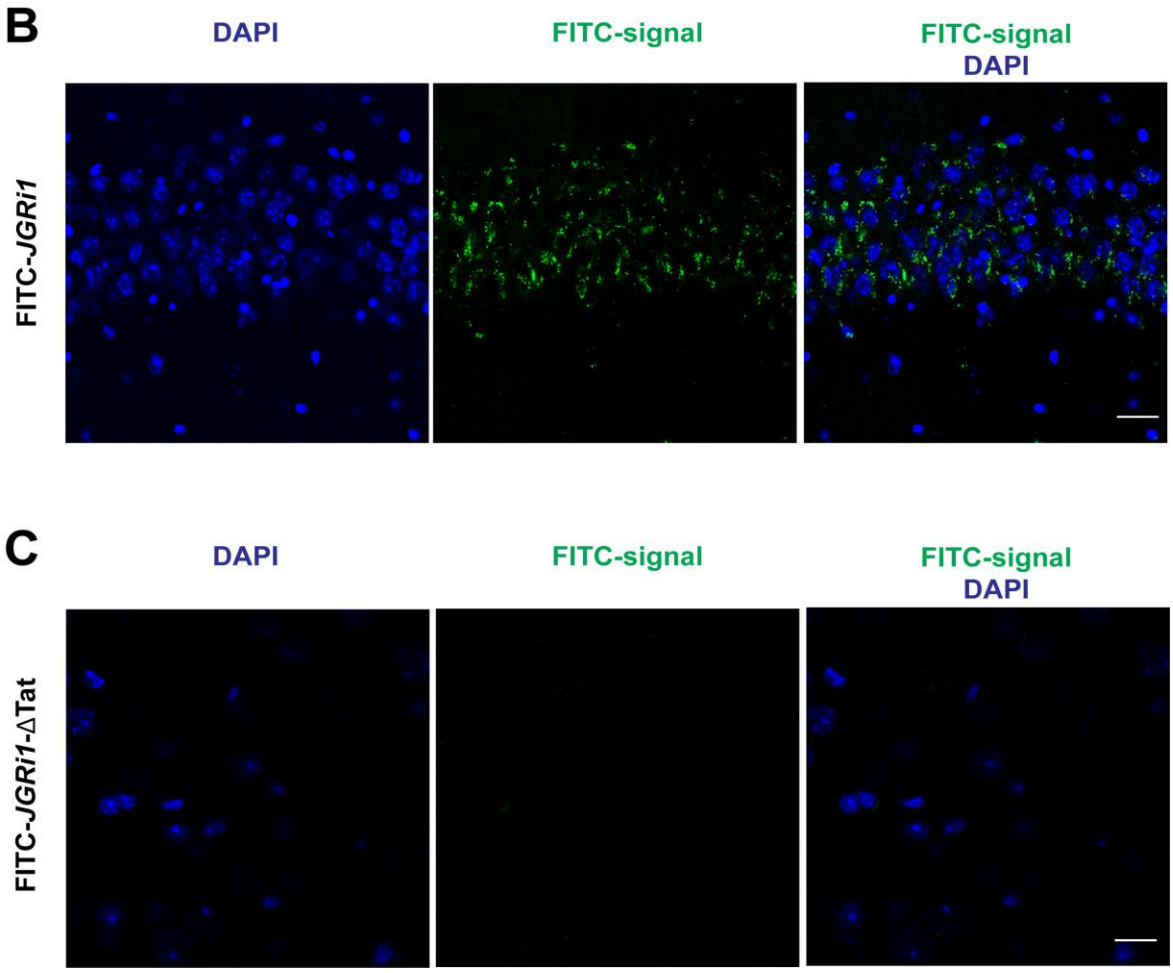

Fig. 35
***JGRi1* distribution in cerebral tissue.**
A) FITC-*JGRi1* (20 mg/kg) was administered intraperitoneally and its brain distribution was detected by confocal microscopy. Cortical tissue has been examined at several time points and the FITC fluorescence was detected until 24 h after injection. Scale bar = 15 μm.
B) FITC-*JGRi1* (20 mg/kg) was intraperitoneally administered and its brain distribution was detected by confocal microscopy. Hippocampal tissue has been examined 3 h after injection and the FITC fluorescence was detected. Scale bar = 15 μm.
C) FITC-*JGRi1*-ΔTat (20 mg/kg) was intraperitoneally administered and its brain distribution was detected by confocal microscopy. Cortical tissue has been examined 3 h after injection but no FITC fluorescence was detected in this case. Scale bar = 15 μm.

JGRi1 distribution and activity following *in vivo* intraperitoneal injection

Wild-type mice were injected in the peritoneum with a single dose of *JGRi1* or vehicle and sacrificed to prepare cortical synaptosomes following 2 or 24 h post Ip injection. NMDA-evoked vesicle release was measured through FM1-43 destaining. *JGRi1* treated mice showed

lower neurotransmitter release with respect to vehicle alone (2h: -23% ± 7% *JGRi1* vs. vehicle; 24h: -26% ± 4 *JGRi1* vs. vehicle) (**p < 0.01) (**Fig. 36A**), demonstrating that a single injection of the peptide, up to 24 h, is already efficacious in inhibiting NMDA receptor activity.

The p-JNK/STX1a interaction-disrupting efficacy of the peptide was tested also in synaptosomes prepared from mice injected intraperitoneally with a single dose of *JGRi1* and sacrificed after 24 h. Synaptosomes were stimulated with NMDA (100 µM) + glycine (1 µM) and then immunoprecipitated for p-JNK.

NMDA treatment induced a relevant increase in the level of p-JNK in synaptosomes from vehicle animal, moreover underlining a stronger interaction with STX1a with respect to control. p-STX1a levels were also increased by NMDA treatment, as expected.

Notably, *JGRi1* efficiently disrupted JNK/STX1a interaction as indicated by the drastically decreased level of STX1a, as well as of its phosphorylated form (**Fig. 36B**).

In an additional experiment, a single dose of *JGRi1* per day administered intraperitoneally for 7 days demonstrated again that when mouse cortical synaptosomes are stimulated with NMDA, the p-JNK levels upon immunoprecipitation were increased in non-treated and treated animals, but the interaction with STX1a was completely abolished only in preparations from *JGRi1* injected animals. This result once more demonstrated the efficacy of the peptide in disrupting JNK/STX1a interaction (**Fig. 36C**).

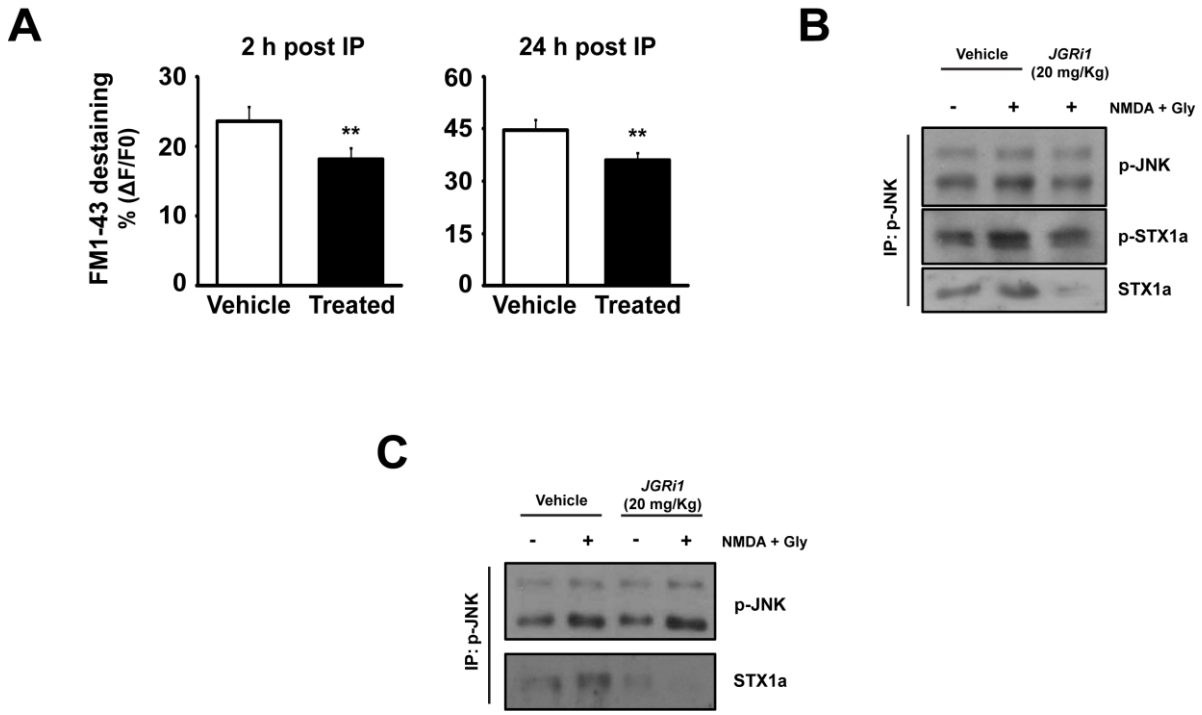

Fig. 36

***JGRi1* inhibits glutamate release and prevents JNK2/STX1a interaction following *in vivo* administration.**

A) *JGRi1* (20 mg/kg) was intraperitoneally (Ip) administered to wild-type mice. After 2 h or 24 h from injection, cortices were used to prepare synaptosomes and to test the exocytosis evoked by NMDA (100 µM) + glycine (1 µM) stimulus, measured as FM1-43 destaining in a time-lapse image setting. Injected *JGRi1* was able to reduce NMDA-evoked exocytosis in both time points, with comparable efficiency (n = 3, **p < 0.01 vs. control, *t*-test).

B) Mice were treated Ip with 1 injection of either vehicle or *JGRi1* (20 mg/kg) and sacrificed after 24 h. The cortices were used to prepare synaptosomes, subsequently stimulated with NMDA (100 µM) + glycine (1 µM), as indicated. Synaptosomes were then IP for p-JNK and probed for p-JNK, STX1a and p-STX1a.

NMDA stimulus alone, as expected, was able to increase the interaction between p-JNK and p-STX1a, as indicated by the increased bands signal from the two phosphorylated proteins. *JGRi1* in turn was able to decrease the level of both STX1a and p-STX1a, confirming the efficacy of the disruption activity of the peptide.

C) Mice were treated Ip with 1 injection per day of vehicle or *JGRi1* (20 mg/kg) and after 7 days the cortices were used to prepare synaptosomes further stimulated by NMDA (100 µM) + glycine (1 µM), as indicated. Synaptosomes were then IP for p-JNK and probed for p-JNK and STX1a. NMDA alone increased the interaction between p-JNK and STX1a while *JGRi1* reduced their interaction in both control and NMDA conditions.

JGRi1 efficiently distributes in the cortex after ICV *in vivo* injection

Single ICV injection of FITC-*JGRi1* (16ng/5µl) showed that the peptide was able to reach the cortical tissue and be maintained there over 24 h. On the other hand, the peptide variant lacking the Tat portion (FITC-*JGRi1*-ΔTat), injected at the same concentration, was not. *JGRi1* fluorescence was intensely found around cell nuclei stained by DAPI (**Fig. 37**).

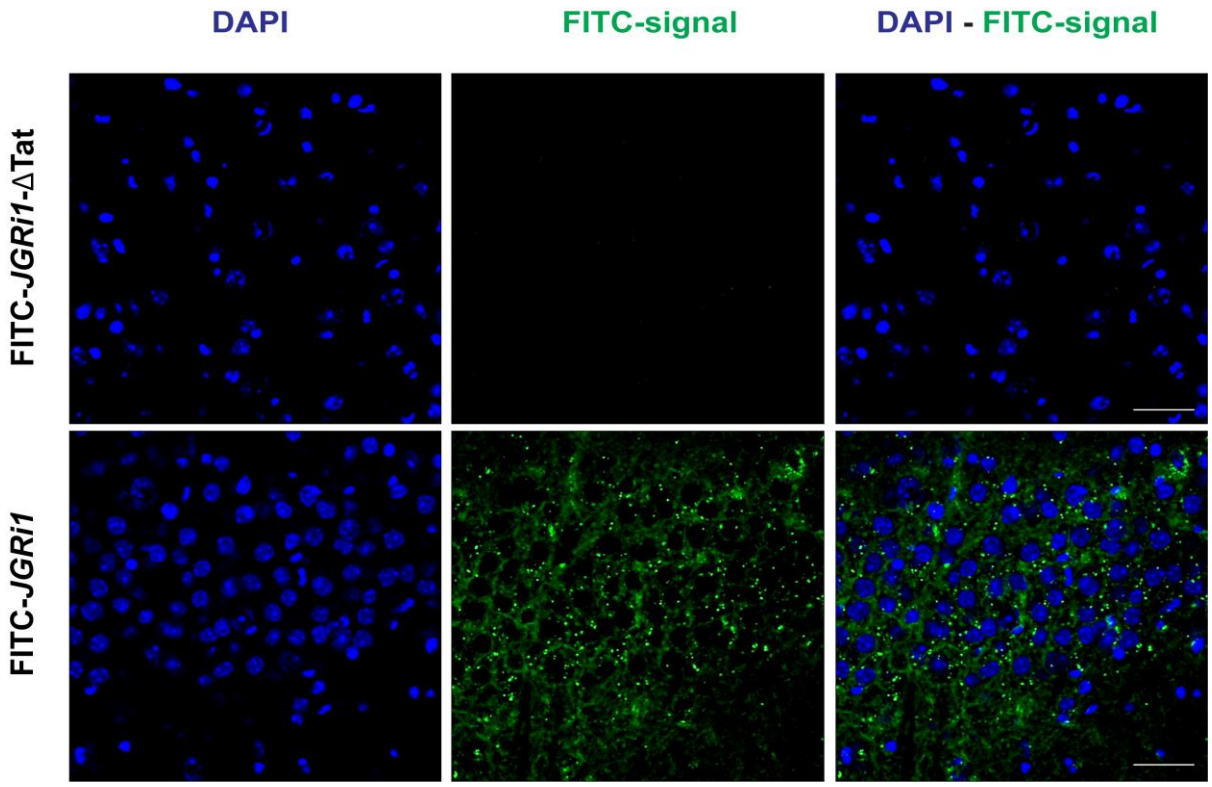

Fig. 37
***JGRi1* distributes in the cortex following *in vivo* ICV administration.**
A) FITC-*JGRi1* (16ng/5µl, ICV) and FITC-*JGRi1*-ΔTat (16ng/5µl, ICV) were administered with a single intracerebroventricular injection to wild-type mice. The brains were sliced after 24h. FITC-*JGRi1*-ΔTat was not able to reach the cortex as shown by the absence of FITC fluorescence (first row of confocal images) while FITC-*JGRi1* was efficiently distributed in the cortex parenchyma as indicated by the green fluorescence presence (second row of confocal images). Scale bar = 25 µm.

JGRi1 disrupts JNK/STX1a interaction and affects STX1a activation in the OGD ischemia model

Preliminary data have been collected to define the JNK2/STX1a interaction also in mouse cortical slices under the OGD (oxygen/glucose deprivation) ischemic paradigm, followed by immunoprecipitation for p-JNK.

As already observed in the synaptic compartment, *excitotoxicity* mimicked by the shortage of nutrient and oxygen supply to cortical neurons promoted a valuable increase in the phosphorylation of JNK, furthermore accompanied by the augmented interaction with the activated p-STX1a (**Fig. 38A**, *unpublished data*).

SNAP25 was instead not pulled down in the JNK/STX complex, as already reported (Cheng et al., 2013).

Notably, pretreatment with *JGRi1* (10 µM) reduced both p-JNK levels as well as the interaction with the phosphorylated STX1a (**Fig. 38A**, *unpublished data*).

To support this result, the same samples were analysed by Western blot in order to evaluate the activation of STX and JNK isoforms.

OGD to cortical neurons promoted a valuable increase in JNK2 phosphorylation, and, interestingly, in this setting also the phosphorylation of JNK1 resulted augmented, possibly due to a major involvement of this isoform in apoptotic cell death (Dhanasekaran and Reddy, 2008; Wang et al., 2007).

On the other hand, pretreatment with *JGRi1* (10 µM) rescued the increase in JNK phosphorylation compared to OGD alone (**Fig. 38B**, *unpublished data*).

Coherently with previous findings, OGD additionally increased STX1a phosphorylation whereas, as expected, *JGRi1* (10 µM) administered 1 h before the insult prevented it (**Fig. 38C**, *unpublished data*).

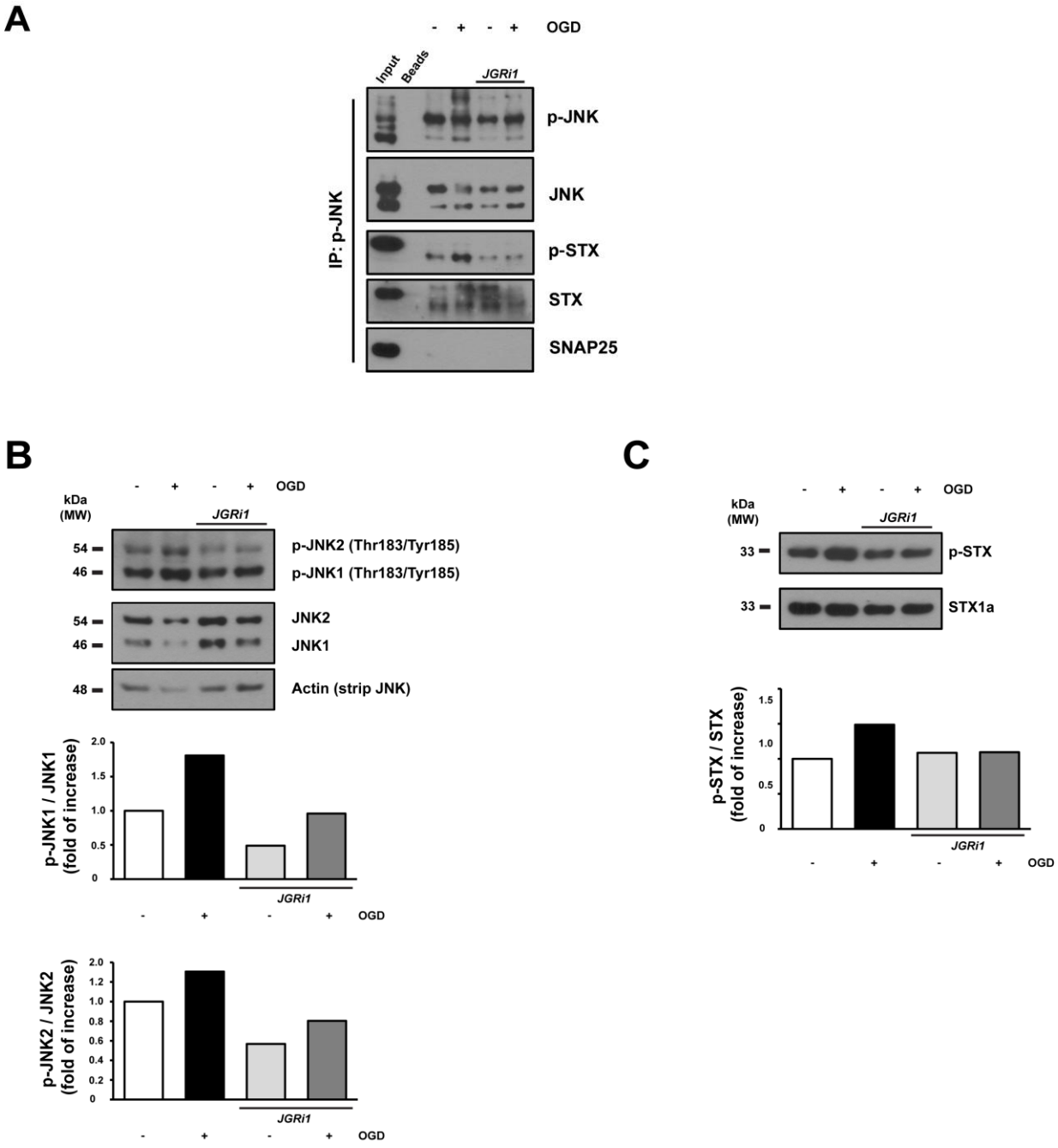

Fig. 38

***JGRi1* disrupts JNK/STX1a interaction in the OGD ischemia model** (*unpublished data*).

A) p-JNK IP experiment on slices subjected to OGD. JNK phosphorylation was clearly augmented by deprivation of oxygen and glucose whilst it was restored by 1 h pretreatment with *JGRi1* (10 µM). p-STX1a as well resulted increased under OGD injury, suggesting the occurrence of JNK/STX interaction also in this experimental model. By contrast, *JGRi1* reduced p-STX1a level, whereas SNAP25 was not involved in p-JNK pull-down.

B) Western blotting analysis on slices subjected to OGD. Under this experimental setting, both p-JNK1 and p-JNK2 levels were augmented, as indicated by higher band reactivity. *JGRi1* (10 µM) was able to rescue the phosphorylation state of both JNK isoforms.

C) OGD insult on cortical neurons increased STX1a phosphorylation that was in turn prevented by pretreatment with *JGRi1* (10 µM), confirming the data already observed in cortical synaptosomes.

In vivo brain ischemia is rescued by *JGRi1* administration in the MCAo mouse model

The neuroprotective effect of *JGRi1* during brain ischemia was assessed in mice subjected to 1 h of middle cerebral artery occlusion (MCAo), followed by 24 h of reperfusion. As shown in **Fig. 39**, ICV injection of *JGRi1* (16ng/5µl) 30 minutes before the induction of ischemia effectively reduced both infarcted areas and volumes in cortical areas when compared to control mice (64 ± 9 and 43 ± 6 mm^3 in saline- and *JGRi1*-treated mice, respectively; n = 8 per group, *p < 0.05).

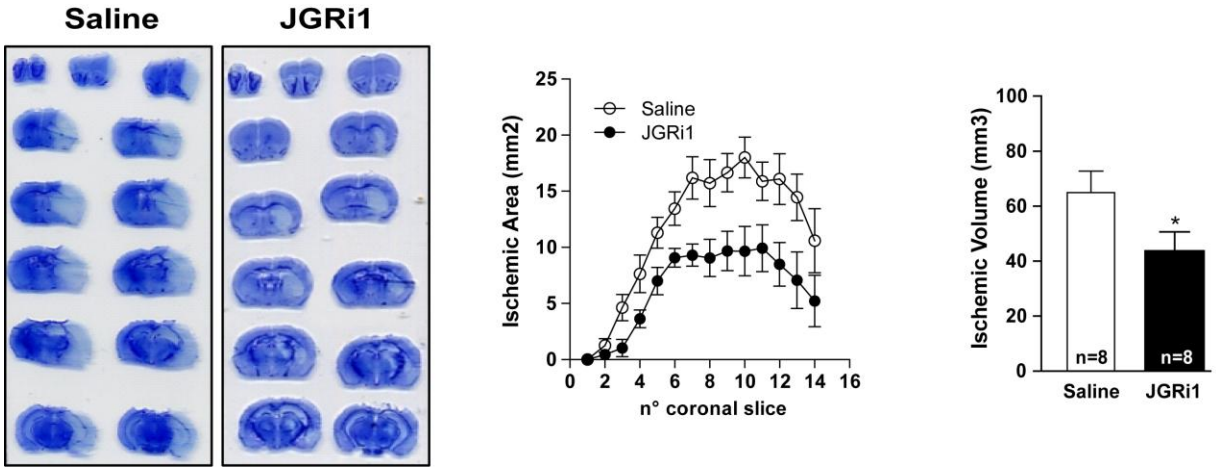

Fig. 39
***JGRi1* rescues infarct insult in the MCAo mouse model.**
Visualization of infarct distribution (pale areas) in toluidine blue-stained coronal brain slices of representative saline- or *JGRi1*-treated mice (left). Effects of *JGRi1* (16ng/5µl, ICV) administered 30 minutes before inducing ischemia upon infarcted areas (in mm^2; centre) and infarcted volumes (in mm^3; right) of mice subjected to 1 h MCAo followed by 24 h reperfusion. Data represent the mean ± SEM of 8 mice per group. *p < 0.05, Student's *t*-test.

Genetic study of *STX1A* SNPs in blood human samples from stroke patients

Taking into account the importance of the STX1a protein in the mechanism of SNARE trafficking so far described, a pilot study was conducted on human blood samples of a group of stroke patients, with the aim of assessing the presence and the implication of *STX1A* single nucleotide polymorphisms (SNPs).

In the other hand, JNK2 sequence is strongly conserved and does not present any SNP.

The SNPs chosen for the gene *STX1A* have been already reported to be associated with pathologies in which *excitotoxicity* plays an important role, *i.e.* migraine and autism (Corominas et al., 2009; Nakamura et al., 2008). Analysing the *STX1A* gene sequence, three interesting polymorphisms have been identified within introns sequence, namely *rs4717806*, *rs6951030* and *rs2293489*, with the latter being located in *WBSCR22* gene, ~6 kbp upstream to 5' UTR *STX1A* gene (**Fig. 40A**). The analysis of *rs2293489* and *rs4717806* SNPs showed significant differences between Acute Ischemic Stroke (AIS) and Healthy Control (HC) subjects in both genotype distributions (p_c= 0.024; p_c= 0.048 respectively) and allele frequencies (p= 0.007; p= 0.012 respectively) (**Tab. 2**), while no significant association was found for *rs6951030* (data not shown).

The logistic regression analysis performed for *rs2293489* and *rs4717806* showed a correlation between T and A nucleotides respectively with high Mini Mental State Evaluation (MMSE) scores (p_c= 0.004, β= 1.33; p_c= 0.012, β= 1.17).

Due to the strong Linkage disequilibrium (r^2= 0.91) between *rs2293489* and *rs4717806*, the haplotype analysis was performed excluding *rs6951030* (**Fig. 40B**). T-A haplotype is more frequent in HC (p= 0.01) while C-T haplotype is more represented among AIS patients (p= 0.01) (**Tab. 3** and **Fig. 40C**).

Plink analysis showed that *rs2293489*/*rs4717806* T-A haplotype is significantly associated with higher MMSE scores (p_c= 0.007; positive value β= 1.20) whereas C-T with lower MMSE scores (p_c= 0.003; negative value β= -1.32) (**Tab. 4**).

The results were confirmed after covariate (age, sex) correction.

A

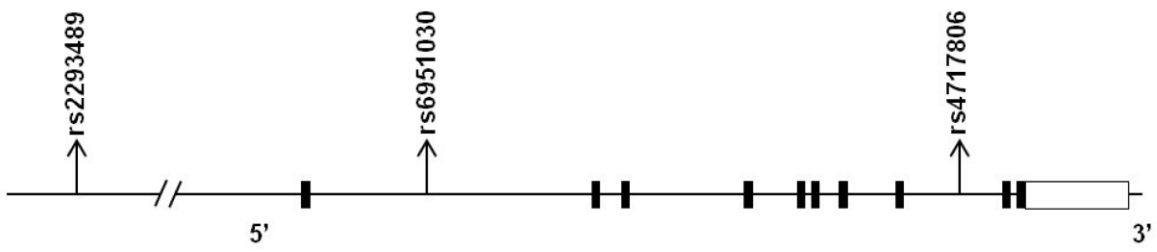

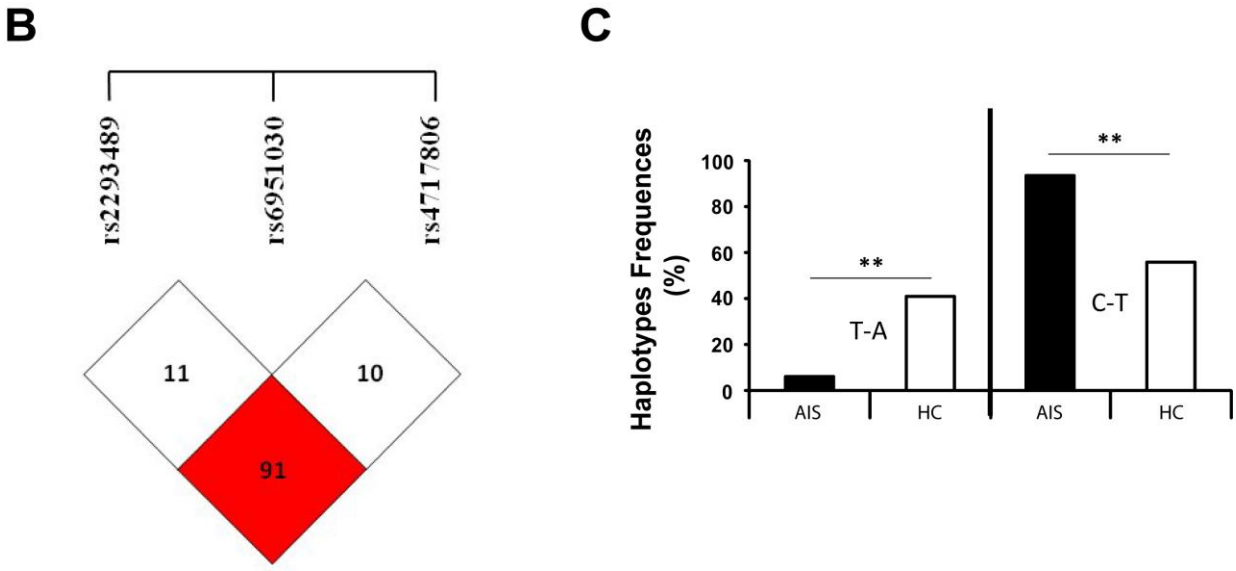

Fig. 40

A) Genomic sequence of *STX1A* and tested SNPs localization. Exons are indicated by boxes, introns are indicated by lines. SNPs positions are denoted by arrows.

B) Linkage Disequilibrium Plot for tested SNPs; r^2 values are reported.

C) Haplotype of *STX1A rs2293489*/*rs4717806* frequencies distribution in AIS and HC subjects. $^{**}p_c = 0.01$

STX1A SNPs	AIS	HC	p_c value	OR [95% CI]
rs2293489				
Genotypes (%)			**0.024**	
CC	87.5	29.4	0.021	14.77 [1.72-409.2]
CT	12.5	52.9	0.142	0.137 [0.005-1.156]
TT	0	17.6	0.590	0 [0.0-3.633]
Alleles (%)			**0.007**	11.842 [1.40-100.1]
C	93.8	55.9	**0.007**	11.38 [1.719-267.2]
T	6.2	44.1	**0.007**	0.088 [0.003-0.581]
rs4717806				
Genotypes (%)			**0.048**	
AA	0	17.6	0.590	0 [0.0-3.633]
AT	12.5	47.1	0.238	0.171 [0.006-1.458]
TT	87.5	35.3	**0.042**	11.53 [1.361-315]
Alleles (%)			**0.012**	0.095 [0.01-0.86]
A	6.2	41.2	**0.012**	0.099 [0.004-0.657]
T	93.8	58.8	**0.012**	10.11 [1.521-237.9]

Tab. 2
Genotype and allele distributions of *STX1A* SNPs *rs2293489* and *rs4717806* in AIS patients and HC.
AIS: Acute Ischemic Stroke, HC: Healthy Controls, p_c: Pearson's p value; OR: odd ratio; 95% CI: interval of confidence.
Significant p_c values are reported in bold.

SNP1	SNP2	Haplotype	χ^2	p value	OR	95% CI
rs2293489	***rs4717806***	T-A	6.64	0.01	0.09	0.01-0.76
		C-T	6.64	0.01	11.05	1.30-93.82

Tab. 3
Haplotype distribution of *STX1A rs2293489/rs4717806* in AIS patients and HC.
OR: odd ratio; 95% CI: interval of confidence.

SNP1	SNP2	Haplotype	Beta	STAT	p_c value
rs2293489	***rs4717806***	T-A	1.20	2.937	**0.007**
		C-T	-1.32	-3.327	**0.003**

Tab. 4
Analysis of *STX1A* haplotype *rs2293489/rs4717806* in relation to MMSE score in AIS patients and HC subjects.

DISCUSSION

The breakthroughs achieved by virtue of a deeper scientific knowledge and an improved medico-technical expertise have so far attempted to find new therapeutic opportunities in the field of neuroprotection.

Nevertheless, cerebral ischemia still represents a pathology with roughly no prophylaxis, limited clinical management, and almost poor prognosis.

Stroke survivors are generally enslaved by two *sequelae*: either a second, possibly fatal acute stroke or multiple chronic ischemic events, with the risk of recurrence ranging between 5% and 20% per year (Gupta et al., 2014). Additionally, the damage correlated to the reperfusion injury may be as threatening as the ischemic injury itself.

Consequently, besides monitoring risk factors in predisposed subjects, the principal goal in managing stroke patients is to prevent further cerebrovascular events, since no real primary prevention does exist.

Recommended approaches for secondary prevention include addressing modifiable risk factors (high blood pressure and cholesterol), initiating long-term antithrombotic therapy, and intervening surgically, when indicated. Unfortunately, the majority of patients are not suitable candidates for mechanical or pharmacological thrombolysis, the intervention that presently represents the unique FDA-approved treatment for ischemia. In addition, the consensus in the stroke medical literature asserts that most of the neuronal demise arises because ischemia occurs within a dramatically brief time period, leaving behind a ridiculously narrow therapeutic window for neuroprotective cares.

Combining preclinical and clinical evidence, the time from symptom onset to the provision of a feasible intervention for substantial reduction of damage might be as short as 1 hour, generally referred to as the "*golden hour*" (Chamorro et al., 2016). The rapid progression of brain damage seems indeed to be almost irreversible already following 3 to 4.5 hours from symptoms onset, as observed from MRI and CT scans.

It appears therefore obvious how urgent and critical should be a robust identification of the biochemical mechanisms underlying the ischemic cascade, in order to develop and provide more effective and convincing treatments to improve recovery from brain damage or, hopefully, even prevent that damage.

The major regulatory site for neuronal activity-mediated chemical transmission is the presynaptic nerve terminal, embedded with a plethora of metabotropic and ionotropic receptors. Among those, NMDA receptors are well-known supporters of the *excitotoxic* glutamate spillover undermining neurons during cerebral ischemia (Lai et al., 2014).

Sadly, the efforts of both preclinical research and pharmaceutical industries to develop an efficient NMDAR inhibitor to contrast *excitotoxicity* have been unsuccessful over the last decades (Chamorro et al., 2016; Ikonomidou and Turski, 2002). One of the possible explanation for such widespread discouraging clinical trials failure of NMDAR inhibitors might be the inappropriate pharmacological action of these molecules that generally directly block the receptor activity, thereby compromising also the normal neurotransmission in certain areas of the brain, ultimately leading to harmful adverse effects (Lipton, 2004).

In an attempt to circumvent past reminiscences of ruinous experimental efforts, and moreover considering the poor risks-benefits ratio as well as the limited time widow for appropriate intervention in pan-NMDAR-mediated glutamate blockade, we focused our speculations on eventual intracellular partners of the NMDA receptors with the aim of disclosing novel therapeutic targets that might be more specific, safer and with a delayed opportunity for intervention.

Additionally, beside several evidences reporting the effects of cerebral ischemia at postsynaptic sites (*i.e.* intracellular Ca^{2+} overload, activation of Ca^{2+}-induced proteolytic enzymes, generation of free radicals), we chose to take into consideration the presynaptic terminal, specifically intervening on the modulation of the excessive release of excitatory neurotransmitter.

Herein, we introduce a new molecule specifically designed and produced to inhibit the presynaptic NMDA receptor activity, via the blockade of an intracellular downstream pathway that we discovered.

In a recent published work, we already demonstrated that the presynaptic release of glutamate evoked by NMDA during *excitotoxic* conditions is specifically mediated by the cooperation between NMDARs and the JNK2 isoform. For the purposes of these previous findings, the presynaptic expression of JNK was assessed by using a synaptic fractionation protocol supported by immunogold staining, while JNK protein activity was inhibited by means of a commercial cell-permeable peptide (*L-JNKi1*) containing a JNK-binding domain (JBD) effector linked to a cargo sequence.

Coherently, both *L-JNKi1* treated synaptosomes and JNK2 knock-out mice exhibited a drastic reduction of glutamate release upon NMDA overstimulation in cortical nerve endings (Nisticò et al., 2015).

Due to the fact that *L-JNKi1* competes with JBDs to disrupt the interaction between all JNKs and their scaffolding protein JIP, and also considering that JNK2 appeared as the critical player involved in NMDAR overactivation, the present work is the natural prosecution of previous evidences.

We indeed investigated a possible molecular mechanism to justify the specific involvement of JNK2 in this presynaptic phenomenon, unveiling for the first time that the mechanism by which NMDA controls glutamate overflow might pass through the interaction between JNK2, presynaptic JIP and other proteins of the release machinery, specifically addressing to the strong JNK2/STX1a interplay occurring upon the massive *excitotoxic* glutamate overflow.

The observation that JNK2 is expressed in high proportion at synaptic *puncta* supports our functional data, demonstrating that JNK2 can actually interfere with the SNARE complex machinery and potentially modulate glutamate release (Nisticò et al., 2015).

In parallel, STX1a is a presynaptic *t*-SNARE protein that belongs to the SNARE complex machinery and primarily regulates the presynaptic neurotransmitter release (Brunger et al., 1998), including glutamate (Acuna et al., 2014). Although its physiological activity is complex and not yet fully elucidated, STX1a phosphorylation at Ser14 driven by casein kinase II is thought to be a crucial step for the protein activation and subsequent assembly of the SNARE complex. Furthermore, the raising of the intracellular Ca^{2+} concentration in charge of presynaptic membrane depolarization upon NMDA or KCl stimuli is likely the signal that triggers STX1a phosphorylation (Foletti et al., 2000; Tian et al., 2003).

Considering the strong implication of both proteins in this intracellular signaling, we evaluated the possible interaction between JNK2 and STX1a as a novel molecular pathway to target to specifically inhibit presynaptic NMDA receptor overactivation in the frame of ischemic *excitotoxicity*.

It is currently definitely ascertained that neuronal exposure to NMDA induces marked swelling of cell bodies within 1 hour, followed by total neuronal degeneration over the next 48 hours (Centeno et al., 2007).

In this frame, our biological inquiry began by confirming that the expression of both JNK2 and phosphorylated STX1a is increased at synaptic level by convenient NMDA stimulation.

We assessed the actual occurrence of a physical contact between the two proteins by means of immunoprecipitation assays that proved the pull-down of STX1a carried by the activated JNK.

In order to identify a possible region of contact between the two proteins, a protein docking approach led to the identification of an amino acidic sequence of STX1a univocally interacting with JNK2. This specific common contact surface was then exploited to produce *JGRi1*, a cell-permeable peptide (CPP) containing the Tat amino acid sequence to confer cell permeability (Chauhan et al., 2007).

Taking advantage of the fluorescein-tagged version of the peptide, we were effectively able to assess the widespread diffusion of FITC-*JGRi1* in cortical and hippocampal brain districts over 24 hours from intraperitoneal and intracerebroventricular administration. On the other hand, the FITC-*JGRi1*-ΔTat version lacked any evidence of fluorescence at confocal observation.

Thus far, CPPs are becoming widely used pharmacological tools to specifically interfere with protein function at intracellular level (Borsello et al., 2003a; Cimini et al., 2016), so that some of them are prominently following the pharmaceutical clinical development for distinct human pathologies (Dinca et al., 2016a; Guidotti et al., 2017).

In line with this panorama, our peptide *JGRi1* demonstrated to be able to efficiently disrupt the presynaptic JNK2/STX1a protein-protein interaction, in turn impeding STX1a phosphorylation at Ser14, preventing the SNARE complex formation, and ultimately reducing the *excitotoxic* NMDA-evoked release of glutamate within the ischemic cascade.

Parallel findings from another research group recently evidenced that both STX1a and STX2 contain a JNK binding domain (JBD) respectively at 151-155 and 261-270 amino acid residues. In their experimental conditions, JNK1 was co-immunoprecipitated with both STX1a and 2 while JNK2 and 3 preferentially interacted with STX2 (Biggi et al., 2017).

In our computational analysis we unveiled a different amino acid cluster (90-103 and 105-109 amino acid residues) besides the classical JBD that appears highly conserved and specific for JNK2 compared to JNK1 and JNK3, being those two proteins more similar among them.

We identified the JNK2/STX1a interaction in this specific sequence and, consequently, we designed and synthetized *JGRi1* exactly on that.

Coherently with our expectations, *JGRi1* efficiently disrupted JNK2/STX1a interplay with high target specificity, without affecting JNK1/ nor JNK3/STX1a eventual interactions, as

evidenced in overexpressing experiments performed in HEK-293 cells and synaptosomal preparations.

Moreover, we did not obtain any evidence of SNAP25 involvement in this initial stage of the SNARE complex formation, possibly due to its partial assembly in a primed structure with STX1a in resting states, followed by an only belated participation to the release machinery (Dawidowski and Cafiso, 2016; Vogel et al., 2000).

Under a functional point of view, the strong neuroprotective efficacy of *JGRi1* is especially worth to be mentioned. Indeed, we tested *JGRi1* on several experimental paradigms, delineating an encouraging widespread activity of neuronal death rescue.

JGRi1 reduced presynaptic NMDA-evoked neurotransmitter release from synaptic vesicles in synaptosomal preparations, as evaluated via Synaptogreen destaining or tritiated [^{3}H]D-aspartate β–emitting radiation.

Our peptide also blocked spontaneous presynaptic NMDA currents in electrophysiology experiments, and prevented NMDA-elicited neuronal death in neurochemical assays.

In a more therapeutic perspective, we reproduced the oxygen/glucose deprivation (OGD) model of ischemia in mouse cortical slices. In shortage of nutrient and oxygen supply, *JGRi1* was again able to interfere with JNK2/STX1a interaction, restoring the levels of phosphorylated proteins back to the control undeprived ones.

Finally, we performed an *in vivo* experiment using the well characterized model of transient focal brain ischemia produced in mouse via the occlusion of the middle cerebral artery (MCAo) (Muzzi et al., 2012). *JGRi1* administered as intracerebroventricular injection 30 min before ischemia induction demonstrated a valuable neuroprotective effect on infarcted cerebral tissue. Upon *JGRi1* pretreatment, indeed, both injured area and volume were significantly reduced, with an almost complete protection in cortical regions.

This striking result, obtained for the first time with a specific presynaptic JNK2 inhibitor, suggests that prevention of *excitotoxicity* can really represent a valuable and efficient approach to reduce brain damage. Since glutamate blood levels can be easily measured and assessed as a biomarker for stroke (Jickling and Sharp, 2011), we believe that safe anti-*excitotoxic* drugs like *JGRi1* could be particularly useful in the clinical practice within a proper time window, aiming not only at the perspective of containing ongoing neuronal demise, but especially at preventing and protecting the brain from recurrent ischemic episodes.

In conclusion, the possibility to finely predict a pathology onset with specific biomarkers undoubtedly represents a major fundamental goal of preventive medicine, particularly when these pathologies plod along in finding a suitable therapeutic treatment.

The evaluation of genetic predisposition in this context is an important yet valuable issue to consider.

Given the key role played by STX1a in the mechanism of vesicle release, we wonder whether there could be any genomic participation to stroke susceptibility, hypothesizing that it should be interesting to study the genetic variants of *STX1A* gene.

We did not consider JNK2 in the genomic analysis since its sequence is conversely highly conserved.

From a careful examination of the scientific literature, we identified three single nucleotide polymorphisms (SNPs) of *STX1A* already associated with migraine and autisms (Corominas et al., 2009; Nakamura et al., 2008), other pathologies wherein *excitotoxicity* contributes to the etiology. We therefore ran a pilot study to analyse the SNPs profiles from blood samples of a cohort of acute ischemic stroke (AIS) patients, in order to confirm the clinical relevance of our data.

The genotype analysis evidenced that two of these polymorphisms (*rs229489* C/T and *rs4717806* A/T) are significantly associated with AIS both for alleles (C and T respectively) and for homozygous genotypes (CC and TT respectively). In line with these findings, the haplotype *rs2293489*/*rs4717806* C-T is more frequent in AIS patients with a positive risk related to stroke and, as expected, is associated with lower MMSE scores. Conversely, the logistic regression analysis showed that *rs2293489* (T) and *rs4717806* (A) alleles are instead associated with higher MMSE scores, in agreement with the protective role already described for autism, concerning the *rs4717806* (A) allele (Corominas et al., 2009).

Overall, we have associated here for the first time these intronic SNPs on *STX1A* gene with the susceptibility to acute ischemic stroke in the Caucasian population, speculating a potential role for STX1a expression, in addition to *cis*- and *trans*-acting factors, to its implication in the excessive glutamate release from presynaptic sites in times of *excitotoxicity* (Durdiaková et al., 2014; Nakamura et al., 2011, 2008).

Glutamate-mediated injury remains a fundamental yet unmet clinical target. So far, several research attempts tried to disclose novel drugs or pharmacological approaches in the field of neuroprotection for either preventive therapy or ongoing post-stroke clinical management.

At present, patients subjected to chronic stroke recurrence are mostly managed with anticoagulants like aspirin, either alone or in combination with some other cardiovascular drugs including clopidogrel or dipyridamole. The rate of clinical success remains in any case very modest, since no specific drug has be so far formulated to purposely tackle *excitotoxicity* (Diener, 2006). Even the promising NMDAR inhibitors failed in their goal, due to their lack of selectivity of action and consequent undesired adverse effects.

In this demoralizing scenario sprinkled by the withdrawal of many new molecules from clinical trials, we yearn to propose a novel tool effectively able to address a precise intracellular molecular mechanism, in order to ensure the pharmacological safety and avoid any unpleasant off-target consequence. Additionally, we make it cell-permeable and we tested it in a plethora of different experimental paradigms mimicking *in vivo* human ischemia, in order to assess the real neuroprotective efficacy.

In the present medical panorama poor in neuroprotective agents, we hope that *JGRi1* could represent the difference. On purpose, *JGRi1* was patented with the indication of *"cell-permeable peptide system for treating diseases caused by excitotoxicity"* (n° WO 2015150934 A1) and is presently following the pharmaceutical development for clinical translatability and trial inclusion in the setting of *excitotoxicity*-linked pathologies.

If there is a reason in science, and undoubtedly there is, our present reason is the attempt to offer a chance for a respectable life to people torn apart by devastating ischemic attacks.

JGRi1 could be the instrument to sublimate our reason.

REFERENCES

Abeti, R., Abramov, A.Y., 2015. Mitochondrial Ca2+ in neurodegenerative disorders. Pharmacol. Res. 99, 377–381. doi:10.1016/j.phrs.2015.05.007.

Acuna, C., Guo, Q., Burré, J., Sharma, M., Sun, J., Südhof, T.C., 2014. Microsecond Dissection of Neurotransmitter Release: SNARE-Complex Assembly Dictates Speed and Ca2+ Sensitivity. Neuron 82, 1088–1100. doi:10.1016/j.neuron.2014.04.020.

Aksenova, M. V, Burbaeva, G.S., Kandror, K. V, Kapkov, D. V, Stepanov, A.S., 1991. The decreased level of casein kinase 2 in brain cortex of schizophrenic and Alzheimer's disease patients. FEBS Lett. 279, 55–7.

Alessandrini, A., Namura, S., Moskowitz, M.A., Bonventre, J. V, 1999. MEK1 protein kinase inhibition protects against damage resulting from focal cerebral ischemia. Proc. Natl. Acad. Sci. U. S. A. 96, 12866–9.

Allan, S.M., Tyrrell, P.J., Rothwell, N.J., 2005. Interleukin-1 and neuronal injury. Nat. Rev. Immunol. 5, 629–640. doi:10.1038/nri1664.

Allgaier, M., Allgaier, C., 2014. An update on drug treatment options of Alzheimer's disease. Front. Biosci. (Landmark Ed. 19, 1345–54.

Alper, B.S., Malone-Moses, M., McLellan, J.S., Prasad, K., Manheimer, E., 2015. Thrombolysis in acute ischaemic stroke: time for a rethink? BMJ 350, h1075.

Amaral, E., Guatimosim, S., Guatimosim, C., 2011. Using the Fluorescent Styryl Dye FM1-43 to Visualize Synaptic Vesicles Exocytosis and Endocytosis in Motor Nerve Terminals, in: Methods in Molecular Biology (Clifton, N.J.). pp. 137–148. doi:10.1007/978-1-60761-950-5_8.

Andersen, L.P.H., Gögenur, I., Rosenberg, J., Reiter, R.J., 2016. The Safety of Melatonin in Humans. Clin. Drug Investig. 36, 169–175. doi:10.1007/s40261-015-0368-5.

Ansari, S., McConnell, D.J., Velat, G.J., Waters, M.F., Levy, E.I., Hoh, B.L., Mocco, J., 2011. Intracranial Stents for Treatment of Acute Ischemic Stroke: Evolution and Current Status. World Neurosurg. 76, S24–S34. doi:10.1016/j.wneu.2011.02.031.

Bai, F., Witzmann, F.A., 2007. Synaptosome proteomics. Subcell. Biochem. 43, 77–98.

Bailey, E.L., Smith, C., Sudlow, C.L.M., Wardlaw, J.M., 2012. Pathology of Lacunar Ischemic Stroke in Humans - A Systematic Review. Brain Pathol. 22, 583–591. doi:10.1111/j.1750-3639.2012.00575.x.

Bailey, R.R., 2017. Promoting Physical Activity and Nutrition in People With Stroke. Am. J. Occup. Ther. 71, 7105360010p1. doi:10.5014/ajot.2017.021378.

Balasubramanian, S., Klein, J., Burdet, E., 2010. Robot-assisted rehabilitation of hand function. Curr. Opin. Neurol. 23, 661–670. doi:10.1097/WCO.0b013e32833e99a4.

Balasubramanian, K., Schroit, A.J., 2003. Aminophospholipid Asymmetry: A Matter of Life and Death. Annu. Rev. Physiol. 65, 701–734. doi:10.1146/annurev.physiol.65.092101.142459.

Banerjee, A., Larsen, R.S., Philpot, B.D., Paulsen, O., 2016. Roles of Presynaptic NMDA Receptors in Neurotransmission and Plasticity. Trends Neurosci. 39, 26–39. doi:10.1016/j.tins.2015.11.001.

Barclay, R.E., Stevenson, T.J., Poluha, W., Ripat, J., Nett, C., Srikesavan, C.S., 2015. Interventions for improving community ambulation in individuals with stroke. Cochrane database Syst. Rev. CD010200. doi:10.1002/14651858.CD010200.pub2.

Bechara, C., Sagan, S., 2013. Cell-penetrating peptides: 20 years later, where do we stand? FEBS Lett. 587, 1693–1702. doi:10.1016/j.febslet.2013.04.031.

Becker, K.J., Dankwa, D., Lee, R., Schulze, J., Zierath, D., Tanzi, P., Cain, K., Dressel, A., Shibata, D., Weinstein, J., 2014. Stroke, IL-1ra, IL1RN, Infection and Outcome. Neurocrit. Care 21, 140–146. doi:10.1007/s12028-013-9899-x.

Beckman, J.S., 1996. Oxidative Damage and Tyrosine Nitration from Peroxynitrite. Chem. Res. Toxicol. 9, 836–844. doi:10.1021/tx9501445.

Bektas, H., Wu, T.-C., Kasam, M., Harun, N., Sitton, C.W., Grotta, J.C., Savitz, S.I., 2010. Increased Blood-Brain Barrier Permeability on Perfusion CT Might Predict Malignant Middle Cerebral Artery Infarction. Stroke 41, 2539–2544. doi:10.1161/STROKEAHA.110.591362.

Berg, J.S., Brunetti-Pierri, N., Peters, S.U., Kang, S.-H.L., Fong, C., Salamone, J., Freedenberg, D., Hannig, V.L., Prock, L.A., Miller, D.T., Raffalli, P., Harris, D.J., Erickson, R.P., Cunniff, C., Clark, G.D., Blazo, M.A., Peiffer, D.A., Gunderson, K.L., Sahoo, T., Patel, A., Lupski, J.R., Beaudet, A.L., Cheung, S.W., 2007. Speech delay and autism spectrum behaviors are frequently associated with duplication of the 7q11.23 Williams-Beuren syndrome region. Genet. Med. 9, 427–41. doi:10.1097GIM.0b013e3180986192.

Betancur, C., Corbex, M., Spielewoy, C., Philippe, A., Laplanche, J.-L., Launay, J.-M., Gillberg, C., Mouren-Siméoni, M.-C., Hamon, M., Giros, B., Nosten-Bertrand, M., Leboyer, M., 2002. Serotonin transporter gene polymorphisms and hyperserotonemia in autistic disorder. Mol. Psychiatry 7, 67–71. doi:10.1038/sj/mp/4000923.

Bethea, J.R., Dietrich, W.D., 2002. Targeting the host inflammatory response in traumatic spinal cord injury. Curr. Opin. Neurol. 15, 355–60.

Biggi, S., Buccarello, L., Sclip, A., Lippiello, P., Tonna, N., Rumio, C., Di Marino, D., Miniaci, M.C., Borsello, T., 2017. Evidence of Presynaptic Localization and Function of the c-Jun N-Terminal Kinase. Neural Plast. 2017, 1–14. doi:10.1155/2017/6468356.

Borsello, T., Clarke, P.G.H., Hirt, L., Vercelli, A., Repici, M., Schorderet, D.F., Bogousslavsky, J., Bonny, C., 2003a. A peptide inhibitor of c-Jun N-terminal kinase protects against excitotoxicity and cerebral ischemia. Nat. Med. 9, 1180–1186. doi:10.1038/nm911.

Borsello, T., Croquelois, K., Hornung, J.-P., Clarke, P.G.H., 2003b. N-methyl-d-aspartate-triggered neuronal death in organotypic hippocampal cultures is endocytic, autophagic and mediated by the c-Jun N-terminal kinase pathway. Eur. J. Neurosci. 18, 473–85.

Brady, M.C., Kelly, H., Godwin, J., Enderby, P., Campbell, P., 2016. Speech and language therapy for aphasia following stroke. Cochrane database Syst. Rev. CD000425. doi:10.1002/14651858.CD000425.pub4.

Bramlett, H., Dietrich, D., 2002. Quantitative structural changes in white and gray matter 1 year following traumatic brain injury in rats. Acta Neuropathol. 103, 607–614. doi:10.1007/s00401-001-0510-8.

Bramlett, H.M., Dietrich, W.D., 2004. Pathophysiology of Cerebral Ischemia and Brain Trauma: Similarities and Differences. J. Cereb. Blood Flow Metab. 24, 133–150. doi:10.1097/01.WCB.0000111614.19196.04.

Brassai, A., Suvanjeiev, R.-G., Bán, E.-G., Lakatos, M., 2015. Role of synaptic and nonsynaptic glutamate receptors in ischaemia induced neurotoxicity. Brain Res. Bull. 112, 1–6. doi:10.1016/j.brainresbull.2014.12.007.

Broughton, B.R.S., Reutens, D.C., Sobey, C.G., 2009. Apoptotic Mechanisms After Cerebral Ischemia. Stroke 40, e331–e339. doi:10.1161/STROKEAHA.108.531632.

Brouns, R., De Smedt, V.H., 2012. Biochemical pathways and their clinical applications in acute ischemic stroke. ResearchGate.

Brunger, A.T., Sutton, R.B., Fasshauer, D., Jahn, R., 1998. Crystal structure of a SNARE complex involved in synaptic exocytosis at 2.4 A resolution. Nature 395, 347–353. doi:10.1038/26412.

Bruno, A., Shah, N., Lin, C., Close, B., Hess, D.C., Davis, K., Baute, V., Switzer, J.A., Waller, J.L., Nichols, F.T., 2010. Improving Modified Rankin Scale Assessment With a Simplified Questionnaire. Stroke 41, 1048–1050. doi:10.1161/STROKEAHA.109.571562.

Bullock, M.R., Merchant, R.E., Carmack, C.A., Doppenberg, E., Shah, A.K., Wilner, K.D., Ko, G., Williams, S.A., 1999. An Open-Label Study of CP-101,606 in Subjects with a Severe Traumatic Head Injury or Spontaneous Intracerebral Hemorrhage. Ann. N. Y. Acad. Sci. 890, 51–58. doi:10.1111/j.1749-6632.1999.tb07980.x.

Burré, J., Sharma, M., Tsetsenis, T., Buchman, V., Etherton, M.R., Südhof, T.C., 2010. Alpha-synuclein promotes SNARE-complex assembly in vivo and in vitro. Science 329, 1663–7. doi:10.1126/science.1195227.

Campos, F., Pérez-Mato, M., Agulla, J., Blanco, M., Barral, D., Almeida, Á., Brea, D., Waeber, C., Castillo, J., Ramos-Cabrer, P., 2012. Glutamate Excitoxicity Is the Key Molecular Mechanism Which Is Influenced by Body Temperature during the Acute Phase of Brain Stroke. PLoS One 7, e44191. doi:10.1371/journal.pone.0044191.

Canazza, A., Minati, L., Boffano, C., Parati, E., Binks, S., 2014. Experimental Models of Brain Ischemia: A Review of Techniques, Magnetic Resonance Imaging, and Investigational Cell-Based Therapies. Front. Neurol. 5, 19. doi:10.3389/fneur.2014.00019.

Cao, F., Hata, R., Zhu, P., Niinobe, M., Sakanaka, M., 2009. Up-regulation of syntaxin1 in ischemic cortex after permanent focal ischemia in rats. Brain Res. 1272, 52–61. doi:10.1016/j.brainres.2009.03.047.

Cao, Z., Balasubramanian, A., Marrelli, S.P., 2014. Pharmacologically induced hypothermia via TRPV1 channel agonism provides neuroprotection following ischemic stroke when initiated 90 min after reperfusion. AJP Regul. Integr. Comp. Physiol. 306, R149–R156. doi:10.1152/ajpregu.00329.2013.

Castillo, M.A., Ghose, S., Tamminga, C.A., Ulery-Reynolds, P.G., 2010. Deficits in Syntaxin 1 Phosphorylation in Schizophrenia Prefrontal Cortex. Biol. Psychiatry 67, 208–216. doi:10.1016/j.biopsych.2009.07.029.

Centeno, C., Repici, M., Chatton, J.-Y., Riederer, B.M., Bonny, C., Nicod, P., Price, M., Clarke, P.G.H., Papa, S., Franzoso, G., Borsello, T., 2007. Role of the JNK pathway in NMDA-mediated excitotoxicity of cortical neurons. Cell Death Differ. 14, 240–253. doi:10.1038/sj.cdd.4401988.

Chamorro, Á., Amaro, S., Castellanos, M., Segura, T., Arenillas, J., Martí-Fábregas, J., Gállego, J., Krupinski, J., Gomis, M., Cánovas, D., Carné, X., Deulofeu, R., Román, L.S., Oleaga, L., Torres, F., Planas, A.M., URICO-ICTUS Investigators, 2014. Safety and efficacy of uric acid in patients with acute stroke (URICO-ICTUS): a randomised, double-blind phase 2b/3 trial. Lancet Neurol. 13, 453–460. doi:10.1016/S1474-4422(14)70054-7.

Chamorro, Á., Dirnagl, U., Urra, X., Planas, A.M., 2016. Neuroprotection in acute stroke: targeting excitotoxicity, oxidative and nitrosative stress, and inflammation. Lancet. Neurol. 15, 869–881. doi:10.1016/S1474-4422(16)00114-9.

Chauhan, A., Tikoo, A., Kapur, A.K., Singh, M., 2007. The Taming of the Cell Penetrating Domain of the HIV Tat: Myths and Realities. J. Control. Release 117, 148. doi:10.1016/j.jconrel.2006.10.031.

Chen, G.Y., Nuñez, G., 2010. Sterile inflammation: sensing and reacting to damage. Nat. Rev. Immunol. 10, 826–837. doi:10.1038/nri2873.

Chen, S., Li, S., 2012. The Na+/Ca2+ exchanger in cardiac ischemia/reperfusion injury. Med. Sci. Monit. 18, RA161–5. doi:10.12659/msm.883533.

Cheng, J., Liu, W., Duffney, L.J., Yan, Z., 2013. SNARE proteins are essential in the potentiation of NMDA receptors by group II metabotropic glutamate receptors. J. Physiol. 591, 3935–47. doi:10.1113/jphysiol.2013.255075.

Cho, S., Wood, A., Bowlby, M.R., 2007. Brain slices as models for neurodegenerative disease and screening platforms to identify novel therapeutics. Curr. Neuropharmacol. 5, 19–33.

Choi, K.-E., Hall, C.L., Sun, J.-M., Wei, L., Mohamad, O., Dix, T.A., Yu, S.P., 2012. A novel stroke therapy of pharmacologically induced hypothermia after focal cerebral ischemia in mice. FASEB J. 26, 2799–2810. doi:10.1096/fj.11-201822.

Choi, S.Y., Choi, E.Y., Han, K., Park, J., Kim, K.-A., Bahn, J.H., Kwon, H.Y., Lee, H.J., Ryu, J., Lee, K.S., 2002. Mutational analysis of a human immunodeficiency virus type 1 Tat protein transduction domain which is required for delivery of an exogenous protein into mammalian cells. J. Gen. Virol. 83, 1173–1181. doi:10.1099/0022-1317-83-5-1173.

Cimarosti, H., Henley, J.M., 2008. Investigating the Mechanisms Underlying Neuronal Death in Ischemia Using In Vitro Oxygen-Glucose Deprivation: Potential Involvement of Protein SUMOylation. Neurosci. 14, 626–636. doi:10.1177/1073858408322677.

Cimarosti, H., Rodnight, R., Tavares, A., Paiva, R., Valentim, L., Rocha, E., Salbego, C., 2001. An investigation of the neuroprotective effect of lithium in organotypic slice cultures of rat hippocampus exposed to oxygen and glucose deprivation. Neurosci. Lett. 315, 33–6.

Cimini, S., Sclip, A., Mancini, S., Colombo, L., Messa, M., Cagnotto, A., Di Fede, G., Tagliavini, F., Salmona, M., Borsello, T., 2016. The cell-permeable A?1-6A2VTAT(D) peptide reverts synaptopathy induced by A?1-42wt. Neurobiol. Dis. 89, 101–111. doi:10.1016/j.nbd.2015.12.013.

Clark, W.M., Wechsler, L.R., Sabounjian, L.A., Schwiderski, U.E., Citicoline Stroke Study Group, 2001. A phase III randomized efficacy trial of 2000 mg citicoline in acute ischemic stroke patients. Neurology 57, 1595–602.

Coffey, E.T., 2014. Nuclear and cytosolic JNK signalling in neurons. Nat. Rev. Neurosci. 15, 285–299. doi:10.1038/nrn3729.

Coghlan, S., Horder, J., Inkster, B., Mendez, M.A., Murphy, D.G., Nutt, D.J., 2012. GABA system dysfunction in autism and related disorders: From synapse to symptoms. Neurosci. Biobehav. Rev. 36, 2044–2055.

doi:10.1016/j.neubiorev.2012.07.005.
Colbourne, F., Grooms, S.Y., Zukin, R.S., Buchan, A.M., Bennett, M.V.L., 2003. Hypothermia rescues hippocampal CA1 neurons and attenuates down-regulation of the AMPA receptor GluR2 subunit after forebrain ischemia. Proc. Natl. Acad. Sci. 100, 2906–2910. doi:10.1073/pnas.2628027100.
Collingridge, G.L., Lester, R.A., 1989. Excitatory amino acid receptors in the vertebrate central nervous system. Pharmacol. Rev. 41, 143–210.
Cook, D.J., Teves, L., Tymianski, M., 2012. Treatment of stroke with a PSD-95 inhibitor in the gyrencephalic primate brain. Nature 483, 213–217. doi:10.1038/nature10841.
Corlew, R., Wang, Y., Ghermazien, H., Erisir, A., Philpot, B.D., 2007. Developmental Switch in the Contribution of Presynaptic and Postsynaptic NMDA Receptors to Long-Term Depression. J. Neurosci. 27, 9835–9845. doi:10.1523/JNEUROSCI.5494-06.2007.
Corominas, R., Ribasés, M., Cuenca-León, E., Narberhaus, B., Serra, S.A., del Toro, M., Roig, M., Fernández-Fernández, J.M., Macaya, A., Cormand, B., 2009. Contribution of syntaxin 1A to the genetic susceptibility to migraine: A case–control association study in the Spanish population. Neurosci. Lett. 455, 105–109. doi:10.1016/j.neulet.2009.03.011.
Danton, G.H., Prado, R., Truettner, J., Watson, B.D., Dietrich, W.D., 2002. Endothelial Nitric Oxide Synthase Pathophysiology after Nonocclusive Common Carotid Artery Thrombosis in Rats. J. Cereb. Blood Flow Metab. 22, 612–619. doi:10.1097/00004647-200205000-00013.
Dávalos, A., Alvarez-Sabín, J., Castillo, J., Díez-Tejedor, E., Ferro, J., Martínez-Vila, E., Serena, J., Segura, T., Cruz, V.T., Masjuan, J., Cobo, E., Secades, J.J., International Citicoline Trial on acUte Stroke (ICTUS) trial investigators, 2012. Citicoline in the treatment of acute ischaemic stroke: an international, randomised, multicentre, placebo-controlled study (ICTUS trial). Lancet 380, 349–357. doi:10.1016/S0140-6736(12)60813-7.
Dávalos, A., Castillo, J., Alvarez-Sabín, J., Secades, J.J., Mercadal, J., López, S., Cobo, E., Warach, S., Sherman, D., Clark, W.M., Lozano, R., 2002. Oral citicoline in acute ischemic stroke: an individual patient data pooling analysis of clinical trials. Stroke 33, 2850–7.
Davis, R.J., 2000. Signal transduction by the JNK group of MAP kinases. Cell 103, 239–52.
Dawidowski, D., Cafiso, D.S., 2016. Munc18-1 and the Syntaxin-1 N Terminus Regulate Open-Closed States in a t-SNARE Complex. Structure 24, 392–400. doi:10.1016/j.str.2016.01.005.
De Butte, M., Fortin, T., Pappas, B.A., 2002. Pinealectomy: behavioral and neuropathological consequences in a chronic cerebral hypoperfusion model. Neurobiol. Aging 23, 309–17.
Deák, F., Xu, Y., Chang, W.-P., Dulubova, I., Khvotchev, M., Liu, X., Südhof, T.C., Rizo, J., 2009. Munc18-1 binding to the neuronal SNARE complex controls synaptic vesicle priming. J. Cell Biol. 184, 751–764. doi:10.1083/jcb.200812026.
del Zoppo, G., Ginis, I., Hallenbeck, J.M., Iadecola, C., Wang, X., Feuerstein, G.Z., 2000. Inflammation and stroke: putative role for cytokines, adhesion molecules and iNOS in brain response to ischemia. Brain Pathol. 10, 95–112.
Dennis, S.H., Jaafari, N., Cimarosti, H., Hanley, J.G., Henley, J.M., Mellor, J.R., 2011. Oxygen/glucose deprivation induces a reduction in synaptic AMPA receptors on hippocampal CA3 neurons mediated by mGluR1 and adenosine A3 receptors. J. Neurosci. 31, 11941–52. doi:10.1523/JNEUROSCI.1183-11.2011.
Derdeyn, C.P., Chimowitz, M.I., 2007. Angioplasty and Stenting for Atherosclerotic Intracranial Stenosis: Rationale for a Randomized Clinical Trial. Neuroimaging Clin. N. Am. 17, 355–363. doi:10.1016/j.nic.2007.05.001.
Dewar, D., Underhill, S.M., Goldberg, M.P., 2003. Oligodendrocytes and Ischemic Brain Injury. J. Cereb. Blood Flow Metab. 23, 263–274. doi:10.1097/01.WCB.0000053472.41007.F9.
Dhamoon, M.S., Moon, Y.P., Paik, M.C., Boden-Albala, B., Rundek, T., Sacco, R.L., Elkind, M.S. V, 2010. Quality of life declines after first ischemic stroke. The Northern Manhattan Study. Neurology 75, 328–34. doi:10.1212/WNL.0b013e3181ea9f03.
Dhanasekaran, D.N., Reddy, E.P., 2008. JNK signaling in apoptosis. Oncogene 27, 6245–6251. doi:10.1038/onc.2008.301.
Diener, H.-C., 2006. Secondary Stroke Prevention with Antiplatelet Drugs: Have We Reached the Ceiling? Int. J. Stroke 1, 4–8. doi:10.1111/j.1747-4949.2005.00016.x.

Dinarello, C.A., van der Meer, J.W.M., 2013. Treating inflammation by blocking interleukin-1 in humans. Semin. Immunol. 25, 469–484. doi:10.1016/j.smim.2013.10.008.

Dinca, A., Chien, W.-M., Chin, M., 2016. Intracellular Delivery of Proteins with Cell-Penetrating Peptides for Therapeutic Uses in Human Disease. Int. J. Mol. Sci. 17, 263. doi:10.3390/ijms17020263.

Dirnagl, U., Endres, M., 2014. Found in Translation: Preclinical Stroke Research Predicts Human Pathophysiology, Clinical Phenotypes, and Therapeutic Outcomes. Stroke 45, 1510–1518. doi:10.1161/STROKEAHA.113.004075.

Dirnagl, U., Iadecola, C., Moskowitz, M.A., 1999. Pathobiology of ischaemic stroke: an integrated view. Trends Neurosci. 22, 391–7.

Doğgan, A., Rao, A.M., Başkaya, M.K., Rao, V.L.R., Rastl, J., Donaldson, D., Dempsey, R.J., 1997. Effects of ifenprodil, a polyamine site NMDA receptor antagonist, on reperfusion injury after transient focal cerebral ischemia. J. Neurosurg. 87, 921–926. doi:10.3171/jns.1997.87.6.0921.

Dong, C., Yang, D.D., Wysk, M., Whitmarsh, A.J., Davis, R.J., Flavell, R.A., 1998. Defective T cell differentiation in the absence of Jnk1. Science 282, 2092–5.

Dunkley, P.R., Jarvie, P.E., Robinson, P.J., 2008. A rapid Percoll gradient procedure for preparation of synaptosomes. Nat. Protoc. 3, 1718–1728. doi:10.1038/nprot.2008.171.

Durdiaková, J., Warrier, V., Banerjee-Basu, S., Baron-Cohen, S., Chakrabarti, B., 2014. STX1A and Asperger syndrome: a replication study. Mol. Autism 5, 14. doi:10.1186/2040-2392-5-14.

Dziedzic, T., 2015. Systemic inflammation as a therapeutic target in acute ischemic stroke. Expert Rev. Neurother. 15, 523–531. doi:10.1586/14737175.2015.1035712.

Edwardson MA, Dromerick D.A., 2017. Ischemic stroke prognosis in adults. URL https://www.uptodate.com/contents/ischemic-stroke-prognosis-in-adults.

Elliott, M.R., Chekeni, F.B., Trampont, P.C., Lazarowski, E.R., Kadl, A., Walk, S.F., Park, D., Woodson, R.I., Ostankovich, M., Sharma, P., Lysiak, J.J., Harden, T.K., Leitinger, N., Ravichandran, K.S., 2009. Nucleotides released by apoptotic cells act as a find-me signal to promote phagocytic clearance. Nature 461, 282–286. doi:10.1038/nature08296.

Eltzschig, H.K., Eckle, T., 2011. Ischemia and reperfusion—from mechanism to translation. Nat. Med. 17, 1391–1401. doi:10.1038/nm.2507.

Emberson, J., Lees, K.R., Lyden, P., Blackwell, L., Albers, G., Bluhmki, E., Brott, T., Cohen, G., Davis, S., Donnan, G., Grotta, J., Howard, G., Kaste, M., Koga, M., von Kummer, R., Lansberg, M., Lindley, R.I., Murray, G., Olivot, J.M., Parsons, M., Tilley, B., Toni, D., Toyoda, K., Wahlgren, N., Wardlaw, J., Whiteley, W., del Zoppo, G.J., Baigent, C., Sandercock, P., Hacke, W., Stroke Thrombolysis Trialists' Collaborative Group, 2014. Effect of treatment delay, age, and stroke severity on the effects of intravenous thrombolysis with alteplase for acute ischaemic stroke: a meta-analysis of individual patient data from randomised trials. Lancet (London, England) 384, 1929–35. doi:10.1016/S0140-6736(14)60584-5.

Engel, O., Kolodziej, S., Dirnagl, U., Prinz, V., 2011. Modeling stroke in mice - middle cerebral artery occlusion with the filament model. J. Vis. Exp. doi:10.3791/2423.

Enlimomab Acute Stroke Trial Investigators, 2001. Use of anti-ICAM-1 therapy in ischemic stroke: results of the Enlimomab Acute Stroke Trial. Neurology 57, 1428–34.

Esposito, S., Pristerà, A., Maresca, G., Cavallaro, S., Felsani, A., Florenzano, F., Manni, L., Ciotti, M.T., Pollegioni, L., Borsello, T., Canu, N., 2012. Contribution of serine racemase/d-serine pathway to neuronal apoptosis. Aging Cell 11, 588–598. doi:10.1111/j.1474-9726.2012.00822.x.

Evans, G.J.O., 2015. The synaptosome as a model system for studying synaptic physiology. Cold Spring Harb. Protoc. 2015, 421–4. doi:10.1101/pdb.top074450.

Fagan, S.C., Waller, J.L., Nichols, F.T., Edwards, D.J., Pettigrew, L.C., Clark, W.M., Hall, C.E., Switzer, J.A., Ergul, A., Hess, D.C., 2010. Minocycline to Improve Neurologic Outcome in Stroke (MINOS): A Dose-Finding Study. Stroke 41, 2283–2287. doi:10.1161/STROKEAHA.110.582601.

Feigin, V.L., Anderson, C.S., Rodgers, A., Anderson, N.E., Gunn, A.J., 2002. The emerging role of induced hypothermia in the management of acute stroke. J. Clin. Neurosci. 9, 502–7.

Feigin, V.L., Forouzanfar, M.H., Krishnamurthi, R., Mensah, G.A., Connor, M., Bennett, D.A., Moran, A.E., Sacco, R.L., Anderson, L., Truelsen, T., O'Donnell, M., Venketasubramanian, N., Barker-Collo, S., Lawes, C.M.M., Wang, W., Shinohara, Y., Witt, E., Ezzati, M., Naghavi, M., Murray, C., Global Burden

of Diseases, Injuries, and Risk Factors Study 2010 (GBD 2010) and the GBD Stroke Experts Group, 2014. Global and regional burden of stroke during 1990-2010: findings from the Global Burden of Disease Study 2010. Lancet (London, England) 383, 245–54.

Feligioni, M., Holman, D., Haglerod, C., Davanger, S., Henley, J.M., 2006. Ultrastructural localisation and differential agonist-induced regulation of AMPA and kainate receptors present at the presynaptic active zone and postsynaptic density. J. Neurochem. 99, 549–560. doi:10.1111/j.1471-4159.2006.04087.x.

Feng, S., Yang, Q., Liu, M., Li, W., Yuan, W., Zhang, S., Wu, B., Li, J., 2011. Edaravone for acute ischaemic stroke, in: Liu, M. (Ed.), Cochrane Database of Systematic Reviews. John Wiley & Sons, Ltd, Chichester, UK, p. CD007230. doi:10.1002/14651858.CD007230.pub2.

Fernandez, I., Ubach, J., Dulubova, I., Zhang, X., Südhof, T.C., Rizo, J., 1998. Three-dimensional structure of an evolutionarily conserved N-terminal domain of syntaxin 1A. Cell 94, 841–9.

Fisher, M., Feuerstein, G., Howells, D.W., Hurn, P.D., Kent, T.A., Savitz, S.I., Lo, E.H., STAIR Group, 2009. Update of the Stroke Therapy Academic Industry Roundtable Preclinical Recommendations. Stroke 40, 2244–2250. doi:10.1161/STROKEAHA.108.541128.

Foletti, D.L., Lin, R., Finley, M.A., Scheller, R.H., 2000. Phosphorylated syntaxin 1 is localized to discrete domains along a subset of axons. J. Neurosci. 20, 4535–44.

Förstermann, U., Boissel, J.P., Kleinert, H., 1998. Expressional control of the "constitutive" isoforms of nitric oxide synthase (NOS I and NOS III). FASEB J. 12, 773–90.

Francoeur, C.L., Mayer, S.A., 2016. Management of delayed cerebral ischemia after subarachnoid hemorrhage. Crit. Care 20, 277. doi:10.1186/s13054-016-1447-6.

Frantseva, M. V, Carlen, P.L., El-Beheiry, H., 1999. A submersion method to induce hypoxic damage in organotypic hippocampal cultures. J. Neurosci. Methods 89, 25–31.

Frasca, A., Aalbers, M., Frigerio, F., Fiordaliso, F., Salio, M., Gobbi, M., Cagnotto, A., Gardoni, F., Battaglia, G.S., Hoogland, G., Di Luca, M., Vezzani, A., 2011. Misplaced NMDA receptors in epileptogenesis contribute to excitotoxicity. Neurobiol. Dis. 43, 507–515. doi:10.1016/j.nbd.2011.04.024.

Fryer, C.E., Luker, J.A., McDonnell, M.N., Hillier, S.L., 2016. Self management programmes for quality of life in people with stroke, in: Hillier, S.L. (Ed.), Cochrane Database of Systematic Reviews. John Wiley & Sons, Ltd, Chichester, UK, p. CD010442. doi:10.1002/14651858.CD010442.pub2.

Fu, Y., Zhang, N., Ren, L., Yan, Y., Sun, N., Li, Y.-J., Han, W., Xue, R., Liu, Q., Hao, J., Yu, C., Shi, F.-D., 2014. Impact of an immune modulator fingolimod on acute ischemic stroke. Proc. Natl. Acad. Sci. U. S. A. 111, 18315–20. doi:10.1073/pnas.1416166111.

Fukuyama, N., Takizawa, S., Ishida, H., Hoshiai, K., Shinohara, Y., Nakazawa, H., 1998. Peroxynitrite Formation in Focal Cerebral Ischemia—Reperfusion in Rats Occurs Predominantly in the Peri-Infarct Region. J. Cereb. Blood Flow Metab. 18, 123–129. doi:10.1097/00004647-199802000-00001.

Gabriel, S.M., Haroutunian, V., Powchih, P., Honer, W.G., Davidson, M., Davies, P., Davis, K.L., 1997. Increased Concentrations of Presynaptic Proteins in the Cingulate Cortex of Subjects With Schizophrenia. Arch. Gen. Psychiatry 54, 559. doi:10.1001/archpsyc.1997.01830180077010.

Gambrill, A.C., Barria, A., 2011. NMDA receptor subunit composition controls synaptogenesis and synapse stabilization. Proc. Natl. Acad. Sci. 108, 5855–5860. doi:10.1073/pnas.1012676108.

Gelderblom, M., Leypoldt, F., Steinbach, K., Behrens, D., Choe, C.-U., Siler, D.A., Arumugam, T. V., Orthey, E., Gerloff, C., Tolosa, E., Magnus, T., 2009. Temporal and Spatial Dynamics of Cerebral Immune Cell Accumulation in Stroke. Stroke 40, 1849–1857. doi:10.1161/STROKEAHA.108.534503.

Gerber, S.H., Rah, J.-C., Min, S.-W., Liu, X., de Wit, H., Dulubova, I., Meyer, A.C., Rizo, J., Arancillo, M., Hammer, R.E., Verhage, M., Rosenmund, C., Sudhof, T.C., 2008. Conformational Switch of Syntaxin-1 Controls Synaptic Vesicle Fusion. Science (80). 321, 1507–1510. doi:10.1126/science.1163174.

Gilad, R., 2012. Management of Seizures following a Stroke. Drugs Aging 29, 533–538. doi:10.2165/11631540-00.

Ginsberg, M.D., 2016. Expanding the concept of neuroprotection for acute ischemic stroke: The pivotal roles of reperfusion and the collateral circulation. Prog. Neurobiol. 145-146, 46–77. doi:10.1016/j.pneurobio.2016.09.002.

Ginsberg, M.D., 2008. Neuroprotection for ischemic stroke: Past, present and future. Neuropharmacology 55, 363–389. doi:10.1016/j.neuropharm.2007.12.007.

Giorgio, V., von Stockum, S., Antoniel, M., Fabbro, A., Fogolari, F., Forte, M., Glick, G.D., Petronilli, V., Zoratti, M., Szabo, I., Lippe, G., Bernardi, P., 2013. Dimers of mitochondrial ATP synthase form the permeability transition pore. Proc. Natl. Acad. Sci. 110, 5887–5892. doi:10.1073/pnas.1217823110.

Giraudo, C.G., Eng, W.S., Melia, T.J., Rothman, J.E., 2006. A Clamping Mechanism Involved in SNARE-Dependent Exocytosis. Science (80). 313, 676–680. doi:10.1126/science.1129450.

Gladkevich, A., Kauffman, H.F., Korf, J., 2004. Lymphocytes as a neural probe: potential for studying psychiatric disorders. Prog. Neuro-Psychopharmacology Biol. Psychiatry 28, 559–576. doi:10.1016/j.pnpbp.2004.01.009.

Gladstone, D.J., Black, S.E., Hakim, A.M., Heart and Stroke Foundation of Ontario Centre of Excellence in Stroke Recovery, 2002. Toward wisdom from failure: lessons from neuroprotective stroke trials and new therapeutic directions. Stroke 33, 2123–36.

Godino, M. del C., Romera, V.G., Sánchez-Tomero, J.A., Pacheco, J., Canals, S., Lerma, J., Vivancos, J., Moro, M.A., Torres, M., Lizasoain, I., Sánchez-Prieto, J., 2013. Amelioration of ischemic brain damage by peritoneal dialysis. J. Clin. Invest. 123, 4359–63. doi:10.1172/JCI67284.

Gonda, X., 2012. Basic pharmacology of NMDA receptors. Curr. Pharm. Des. 18, 1558–67.

González, R.G., 2012. Clinical MRI of acute ischemic stroke. J. Magn. Reson. Imaging 36, 259–271. doi:10.1002/jmri.23595.

Goyal, M., Demchuk, A.M., Menon, B.K., Eesa, M., Rempel, J.L., Thornton, J., Roy, D., Jovin, T.G., Willinsky, R.A., Sapkota, B.L., Dowlatshahi, D., Frei, D.F., Kamal, N.R., Montanera, W.J., Poppe, A.Y., Ryckborst, K.J., Silver, F.L., Shuaib, A., Tampieri, D., Williams, D., Bang, O.Y., Baxter, B.W., Burns, P.A., Choe, H., Heo, J.-H., Holmstedt, C.A., Jankowitz, B., Kelly, M., Linares, G., Mandzia, J.L., Shankar, J., Sohn, S.-I., Swartz, R.H., Barber, P.A., Coutts, S.B., Smith, E.E., Morrish, W.F., Weill, A., Subramaniam, S., Mitha, A.P., Wong, J.H., Lowerison, M.W., Sajobi, T.T., Hill, M.D., 2015. Randomized Assessment of Rapid Endovascular Treatment of Ischemic Stroke. doi.org 1019–1030. doi:10.1056/nejmoa1414905.

Gray, E.G., Whittaker, V.P., 1962. The isolation of nerve endings from brain: an electron-microscopic study of cell fragments derived by homogenization and centrifugation. J. Anat. 96, 79–88.

Green, M., Ishino, M., Loewenstein, P.M., 1989. Mutational analysis of HIV-1 Tat minimal domain peptides: identification of trans-dominant mutants that suppress HIV-LTR-driven gene expression. Cell 58, 215–23.

Green, T., Nayeem, N., 2015. The multifaceted subunit interfaces of ionotropic glutamate receptors. J. Physiol. 593, 73–81. doi:10.1113/jphysiol.2014.273409.

Grilli, M., Summa, M., Salamone, A., Olivero, G., Zappettini, S., Di Prisco, S., Feligioni, M., Usai, C., Pittaluga, A., Marchi, M., 2012. In vitro exposure to nicotine induces endocytosis of presynaptic AMPA receptors modulating dopamine release in rat nucleus accumbens nerve terminals. Neuropharmacology 63, 916–26. doi:10.1016/j.neuropharm.2012.06.049.

Grupke, S., Hall, J., Dobbs, M., Bix, G.J., Fraser, J.F., 2015. Understanding history, and not repeating it. Neuroprotection for acute ischemic stroke: From review to preview. Clin. Neurol. Neurosurg. 129, 1–9. doi:10.1016/j.clineuro.2014.11.013.

Guidotti, G., Brambilla, L., Rossi, D., 2017. Cell-Penetrating Peptides: From Basic Research to Clinics. Trends Pharmacol. Sci. 38, 406–424. doi:10.1016/j.tips.2017.01.003.

Guo, R., Zhang, M., Liu, W., Zhao, C., Cui, Y., Wang, C., Feng, J., Chen, P., 2009. NMDA receptors are involved in upstream of the spinal JNK activation in morphine antinociceptive tolerance. Neurosci. Lett. 467, 95–99. doi:10.1016/j.neulet.2009.10.013.

Gupta, S., Barrett, T., Whitmarsh, A.J., Cavanagh, J., Sluss, H.K., Dérijard, B., Davis, R.J., 1996. Selective interaction of JNK protein kinase isoforms with transcription factors. EMBO J. 15, 2760–70.

Gupta, H. V, Farrell, A.M., Mittal, M.K., 2014. Transient ischemic attacks: predictability of future ischemic stroke or transient ischemic attack events. Ther. Clin. Risk Manag. 10, 27–35. doi:10.2147/TCRM.S54810.

Hacke, W., Kaste, M., Bluhmki, E., Brozman, M., Dávalos, A., Guidetti, D., Larrue, V., Lees, K.R., Medeghri, Z., Machnig, T., Schneider, D., von Kummer, R., Wahlgren, N., Toni, D., ECASS Investigators, 2008. Thrombolysis with alteplase 3 to 4.5 hours after acute ischemic stroke. N. Engl. J. Med. 359, 1317–29. doi:10.1056/NEJMoa0804656.

Hall, E.D., 1997. Brain attack. Acute therapeutic interventions. Free radical scavengers and antioxidants. Neurosurg. Clin. N. Am. 8, 195–206.

Hardingham, G.E., Fukunaga, Y., Bading, H., 2002. Extrasynaptic NMDARs oppose synaptic NMDARs by triggering CREB shut-off and cell death pathways. Nat. Neurosci. 5, 405–14. doi:10.1038/nn835.

Harper, A.M., 1965. Physiology of cerebral bloodflow. Brit. J. Anaesth. (1965), 37, 225 37.

Harpsøe, N.G., Andersen, L.P.H., Gögenur, I., Rosenberg, J., 2015. Clinical pharmacokinetics of melatonin: a systematic review. Eur. J. Clin. Pharmacol. 71, 901–909. doi:10.1007/s00228-015-1873-4.

Harreveld, A. Van, 1959. Compounds in brain extracts causing spreading depression of cerebral cortical activity and contraction of crustacean muscle. J. Neurochem. 3, 300–315. doi:10.1111/j.1471-4159.1959.tb12636.x.

Hill, M.D., Martin, R.H., Mikulis, D., Wong, J.H., Silver, F.L., terBrugge, K.G., Milot, G., Clark, W.M., MacDonald, R.L., Kelly, M.E., Boulton, M., Fleetwood, I., McDougall, C., Gunnarsson, T., Chow, M., Lum, C., Dodd, R., Poublanc, J., Krings, T., Demchuk, A.M., Goyal, M., Anderson, R., Bishop, J., Garman, D., Tymianski, M., ENACT trial investigators, 2012. Safety and efficacy of NA-1 in patients with iatrogenic stroke after endovascular aneurysm repair (ENACT): a phase 2, randomised, double-blind, placebo-controlled trial. Lancet Neurol. 11, 942–950. doi:10.1016/S1474-4422(12)70225-9.

Honer, W.G., Falkai, P., Young, C., Wang, T., Xie, J., Bonner, J., Hu, L., Boulianne, G.L., Luo, Z., Trimble, W.S., 1997. Cingulate cortex synaptic terminal proteins and neural cell adhesion molecule in schizophrenia. Neuroscience 78, 99–110.

Hotchkiss, R.S., Strasser, A., McDunn, J.E., Swanson, P.E., 2009. Cell Death. N. Engl. J. Med. 361, 1570–1583. doi:10.1056/NEJMra0901217.

Howells, D.W., Sena, E.S., Macleod, M.R., 2013. Bringing rigour to translational medicine. Nat. Rev. Neurol. 10, 37–43. doi:10.1038/nrneurol.2013.232.

https://www.nhlbi.nih.gov/health/health-topics/topics/stroke. What Is a Stroke? - NHLBI, NIH.

https://www.nhlbi.nih.gov/health/health-topics/topics/stroke/types. Types of Stroke - NHLBI, NIH.

https://www.nhlbi.nih.gov/health/health-topics/topics/stroke/diagnosis. How Is a Stroke Diagnosed? - NHLBI, NIH.

https:// www.genome.ucsc.edu. UCSC Genome Browser Home.

http://www.bioinf.manchester.ac.uk/naccess/. NACCESS Computer Program.

Iadecola, C., Alexander, M., 2001. Cerebral ischemia and inflammation. Curr. Opin. Neurol. 14, 89–94.

Ikonomidou, C., Turski, L., 2002. Why did NMDA receptor antagonists fail clinical trials for stroke and traumatic brain injury? Lancet. Neurol. 1, 383–6.

Friedman L.K., Ginsberg M.D., Belayev L., Busto R., Alonso O.F, Lin B., Globus M.Y., 2001. Intraischemic but not postischemic hypothermia prevents non-selective hippocampal downregulation of AMPA and NMDA receptor gene expression after global ischemia. Mol. Brain Res. 86, 34–47. doi:10.1016/S0169-328X(00)00252-7.

Ishikawa, M., Cooper, D., Arumugam, T. V., Zhang, J.H., Nanda, A., Granger, D.N., 2004. Platelet–Leukocyte–Endothelial Cell Interactions after Middle Cerebral Artery Occlusion and Reperfusion. J. Cereb. Blood Flow Metab. 24, 907–915. doi:10.1097/01.WCB.0000132690.96836.7F.

Jahn, R., Fasshauer, D., 2012. Molecular machines governing exocytosis of synaptic vesicles. Nature 490, 201–207. doi:10.1038/nature11320.

Jiang, M.Q., Zhao, Y.-Y., Cao, W., Wei, Z.Z., Gu, X., Wei, L., Yu, S.P., 2017. Long-term survival and regeneration of neuronal and vasculature cells inside the core region after ischemic stroke in adult mice. Brain Pathol. 27, 480–498. doi:10.1111/bpa.12425.

Jickling, G.C., Sharp, F.R., 2015. Improving the translation of animal ischemic stroke studies to humans. Metab. Brain Dis. 30, 461–467. doi:10.1007/s11011-014-9499-2.

Jickling, G.C., Sharp, F.R., 2011. Blood Biomarkers of Ischemic Stroke. Neurotherapeutics 8, 349–360. doi:10.1007/s13311-011-0050-4.

Johnson, J., Kotermanski, S., 2006. Mechanism of action of memantine. Curr. Opin. Pharmacol. 6, 61–67. doi:10.1016/j.coph.2005.09.007.

Jones, R.S., Heinemann, U., 1988. Synaptic and intrinsic responses of medical entorhinal cortical cells in normal and magnesium-free medium in vitro. J. Neurophysiol. 59, 1476–96.

Jovin, T.G., Chamorro, A., Cobo, E., de Miquel, M.A., Molina, C.A., Rovira, A., San Román, L., Serena, J., Abilleira, S., Ribó, M., Millán, M., Urra, X., Cardona, P., López-Cancio, E., Tomasello, A., Castaño, C.,

Blasco, J., Aja, L., Dorado, L., Quesada, H., Rubiera, M., Hernandez-Pérez, M., Goyal, M., Demchuk, A.M., von Kummer, R., Gallofré, M., Dávalos, A., 2015. Thrombectomy within 8 Hours after Symptom Onset in Ischemic Stroke. doi.org 2296–2306. doi:10.1056/nejmoa1503780.

Kahles, T., Brandes, R.P., 2012. NADPH oxidases as therapeutic targets in ischemic stroke. Cell. Mol. Life Sci. 69, 2345–2363. doi:10.1007/s00018-012-1011-8.

Kalia, L. V, Kalia, S.K., Salter, M.W., 2008. NMDA receptors in clinical neurology: excitatory times ahead. Lancet. Neurol. 7, 742–55. doi:10.1016/S1474-4422(08)70165-0.

Kanner, L., 1968. Autistic disturbances of affective contact. Acta Paedopsychiatr. 35, 100–36.

Kennedy, N.J., Martin, G., Ehrhardt, A.G., Cavanagh-Kyros, J., Kuan, C.-Y., Rakic, P., Flavell, R.A., Treistman, S.N., Davis, R.J., 2007. Requirement of JIP scaffold proteins for NMDA-mediated signal transduction. Genes & Dev. 21, 2336–2346. doi:10.1101/gad.1563107.

Kernan, W.N., Ovbiagele, B., Black, H.R., Bravata, D.M., Chimowitz, M.I., Ezekowitz, M.D., Fang, M.C., Fisher, M., Furie, K.L., Heck, D. V., Johnston, S.C. Clay, Kasner, S.E., Kittner, S.J., Mitchell, P.H., Rich, M.W., Richardson, D., Schwamm, L.H., Wilson, J.A., 2014. Guidelines for the Prevention of Stroke in Patients With Stroke and Transient Ischemic Attack. Stroke.

Khatun, S., Chaube, S.K., Bhattacharyya, C.N., 2013. Generation of hydrogen peroxide mediates hanging death-induced neuronal cell apoptosis in the dentate gyrus of the rat brain. Brain Res. Bull. 95, 54–60. doi:10.1016/J.brainresbull.2013.03.002.

Kirshner, H.S., 2008. Therapeutic interventions for prevention of recurrent ischemic stroke. Am. J. Manag. Care 14, S212–26.

Kochubey, O., Lou, X., Schneggenburger, R., 2011. Regulation of transmitter release by Ca2+ and synaptotagmin: insights from a large CNS synapse. Trends Neurosci. 34, 237–246. doi:10.1016/j.tins.2011.02.006.

Kohler, E., Prentice, D.A., Bates, T.R., Hankey, G.J., Claxton, A., van Heerden, J., Blacker, D., 2013. Intravenous Minocycline in Acute Stroke. Stroke 44, 2493–2499. doi:10.1161/STROKEAHA.113.000780.

Kolaczkowska, E., Kubes, P., 2013. Neutrophil recruitment and function in health and inflammation. Nat. Rev. Immunol. 13, 159–175. doi:10.1038/nri3399.

Kondoh, K., Nishida, E., 2007. Regulation of MAP kinases by MAP kinase phosphatases. Biochim. Biophys. Acta - Mol. Cell Res. 1773, 1227–1237.

Kuan, C.-Y., Whitmarsh, A.J., Yang, D.D., Liao, G., Schloemer, A.J., Dong, C., Bao, J., Banasiak, K.J., Haddad, G.G., Flavell, R.A., Davis, R.J., Rakic, P., 2003. A critical role of neural-specific JNK3 for ischemic apoptosis. Proc. Natl. Acad. Sci. 100, 15184–15189. doi:10.1073/pnas.2336254100.

Kuan, C.Y., Yang, D.D., Samanta Roy, D.R., Davis, R.J., Rakic, P., Flavell, R.A., 1999. The Jnk1 and Jnk2 protein kinases are required for regional specific apoptosis during early brain development. Neuron 22, 667–76.

Kuglstatter, A., Ghate, M., Tsing, S., Villaseñor, A.G., Shaw, D., Barnett, J.W., Browner, M.F., 2010. X-ray crystal structure of JNK2 complexed with the p38α inhibitor BIRB796: Insights into the rational design of DFG-out binding MAP kinase inhibitors. Bioorg. Med. Chem. Lett. 20, 5217–5220. doi:10.1016/j.bmcl.2010.06.157.

Kumaria, A., Tolias, C.M., 2009. Normobaric hyperoxia therapy for traumatic brain injury and stroke: a review. Br. J. Neurosurg. 23, 576–584. doi:10.3109/02688690903050352.

Kvrivishvili, G., 2002. Glycine and neuroprotective effect of hypothermia in hypoxic-ischemic brain damage. Neuroreport 13, 1995–2000.

Lai, T.W., Zhang, S., Wang, Y.T., 2014. Excitotoxicity and stroke: Identifying novel targets for neuroprotection. Prog. Neurobiol. 115, 157–188. doi:10.1016/j.pneurobio.2013.11.006.

Lakhan, S.E., Kirchgessner, A., Tepper, D., Leonard, A., 2013. Matrix metalloproteinases and blood-brain barrier disruption in acute ischemic stroke. Front. Neurol. 4, 32. doi:10.3389/fneur.2013.00032.

Landis, S.C., Amara, S.G., Asadullah, K., Austin, C.P., Blumenstein, R., Bradley, E.W., Crystal, R.G., Darnell, R.B., Ferrante, R.J., Fillit, H., Finkelstein, R., Fisher, M., Gendelman, H.E., Golub, R.M., Goudreau, J.L., Gross, R.A., Gubitz, A.K., Hesterlee, S.E., Howells, D.W., Huguenard, J., Kelner, K., Koroshetz, W., Krainc, D., Lazic, S.E., Levine, M.S., Macleod, M.R., McCall, J.M., Moxley III, R.T., Narasimhan, K., Noble, L.J., Perrin, S., Porter, J.D., Steward, O., Unger, E., Utz, U., Silberberg, S.D., 2012. A call for

transparent reporting to optimize the predictive value of preclinical research. Nature 490, 187–191. doi:10.1038/nature11556.

Langhauser, F., Kraft, P., Gob, E., Leinweber, J., Schuhmann, M.K., Lorenz, K., Gelderblom, M., Bittner, S., Meuth, S.G., Wiendl, H., Magnus, T., Kleinschnitz, C., 2014. Blocking of 4 Integrin Does Not Protect From Acute Ischemic Stroke in Mice. Stroke 45, 1799–1806. doi:10.1161/STROKEAHA.114.005000.

Lapchak, P.A., 2010. A critical assessment of edaravone acute ischemic stroke efficacy trials: is edaravone an effective neuroprotective therapy? Expert Opin. Pharmacother. 11, 1753–1763. doi:10.1517/14656566.2010.493558.

Larsen, R.S., Smith, I.T., Miriyala, J., Han, J.E., Corlew, R.J., Smith, S.L., Philpot, B.D., 2014. Synapse-Specific Control of Experience-Dependent Plasticity by Presynaptic NMDA Receptors. Neuron 83, 879–893. doi:10.1016/j.neuron.2014.07.039.

Lee, J., Zhang, J., Yu, S., 2017. Neuroprotective mechanisms and translational potential of therapeutic hypothermia in the treatment of ischemic stroke. Neural Regen. Res. 12, 341. doi:10.4103/1673-5374.202915.

Lee, J.H., Wei, L., Gu, X., Wei, Z., Dix, T.A., Yu, S.P., 2014. Therapeutic Effects of Pharmacologically Induced Hypothermia against Traumatic Brain Injury in Mice. J. Neurotrauma 31, 1417–1430. doi:10.1089/neu.2013.3251.

Lee, J.H., Wei, Z.Z., Cao, W., Won, S., Gu, X., Winter, M., Dix, T.A., Wei, L., Yu, S.P., 2016. Regulation of therapeutic hypothermia on inflammatory cytokines, microglia polarization, migration and functional recovery after ischemic stroke in mice. Neurobiol. Dis. 96, 248–260. doi:10.1016/j.nbd.2016.09.013.

Lee, J.M., Grabb, M.C., Zipfel, G.J., Choi, D.W., 2000. Brain tissue responses to ischemia. J. Clin. Invest. 106, 723–31. doi:10.1172/JCI11003.

Lees, K.R., Zivin, J.A., Ashwood, T., Davalos, A., Davis, S.M., Diener, H.-C., Grotta, J., Lyden, P., Shuaib, A., Hårdemark, H.-G., Wasiewski, W.W., 2006. NXY-059 for Acute Ischemic Stroke. N. Engl. J. Med. 354, 588–600. doi:10.1056/NEJMoa052980.

Leiva-Salinas, C., Wintermark, M., 2010. Imaging of acute ischemic stroke. Neuroimaging Clin. N. Am. 20, 455–68. doi:10.1016/j.nic.2010.07.002.

Lemos, C., Pereira-Monteiro, J., Mendonça, D., Ramos, E.M., Barros, J., Sequeiros, J., Alonso, I., Sousa, A., 2010. Evidence of syntaxin 1A involvement in migraine susceptibility: a Portuguese study. Arch. Neurol. 67, 422–427. doi:10.1001/archneurol.2010.37.

Li, F., Pincet, F., Perez, E., Eng, W.S., Melia, T.J., Rothman, J.E., Tareste, D., 2007. Energetics and dynamics of SNAREpin folding across lipid bilayers. Nat. Struct. Mol. Biol. 14, 890–896. doi:10.1038/nsmb1310.

Li, Z., Zhang, Z., He, Z., Tang, W., Li, T., Zeng, Z., He, L., Shi, Y., 2009. A partition-ligation-combination-subdivision EM algorithm for haplotype inference with multiallelic markers: update of the SHEsis (http://analysis.bio-x.cn). Cell Res. 19, 519–523. doi:10.1038/cr.2009.33.

Liesz, A., Zhou, W., Mracskó, É., Karcher, S., Bauer, H., Schwarting, S., Sun, L., Bruder, D., Stegemann, S., Cerwenka, A., Sommer, C., Dalpke, A.H., Veltkamp, R., 2011. Inhibition of lymphocyte trafficking shields the brain against deleterious neuroinflammation after stroke. Brain 134, 704–720. doi:10.1093/brain/awr008.

Lipton, S.A., 2004. Failures and successes of NMDA receptor antagonists: Molecular basis for the use of open-channel blockers like memantine in the treatment of acute and chronic neurologic insults. NeuroRX 1, 101–110. doi:10.1602/neurorx.1.1.101.

Liu, H., Li, J., Zhao, F., Wang, H., Qu, Y., Mu, D., 2015. Nitric oxide synthase in hypoxic or ischemic brain injury. Rev. Neurosci. 26, 105–17. doi:10.1515/revneuro-2014-0041.

Liu, J., Zhang, C., Tao, W., Liu, M., 2013. Systematic Review and Meta-Analysis of the Efficacy of Sphingosine-1-Phosphate (S1P) Receptor Agonist FTY720 (Fingolimod) in Animal Models of Stroke. Int. J. Neurosci. 123, 163–169. doi:10.3109/00207454.2012.749255.

Liu, X., Wang, L., Wen, A., Yang, J., Yan, Y., Song, Y., Liu, X., Ren, H., Wu, Y., Li, Z., Chen, W., Xu, Y., Li, L., Xia, J., Zhao, G., 2012. Ginsenoside-Rd improves outcome of acute ischaemic stroke - a randomized, double-blind, placebo-controlled, multicenter trial. Eur. J. Neurol. 19, 855–863. doi:10.1111/j.1468-1331.2011.03634.x.

Liu, Y., Wong, T.P., Aarts, M., Rooyakkers, A., Liu, L., Lai, T.W., Wu, D.C., Lu, J., Tymianski, M., Craig,

A.M., Wang, Y.T., 2007. NMDA Receptor Subunits Have Differential Roles in Mediating Excitotoxic Neuronal Death Both In Vitro and In Vivo. J. Neurosci. 27.

Liu, Z., Chopp, M., 2016. Astrocytes, therapeutic targets for neuroprotection and neurorestoration in ischemic stroke. Prog. Neurobiol. 144, 103–20. doi:10.1016/j.pneurobio.2015.09.008.

Llovera, G., Hofmann, K., Roth, S., Salas-Perdomo, A., Ferrer-Ferrer, M., Perego, C., Zanier, E.R., Mamrak, U., Rex, A., Party, H., Agin, V., Fauchon, C., Orset, C., Haelewyn, B., De Simoni, M.-G., Dirnagl, U., Grittner, U., Planas, A.M., Plesnila, N., Vivien, D., Liesz, A., 2015. Results of a preclinical randomized controlled multicenter trial (pRCT): Anti-CD49d treatment for acute brain ischemia. Sci. Transl. Med. 7, 299ra121–299ra121. doi:10.1126/scitranslmed.aaa9853.

Llovera, G., Roth, S., Plesnila, N., Veltkamp, R., Liesz, A., 2014. Modeling Stroke in Mice: Permanent Coagulation of the Distal Middle Cerebral Artery. J. Vis. Exp. e51729. doi:10.3791/51729.

Llull, L., Laredo, C., Renú, A., Pérez, B., Vila, E., Obach, V., Urra, X., Planas, A., Amaro, S., Chamorro, Á., 2015. Uric Acid Therapy Improves Clinical Outcome in Women With Acute Ischemic Stroke. Stroke 46, 2162–2167. doi:10.1161/STROKEAHA.115.009960.

Lo, E.H., Moskowitz, M.A., Jacobs, T.P., 2005. Exciting, Radical, Suicidal: How Brain Cells Die After Stroke. Stroke 36, 189–192. doi:10.1161/01.STR.0000153069.96296.fd.

Lopez-Valdes, H.E., Clarkson, A.N., Ao, Y., Charles, A.C., Carmichael, S.T., Sofroniew, M. V., Brennan, K.C., 2014. Memantine Enhances Recovery From Stroke. Stroke 45, 2093–2100. doi:10.1161/STROKEAHA.113.004476.

Lyaker, M., Tulman, D., Dimitrova, G., Pin, R., Papadimos, T., 2013. Arterial embolism. Int. J. Crit. Illn. Inj. Sci. 3, 77. doi:10.4103/2229-5151.109429.

Mahoney, F.I., Barthel, D.W., 1965. Functional evaluation: the Barthel Index. Md. State Med. J. 14, 61–5.

Manchester, L.C., Coto-Montes, A., Boga, J.A., Andersen, L.P.H., Zhou, Z., Galano, A., Vriend, J., Tan, D.-X., Reiter, R.J., 2015. Melatonin: an ancient molecule that makes oxygen metabolically tolerable. J. Pineal Res. 59, 403–419. doi:10.1111/jpi.12267.

Mangia, S., Giove, F., DiNuzzo, M., 2012. Metabolic Pathways and Activity-Dependent Modulation of Glutamate Concentration in the Human Brain. Neurochem. Res. 37, 2554–2561. doi:10.1007/s11064-012-0848-4.

Marcelli, S., Ficulle, E., Iannuzzi, F., Kövari, E., Nisticò, R., Feligioni, M., 2016. Targeting SUMO-1ylation Contrasts Synaptic Dysfunction in a Mouse Model of Alzheimer's Disease. Mol. Neurobiol. doi:10.1007/s12035-016-0176-9.

McDougle, C.J., Erickson, C.A., Stigler, K.A., Posey, D.J., 2005. Neurochemistry in the pathophysiology of autism. J. Clin. Psychiatry 66 Suppl 10, 9–18.

McPartland, J., Klin, A., 2006. Asperger's syndrome. Adolesc. Med. Clin. 17, 771–88; abstract xiii. doi:10.1016/j.admecli.2006.06.010.

Meschia, J.F., Bushnell, C., Boden-Albala, B., Braun, L.T., Bravata, D.M., Chaturvedi, S., Creager, M.A., Eckel, R.H., Elkind, M.S.V., Fornage, M., Goldstein, L.B., Greenberg, S.M., Horvath, S.E., Iadecola, C., Jauch, E.C., Moore, W.S., Wilson, J.A., American Heart Association Stroke Council, Council on Cardiovascular and Stroke Nursing, Council on Clinical Cardiology, Council on Functional Genomics and Translational Biology, Council on Hypertension, 2014. Guidelines for the Primary Prevention of Stroke. Stroke 45, 3754–3832. doi:10.1161/STR.0000000000000046.

Mirnics, K., Middleton, F.A., Lewis, D.A., Levitt, P., 2001. Analysis of complex brain disorders with gene expression microarrays: schizophrenia as a disease of the synapse. Trends Neurosci. 24, 479–86.

Moretti, A., Ferrari, F., Villa, R.F., 2015. Neuroprotection for ischaemic stroke: Current status and challenges. Pharmacol. Ther. 146, 23–34. doi:10.1016/j.pharmthera.2014.09.003.

Mozaffarian, D., Benjamin, E.J., Go, A.S., Arnett, D.K., Blaha, M.J., Cushman, M., Das, S.R., de Ferranti, S., Després, J.-P., Fullerton, H.J., Howard, V.J., Huffman, M.D., Isasi, C.R., Jiménez, M.C., Judd, S.E., Kissela, B.M., Lichtman, J.H., Lisabeth, et al. American Heart Association Statistics Committee, Stroke Statistics Subcommittee, 2016. Executive Summary: Heart Disease and Stroke Statistics--2016 Update: A Report From the American Heart Association. Circulation 133, 447–54. doi:10.1161/CIR.0000000000000366.

Mukherjee, P.K., DeCoster, M.A., Campbell, F.Z., Davis, R.J., Bazan, N.G., 1999. Glutamate receptor signaling

interplay modulates stress-sensitive mitogen-activated protein kinases and neuronal cell death. J. Biol. Chem. 274, 6493–8.

Mulcahy, N.J., Ross, J., Rothwell, N.J., Loddick, S.A., 2003. Delayed administration of interleukin-1 receptor antagonist protects against transient cerebral ischaemia in the rat. Br. J. Pharmacol. 140, 471–476. doi:10.1038/sj.bjp.0705462.

Munton, R.P., Tweedie-Cullen, R., Livingstone-Zatchej, M., Weinandy, F., Waidelich, M., Longo, D., Gehrig, P., Potthast, F., Rutishauser, D., Gerrits, B., Panse, C., Schlapbach, R., Mansuy, I.M., 2007. Qualitative and Quantitative Analyses of Protein Phosphorylation in Naive and Stimulated Mouse Synaptosomal Preparations. Mol. Cell. Proteomics 6, 283–293. doi:10.1074/mcp.M600046-MCP200.

Murata, Y., Rosell, A., Scannevin, R.H., Rhodes, K.J., Wang, X., Lo, E.H., 2008. Extension of the Thrombolytic Time Window With Minocycline in Experimental Stroke. Stroke 39, 3372–3377. doi:10.1161/STROKEAHA.108.514026.

Muzzi, M., Felici, R., Cavone, L., Gerace, E., Minassi, A., Appendino, G., Moroni, F., Chiarugi, A., 2012. Ischemic neuroprotection by TRPV1 receptor-induced hypothermia. J. Cereb. Blood Flow Metab. 32, 978–82. doi:10.1038/jcbfm.2012.36.

Nakamura, K., Anitha, A., Yamada, K., Tsujii, M., Iwayama, Y., Hattori, E., Toyota, T., Suda, S., Takei, N., Iwata, Y., Suzuki, K., Matsuzaki, H., Kawai, M., Sekine, Y., Tsuchiya, K.J., Sugihara, G., Ouchi, Y., Sugiyama, T., Yoshikawa, T., Mori, N., 2008. Genetic and expression analyses reveal elevated expression of syntaxin 1A (STX1A) in high functioning autism. Int. J. Neuropsychopharmacol. 11, 1073. doi:10.1017/S1461145708009036.

Nakamura, K., Iwata, Y., Anitha, A., Miyachi, T., Toyota, T., Yamada, S., Tsujii, M., Tsuchiya, K.J., Iwayama, Y., Yamada, K., Hattori, E., Matsuzaki, H., Matsumoto, K., Suzuki, K., Suda, S., Takebayashi, K., Takei, N., Ichikawa, H., Sugiyama, T., Yoshikawa, T., Mori, N., 2011. Replication study of Japanese cohorts supports the role of STX1A in autism susceptibility. Prog. Neuro-Psychopharmacology Biol. Psychiatry 35, 454–458. doi:10.1016/j.pnpbp.2010.11.033.

Nakamura, Y., Iga, K., Shibata, T., Shudo, M., Kataoka, K., 1993. Glial plasmalemmal vesicles: A subcellular fraction from rat hippocampal homogenate distinct from synaptosomes. Glia 9, 48–56. doi:10.1002/glia.440090107.

Nishio, N., Taniguchi, W., Sugimura, Y.K., Takiguchi, N., Yamanaka, M., Kiyoyuki, Y., Yamada, H., Miyazaki, N., Yoshida, M., Nakatsuka, T., 2013. Reactive oxygen species enhance excitatory synaptic transmission in rat spinal dorsal horn neurons by activating TRPA1 and TRPV1 channels. Neuroscience 247, 201–212. doi:10.1016/j.neuroscience.2013.05.023.

Nisticò, R., Florenzano, F., Mango, D., Ferraina, C., Grilli, M., Di Prisco, S., Nobili, A., Saccucci, S., D'Amelio, M., Morbin, M., Marchi, M., Mercuri, N.B., Davis, R.J., Pittaluga, A., Feligioni, M., 2015. Presynaptic c-Jun N-terminal Kinase 2 regulates NMDA receptor-dependent glutamate release. Sci. Rep. 5, 9035. doi:10.1038/srep09035.

Nisticò, R., Piccirilli, S., Cucchiaroni, M.L., Armogida, M., Guatteo, E., Giampà, C., Fusco, F.R., Bernardi, G., Nisticò, G., Mercuri, N.B., 2008. Neuroprotective effect of hydrogen peroxide on an in vitro model of brain ischaemia. Br. J. Pharmacol. 153, 1022–9. doi:10.1038/sj.bjp.0707587.

Nor, A.M., Davis, J., Sen, B., Shipsey, D., Louw, S.J., Dyker, A.G., Davis, M., Ford, G.A., 2005. The Recognition of Stroke in the Emergency Room (ROSIER) scale: development and validation of a stroke recognition instrument. Lancet Neurol. 4, 727–734. doi:10.1016/S1474-4422(05)70201-5.

Nour, M., Scalzo, F., Liebeskind, D.S., 2013. Ischemia-reperfusion injury in stroke. Interv. Neurol. 1, 185–99. doi:10.1159/000353125.

O'Collins, V.E., Macleod, M.R., Donnan, G.A., Horky, L.L., van der Worp, B.H., Howells, D.W., 2006. 1,026 Experimental treatments in acute stroke. Ann. Neurol. 59, 467–477. doi:10.1002/ana.20741.

O'Regan, C., Wu, P., Arora, P., Perri, D., Mills, E.J., 2008. Statin Therapy in Stroke Prevention: A Meta-analysis Involving 121,000 Patients. Am. J. Med. 121, 24–33. doi:10.1016/j.amjmed.2007.06.033.

Ohura, T., Hase, K., Nakajima, Y., Nakayama, T., 2017. Validity and reliability of a performance evaluation tool based on the modified Barthel Index for stroke patients. BMC Med. Res. Methodol. 17, 131. doi:10.1186/s12874-017-0409-2

Olmez, I., Ozyurt, H., 2012. Reactive oxygen species and ischemic cerebrovascular disease. Neurochem. Int. 60,

208–212. doi:10.1016/j.neuint.2011.11.009.
Olney, J.W., 1969. Glutamate-induced retinal degeneration in neonatal mice. Electron microscopy of the acutely evolving lesion. J. Neuropathol. Exp. Neurol. 28, 455–474. doi:10.1097/00005072-196907000-00007.
Onetti, Y., Dantas, A.P., Pérez, B., Cugota, R., Chamorro, A., Planas, A.M., Vila, E., Jiménez-Altayó, F., 2015. Middle cerebral artery remodeling following transient brain ischemia is linked to early postischemic hyperemia: A target of uric acid treatment. Am. J. Physiol. - Hear. Circ. Physiol. 308, H862–H874. doi:10.1152/ajpheart.00001.2015.
Orgogozo, J.-M., Rigaud, A.-S., Stöffler, A., Möbius, H.-J., Forette, F., 2002. Efficacy and safety of memantine in patients with mild to moderate vascular dementia: a randomized, placebo-controlled trial (MMM 300). Stroke 33, 1834–9.
Ortiz, G.A., Sacco, R.L., Ortiz, G.A., Sacco, R.L., 2008. National Institutes of Health Stroke Scale (NIHSS), in: Wiley Encyclopedia of Clinical Trials. John Wiley & Sons, Inc., Hoboken, NJ, USA. doi:10.1002/9780471462422.eoct400.
Pacher, P., Beckman, J.S., Liaudet, L., 2007. Nitric Oxide and Peroxynitrite in Health and Disease. Physiol. Rev. 87, 315–424. doi:10.1152/physrev.00029.2006.
Pan, J., Konstas, A.-A., Bateman, B., Ortolano, G.A., Pile-Spellman, J., 2007. Reperfusion injury following cerebral ischemia: pathophysiology, MR imaging, and potential therapies. Neuroradiology 49, 93–102. doi:10.1007/s00234-006-0183-z.
Pellegrino, S., Annoni, C., Contini, A., Clerici, F., Gelmi, M.L., 2012. Expedient chemical synthesis of 75mer DNA binding domain of MafA: an insight on its binding to insulin enhancer. Amino Acids 43, 1995–2003. doi:10.1007/s00726-012-1274-2.
Pieri M., Amadoro G., Carunchio I., Ciotti M.T., Quaresima S., Florenzano F., Calissano P., Possenti R., Zona C., Severini C., 2010. SP protects cerebellar granule cells against β-amyloid-induced apoptosis by down-regulation and reduced activity of Kv4 potassium channels. Neuropharmacology 58, 268–276. doi:10.1016/J.NEUROPHARM.2009.06.029.
Pittaluga, A., Feligioni, M., Longordo, F., Luccini, E., Raiteri, M., 2006. Trafficking of presynaptic AMPA receptors mediating neurotransmitter release: neuronal selectivity and relationships with sensitivity to cyclothiazide. Neuropharmacology 50, 286–96. doi:10.1016/j.neuropharm.2005.09.004.
Pulverer, B.J., Kyriakis, J.M., Avruch, J., Nikolakaki, E., Woodgett, J.R., 1991. Phosphorylation of c-jun mediated by MAP kinases. Nature 353, 670–674. doi:10.1038/353670a0.
Purcell, S., Neale, B., Todd-Brown, K., Thomas, L., Ferreira, M.A.R., Bender, D., Maller, J., Sklar, P., de Bakker, P.I.W., Daly, M.J., Sham, P.C., 2007. PLINK: A Tool Set for Whole-Genome Association and Population-Based Linkage Analyses. Am. J. Hum. Genet. 81, 559–575. doi:10.1086/519795.
Quick, M.W., 2002. Role of syntaxin 1A on serotonin transporter expression in developing thalamocortical neurons. Int. J. Dev. Neurosci. 20, 219–24.
Radermacher, K.A., Wingler, K., Langhauser, F., Altenhöfer, S., Kleikers, P., Hermans, J.J.R., Hrabě de Angelis, M., Kleinschnitz, C., Schmidt, H.H.H.W., 2013. Neuroprotection After Stroke by Targeting NOX4 As a Source of Oxidative Stress. Antioxid. Redox Signal. 18, 1418–1427. doi:10.1089/ars.2012.4797.
Raichle, M.E., 1983. The pathophysiology of brain ischemia. Ann. Neurol. 13, 2–10. doi:10.1002/ana.410130103.
Ramakrishnan, N.A., Drescher, M.J., Drescher, D.G., 2012. The SNARE complex in neuronal and sensory cells. Mol. Cell. Neurosci. 50, 58–69. doi:10.1016/j.mcn.2012.03.009.
Ramos, E., Patiño, P., Reiter, R.J., Gil-Martín, E., Marco-Contelles, J., Parada, E., Los Rios, C. de, Romero, A., Egea, J., 2017. Ischemic brain injury: New insights on the protective role of melatonin. Free Radic. Biol. Med. 104, 32–53. doi:10.1016/j.freeradbiomed.2017.01.005.
Ramos-Cabrer, P., Campos, F., Sobrino, T., Castillo, J., 2011. Targeting the Ischemic Penumbra. Stroke 42, S7–S11. doi:10.1161/STROKEAHA.110.596684.
Rankin, J., 1957. Cerebral Vascular Accidents in Patients over the Age of 60: II. Prognosis. Scott. Med. J. 2, 200–215. doi:10.1177/003693305700200504.
Reinecke, K., Herdegen, T., Eminel, S., Aldenhoff, J.B., Schiffelholz, T., 2013. Knockout of c-Jun N-terminal kinases 1, 2 or 3 isoforms induces behavioural changes. Behav. Brain Res. 245, 88–95.

doi:10.1016/j.bbr.2013.02.013.

Reiter, R.J., Paredes, S.D., Manchester, L.C., Tan, D.-X., 2009. Reducing oxidative/nitrosative stress: a newly-discovered genre for melatonin. Crit. Rev. Biochem. Mol. Biol. 44, 175–200. doi:10.1080/10409230903044914.

Repici, M., Centeno, C., Tomasi, S., Forloni, G., Bonny, C., Vercelli, A., Borsello, T., 2007. Time-course of c-Jun N-terminal kinase activation after cerebral ischemia and effect of D-JNKI1 on c-Jun and caspase-3 activation. Neuroscience 150, 40–49. doi:10.1016/j.neuroscience.2007.08.021.

Rhee, P., Morris, J., Durham, R., Hauser, C., Cipolle, M., Wilson, R., Luchette, F., McSwain, N., Miller, R., 2000. Recombinant humanized monoclonal antibody against CD18 (rhuMAb CD18) in traumatic hemorrhagic shock: results of a phase II clinical trial. Traumatic Shock Group. J. Trauma 49, 611–9; discussion 619–20.

Rickman, C., Duncan, R.R., 2010. Munc18/Syntaxin interaction kinetics control secretory vesicle dynamics. J. Biol. Chem. 285, 3965–72. doi:10.1074/jbc.M109.040402.

Rickman, C., Medine, C.N., Bergmann, A., Duncan, R.R., 2007. Functionally and Spatially Distinct Modes of munc18-Syntaxin 1 Interaction. J. Biol. Chem. 282, 12097–12103. doi:10.1074/jbc.M700227200.

Risinger, C., Bennett, M.K., 1999. Differential phosphorylation of syntaxin and synaptosome-associated protein of 25 kDa (SNAP-25) isoforms. J. Neurochem. 72, 614–24.

Roger, V.L., Go, A.S., Lloyd-Jones, D.M., Adams, R.J., Berry, J.D., Brown, T.M., Carnethon, M.R., Dai, S., de Simone, G., Ford, E.S., Fox, C.S., Fullerton, H.J., Gillespie, C., Greenlund, K.J., Hailpern, S.M., Heit, J.A., Ho, P.M., Howard, V.J., Kissela, B.M., Kittner, S.J., Lackland, D.T., Lichtman, J.H., Lisabeth, L.D., Makuc, D.M., Marcus, G.M., Marelli, A., Matchar, D.B., McDermott, M.M., Meigs, J.B., Moy, C.S., Mozaffarian, D., Mussolino, M.E., Nichol, G., Paynter, N.P., Rosamond, W.D., Sorlie, P.D., Stafford, R.S., Turan, T.N., Turner, M.B., Wong, N.D., Wylie-Rosett, J., American Heart Association Statistics Committee and Stroke Statistics Subcommittee, 2011. Heart disease and stroke statistics--2011 update: a report from the American Heart Association. Circulation 123, e18–e209. doi:10.1161/CIR.0b013e3182009701.

Romanos, E., Planas, A.M., Amaro, S., Chamorro, Á., 2007. Uric Acid Reduces Brain Damage and Improves the Benefits of rt-PA in a Rat Model of Thromboembolic Stroke. J. Cereb. Blood Flow Metab. 27, 14–20. doi:10.1038/sj.jcbfm.9600312.

Roof, R.L., Hall, E.D., 2000. Gender differences in acute CNS trauma and stroke: neuroprotective effects of estrogen and progesterone. J. Neurotrauma 17, 367–88. doi:10.1089/neu.2000.17.367.

Rothwell, P.M., Algra, A., Chen, Z., Diener, H.-C., Norrving, B., Mehta, Z., 2016. Effects of aspirin on risk and severity of early recurrent stroke after transient ischaemic attack and ischaemic stroke: time-course analysis of randomised trials. Lancet (London, England) 388, 365–375. doi:10.1016/S0140-6736(16)30468-8.

Rothwell, P.M., Eliasziw, M., Gutnikov, S.A., Fox, A.J., Taylor, D.W., Mayberg, M.R., Warlow, C.P., Barnett, H.J.M., Carotid Endarterectomy Trialists' Collaboration, 2003. Analysis of pooled data from the randomised controlled trials of endarterectomy for symptomatic carotid stenosis. Lancet (London, England) 361, 107–16.

Ryan, T.J., Emes, R.D., Grant, S.G., Komiyama, N.H., 2008. Evolution of NMDA receptor cytoplasmic interaction domains: implications for organisation of synaptic signalling complexes. BMC Neurosci. 9, 6. doi:10.1186/1471-2202-9-6.

Sanz-Rosa, D., García-Prieto, J., Ibanez, B., 2012. The future: therapy of myocardial protection. Ann. N. Y. Acad. Sci. 1254, 90–98. doi:10.1111/j.1749-6632.2012.06501.x.

Sattler, R., Xiong, Z., Lu, W.Y., Hafner, M., MacDonald, J.F., Tymianski, M., 1999. Specific coupling of NMDA receptor activation to nitric oxide neurotoxicity by PSD-95 protein. Science 284, 1845–8.

Saunders, D.H., Sanderson, M., Brazzelli, M., Greig, C.A., Mead, G.E., 2013. Physical fitness training for stroke patients. Cochrane database Syst. Rev. CD003316. doi:10.1002/14651858.CD003316.pub5.

Saver, J.L., 2006. Time Is Brain--Quantified. Stroke 37, 263–266. doi:10.1161/01.STR.0000196957.55928.ab.

Saver, J.L., Goyal, M., van der Lugt, A., Menon, B.K., Majoie, C.B.L.M., Dippel, D.W., Campbell, B.C., Nogueira, R.G., Demchuk, A.M., Tomasello, A., Cardona, P., Devlin, T.G., Frei, D.F., du Mesnil de Rochemont, R., Berkhemer, O.A., Jovin, T.G., Siddiqui, A.H., van Zwam, W.H., Davis, S.M., Castaño, C.,

Sapkota, B.L., Fransen, P.S., Molina, C., van Oostenbrugge, R.J., Chamorro, Á., Lingsma, H., Silver, F.L., Donnan, G.A., Shuaib, A., Brown, S., Stouch, B., Mitchell, P.J., Davalos, A., Roos, Y.B.W.E.M., Hill, M.D., HERMES Collaborators, 2016. Time to Treatment With Endovascular Thrombectomy and Outcomes From Ischemic Stroke: A Meta-analysis. JAMA 316, 1279–88. doi:10.1001/jama.2016.13647.

Saver, J.L., Starkman, S., Eckstein, M., Stratton, S.J., Pratt, F.D., Hamilton, S., Conwit, R., Liebeskind, D.S., Sung, G., Kramer, I., Moreau, G., Goldweber, R., Sanossian, N., FAST-MAG Investigators and Coordinators, 2015. Prehospital Use of Magnesium Sulfate as Neuroprotection in Acute Stroke. N. Engl. J. Med. 372, 528–536. doi:10.1056/NEJMoa1408827.

Schaller, B., Graf, R., 2004. Cerebral Ischemia and Reperfusion: The Pathophysiologic Concept as a Basis for Clinical Therapy. J. Cereb. Blood Flow Metab. 24, 351–371. doi:10.1097/00004647-200404000-00001.

Sclip, A., Antoniou, X., Colombo, A., Camici, G.G., Pozzi, L., Cardinetti, D., Feligioni, M., Veglianese, P., Bahlmann, F.H., Cervo, L., Balducci, C., Costa, C., Tozzi, A., Calabresi, P., Forloni, G., Borsello, T., 2011. c-Jun N-terminal kinase regulates soluble Aβ oligomers and cognitive impairment in AD mouse model. J. Biol. Chem. 286, 43871–80. doi:10.1074/jbc.M111.297515.

Sclip, A., Tozzi, A., Abaza, A., Cardinetti, D., Colombo, I., Calabresi, P., Salmona, M., Welker, E., Borsello, T., 2014. c-Jun N-terminal kinase has a key role in Alzheimer disease synaptic dysfunction in vivo. Cell Death Dis. 5, e1019. doi:10.1038/cddis.2013.559.

Scullen, T.A., Monlezun, D.J., Siegler, J.E., George, A.J., Schwickrath, M., El Khoury, R., Cho, M.C., Martin-Schild, S., 2015. Cryptogenic Stroke: Clinical Consideration of a Heterogeneous Ischemic Subtype. J. Stroke Cerebrovasc. Dis. 24, 993–999. doi:10.1016/j.jstrokecerebrovasdis.2014.12.024.

Sena, E.S., van der Worp, H.B., Bath, P.M.W., Howells, D.W., Macleod, M.R., 2010. Publication Bias in Reports of Animal Stroke Studies Leads to Major Overstatement of Efficacy. PLoS Biol. 8, e1000344. doi:10.1371/journal.pbio.1000344.

Shen, J., Qiu, X., Jiang, B., Zhang, D., Xin, W., Fung, P.C.W., Zhao, B., 2003. Nitric oxide and oxygen radicals induced apoptosis via bcl-2 and p53 pathway in hypoxia-reoxygenated cardiomyocytes. Sci. China Ser. C Life Sci. 46, 28–39. doi:10.1007/BF03182682.

Shi, Z.-Q., Sunico, C.R., McKercher, S.R., Cui, J., Feng, G.-S., Nakamura, T., Lipton, S.A., 2013. S-nitrosylated SHP-2 contributes to NMDA receptor-mediated excitotoxicity in acute ischemic stroke. Proc. Natl. Acad. Sci. U. S. A. 110, 3137–42. doi:10.1073/pnas.1215501110.

Shuaib, A., Lees, K.R., Lyden, P., Grotta, J., Davalos, A., Davis, S.M., Diener, H.-C., Ashwood, T., Wasiewski, W.W., Emeribe, U., SAINT II Trial Investigators, 2007. NXY-059 for the Treatment of Acute Ischemic Stroke. N. Engl. J. Med. 357, 562–571. doi:10.1056/NEJMoa070240.

Sievers, F., Wilm, A., Dineen, D., Gibson, T.J., Karplus, K., Li, W., Lopez, R., McWilliam, H., Remmert, M., Söding, J., Thompson, J.D., Higgins, D.G., 2011. Fast, scalable generation of high-quality protein multiple sequence alignments using Clustal Omega. Mol. Syst. Biol. 7, 539. doi:10.1038/msb.2011.75.

Simon, R.P., Swan, J.H., Griffiths, T., Meldrum, B.S., 1984. Blockade of N-methyl-D-aspartate receptors may protect against ischemic damage in the brain. Science 226, 850–2.

Singh, M.H., Brooke, S.M., Zemlyak, I., Sapolsky, R.M., 2010. Evidence for caspase effects on release of cytochrome c and AIF in a model of ischemia in cortical neurons. Neurosci. Lett. 469, 179–183. doi:10.1016/j.neulet.2009.11.067.

Sircar, A., Chaudhury, S., Kilambi, K.P., Berrondo, M., Gray, J.J., 2010. A generalized approach to sampling backbone conformations with RosettaDock for CAPRI rounds 13-19. Proteins Struct. Funct. Bioinforma. 78, 3115–3123. doi:10.1002/prot.22765.

Smyth, A.M., Duncan, R.R., Rickman, C., 2010. Munc18-1 and Syntaxin1: Unraveling the Interactions Between the Dynamic Duo. Cell. Mol. Neurobiol. 30, 1309–1313. doi:10.1007/s10571-010-9581-1.

Sommer, C.J., 2017. Ischemic stroke: experimental models and reality. Acta Neuropathol. 133, 245–261. doi:10.1007/s00401-017-1667-0.

Squadrito, G.L., Cueto, R., Splenser, A.E., Valavanidis, A., Zhang, H., Uppu, R.M., Pryor, W.A., 2000. Reaction of Uric Acid with Peroxynitrite and Implications for the Mechanism of Neuroprotection by Uric Acid. Arch. Biochem. Biophys. 376, 333–337. doi:10.1006/abbi.2000.1721.

Stalmans, S., Bracke, N., Wynendaele, E., Gevaert, B., Peremans, K., Burvenich, C., Polis, I., De Spiegeleer, B., 2015. Cell-Penetrating Peptides Selectively Cross the Blood-Brain Barrier In Vivo. PLoS One 10,

e0139652. doi:10.1371/journal.pone.0139652.
Stephenson, F.A., 2006. Structure and trafficking of NMDA and GABA $_{A}$ receptors. Biochem. Soc. Trans. 34, 877–881. doi:10.1042/BST0340877.
Stovner, L.J., Zwart, J.-A., Hagen, K., Terwindt, G.M., Pascual, J., 2006. Epidemiology of headache in Europe. Eur. J. Neurol. 13, 333–345. doi:10.1111/j.1468-1331.2006.01184.x.
Stowe, A.M., Altay, T., Freie, A.B., Gidday, J.M., 2011. Repetitive hypoxia extends endogenous neurovascular protection for stroke. Ann. Neurol. 69, 975–85. doi:10.1002/ana.22367.
Stroke Therapy Academic Industry Roundtable (STAIR), 1999. Recommendations for standards regarding preclinical neuroprotective and restorative drug development. Stroke 30, 2752–8.
Südhof, T.C., 2013a. Neurotransmitter Release: The Last Millisecond in the Life of a Synaptic Vesicle. Neuron 80, 675–690. doi:10.1016/j.neuron.2013.10.022.
Südhof, T.C., 2013b. A molecular machine for neurotransmitter release: synaptotagmin and beyond. Nat. Med. 19, 1227–1231. doi:10.1038/nm.3338.
Südhof, T.C., 2012. The Presynaptic Active Zone. Neuron 75, 11–25. doi:10.1016/j.neuron.2012.06.012.
Südhof, T.C., 2004. The synaptic vesicle cycle. Annu. Rev. Neurosci. 27, 509–547. doi:10.1146/annurev.neuro.26.041002.131412.
Südhof, T.C., 1995. The synaptic vesicle cycle: a cascade of protein–protein interactions. Nature 375, 645–653. doi:10.1038/375645a0.
Sugimori H., Yao H., Ooboshi H., Ibayashi S., Iida M., 2004. Krypton laser-induced photothrombotic distal middle cerebral artery occlusion without craniectomy in mice. Brain Res. Protoc. 13, 189–196. doi:10.1016/J.BRAINRESPROT.2004.06.001.
Sugino, T., Nozaki, K., Hashimoto, N., 2000. Activation of mitogen-activated protein kinases in gerbil hippocampus with ischemic tolerance induced by 3-nitropropionic acid. Neurosci. Lett. 278, 101–4.
Sveinsson, O.A., Kjartansson, O., Valdimarsson, E.M., 2014. Cerebral ischemia/infarction - epidemiology, causes and symptoms. Laeknabladid 100, 271–9.
Szydlowska, K., Tymianski, M., 2010. Calcium, ischemia and excitotoxicity. Cell Calcium 47, 122–129. doi:10.1016/j.ceca.2010.01.003.
Tadano, T., Yonezawa, A., Oyama, K., Kisara, K., Arai, Y., Togashi, M., Kinemuchi, H., 1995. Effects of transient global ischemia and a monoamine oxidase inhibitor ifenprodil on rat brain monoamine metabolism. Prog. Brain Res. 106, 173–80.
Tajima, N., Karakas, E., Grant, T., Simorowski, N., Diaz-Avalos, R., Grigorieff, N., Furukawa, H., 2016. Activation of NMDA receptors and the mechanism of inhibition by ifenprodil. Nature 534, 63–68. doi:10.1038/nature17679.
Taylor, R.A., Sansing, L.H., 2013. Microglial Responses after Ischemic Stroke and Intracerebral Hemorrhage. Clin. Dev. Immunol. 2013, 1–10. doi:10.1155/2013/746068.
Tian, J.-H., Das, S., Sheng, Z.-H., 2003. Ca $^{2+}$ -dependent Phosphorylation of Syntaxin-1A by the Death-associated Protein (DAP) Kinase Regulates Its Interaction with Munc18. J. Biol. Chem. 278, 26265–26274. doi:10.1074/jbc.M300492200.
Toonen, R.F.G., De Vries, K.J., Zalm, R., Südhof, T.C., Verhage, M., 2005. Munc18-1 stabilizes syntaxin 1, but is not essential for syntaxin 1 targeting and SNARE complex formation. J. Neurochem. 93, 1393–1400. doi:10.1111/j.1471-4159.2005.03128.x.
Tournier, C., Hess, P., Yang, D.D., Xu, J., Turner, T.K., Nimnual, A., Bar-Sagi, D., Jones, S.N., Flavell, R.A., Davis, R.J., 2000. Requirement of JNK for stress-induced activation of the cytochrome c-mediated death pathway. Science 288, 870–4.
Tran, H.T., Sanchez, L., Brody, D.L., 2012. Inhibition of JNK by a Peptide Inhibitor Reduces Traumatic Brain Injury–Induced Tauopathy in Transgenic Mice. J. Neuropathol. Exp. Neurol. 71, 116–129. doi:10.1097/NEN.0b013e3182456aed.
Traystman, R.J., 2003. Animal models of focal and global cerebral ischemia. ILAR J. 44, 85–95.
Trotman, M., Vermehren, P., Gibson, C.L., Fern, R., 2015. The Dichotomy of Memantine Treatment for Ischemic Stroke: Dose-Dependent Protective and Detrimental Effects. J. Cereb. Blood Flow Metab. 35, 230–239. doi:10.1038/jcbfm.2014.188.
Vizi, E., Fekete, A., Karoly, R., Mike, A., 2010. Non-synaptic receptors and transporters involved in brain

functions and targets of drug treatment. Br. J. Pharmacol. 160, 785–809. doi:10.1111/j.1476-5381.2009.00624.x.

Vizi, E.S., Kisfali, M., Lőrincz, T., 2013. Role of nonsynaptic GluN2B-containing NMDA receptors in excitotoxicity: Evidence that fluoxetine selectively inhibits these receptors and may have neuroprotective effects. Brain Res. Bull. 93, 32–38. doi:10.1016/j.brainresbull.2012.10.005.

Vogel, K., Cabaniols, J.P., Roche, P.A., 2000. Targeting of SNAP-25 to membranes is mediated by its association with the target SNARE syntaxin. J. Biol. Chem. 275, 2959–65. doi:10.1074/JBC.275.4.2959.

Wan, P., Zhang, Y.-P., Yan, J., Xu, Y.-X., Wang, H.-Q., Yang, R., Zhu, C.-Q., 2010. Glutamate enhances the surface distribution and release of Munc18 in cerebral cortical neurons. Neurosci. Bull. 26, 273–281. doi:10.1007/s12264-010-0411-8.

Wang, H., Naghavi, M., Allen, C., Barber, R.M., Bhutta, Z.A., Carter, A., Casey, D.C., Charlson, F.J., Chen, A.Z., Coates, M.M., Coggeshall, M., Dandona, L., Dicker, D.J., Erskine, H.E., Ferrari, A.J., Fitzmaurice, C., Foreman, K., Forouzanfar, M.H., Fraser, M.S., Fullman, N., Gething, P.W., Goldberg, E.M., Graetz, N., Haagsma, et al., 2016. Global, regional, and national life expectancy, all-cause mortality, and cause-specific mortality for 249 causes of death, 1980–2015: a systematic analysis for the Global Burden of Disease Study 2015. Lancet 388, 1459–1544. doi:10.1016/S0140-6736(16)31012-1

Wang, X., Lo, E.H., 2003. Triggers and Mediators of Hemorrhagic Transformation in Cerebral Ischemia. Mol. Neurobiol. 28, 229–244. doi:10.1385/MN:28:3:229.

Wang, X.-T., Pei, D.-S., Xu, J., Guan, Q.-H., Sun, Y.-F., Liu, X.-M., Zhang, G.-Y., 2007. Opposing effects of Bad phosphorylation at two distinct sites by Akt1 and JNK1/2 on ischemic brain injury. Cell. Signal. 19, 1844–1856. doi:10.1016/j.cellsig.2007.04.005.

Wardlaw, J.M., Murray, V., Berge, E., del Zoppo, G.J., 2014. Thrombolysis for acute ischaemic stroke. Cochrane database Syst. Rev. CD000213. doi:10.1002/14651858.CD000213.pub3.

Wei, S., Sun, J., Li, J., Wang, L., Hall, C.L., Dix, T.A., Mohamad, O., Wei, L., Yu, S.P., 2013. Acute and delayed protective effects of pharmacologically induced hypothermia in an intracerebral hemorrhage stroke model of mice. Neuroscience 252, 489–500. doi:10.1016/j.neuroscience.2013.07.052.

Wei, Y., Sinha, S., Levine, B., 2008. Dual role of JNK1-mediated phosphorylation of Bcl-2 in autophagy and apoptosis regulation. Autophagy 4, 949–51.

Wei, Y., Yemisci, M., Kim, H.-H., Yung, L.M., Shin, H.K., Hwang, S.-K., Guo, S., Qin, T., Alsharif, N., Brinkmann, V., Liao, J.K., Lo, E.H., Waeber, C., 2011. Fingolimod provides long-term protection in rodent models of cerebral ischemia. Ann. Neurol. 69, 119–129. doi:10.1002/ana.22186.

Weston, C.R., Davis, R.J., 2007. The JNK signal transduction pathway. Curr. Opin. Cell Biol. 19, 142–149. doi:10.1016/j.ceb.2007.02.001.

White, B.C., Sullivan, J.M., DeGracia, D.J., O'Neil, B.J., Neumar, R.W., Grossman, L.I., Rafols, J.A., Krause, G.S., 2000. Brain ischemia and reperfusion: molecular mechanisms of neuronal injury. J. Neurol. Sci. 179, 1–33.

Whitmarsh, A.J., Kuan, C.Y., Kennedy, N.J., Kelkar, N., Haydar, T.F., Mordes, J.P., Appel, M., Rossini, A.A., Jones, S.N., Flavell, R.A., Rakic, P., Davis, R.J., 2001. Requirement of the JIP1 scaffold protein for stress-induced JNK activation. Genes Dev. 15, 2421–2432. doi:10.1101/gad.922801.

Whyte, J.R.C., Munro, S., 2002. Vesicle tethering complexes in membrane traffic. J. Cell Sci. 115, 2627–37.

Wilhelm, B.G., Mandad, S., Truckenbrodt, S., Krohnert, K., Schafer, C., Rammner, B., Koo, S.J., Classen, G.A., Krauss, M., Haucke, V., Urlaub, H., Rizzoli, S.O., 2014. Composition of isolated synaptic boutons reveals the amounts of vesicle trafficking proteins. Science (80-.). 344, 1023–1028. doi:10.1126/science.1252884.

Williams, K., 1993. Ifenprodil discriminates subtypes of the N-methyl-D-aspartate receptor: selectivity and mechanisms at recombinant heteromeric receptors. Mol. Pharmacol. 44, 851–9.

Wolf, P.A., Dawber, T.R., Thomas, H.E., Colton, T., Kannel, W.B., 1977. Epidemiology of stroke. Adv. Neurol. 16, 5–19.

Wong, A.H.C., Trakalo, J., Likhodi, O., Yusuf, M., Macedo, A., Azevedo, M.-H., Klempan, T., Pato, M.T., Honer, W.G., Pato, C.N., Van Tol, H.H.M., Kennedy, J.L., 2004. Association between schizophrenia and the syntaxin 1A gene. Biol. Psychiatry 56, 24–29. doi:10.1016/j.biopsych.2004.03.008.

World Health Organisation (1978). Cerebrovascular Disorders. Geneva.

Wroge, C.M., Hogins, J., Eisenman, L., Mennerick, S., 2012. Synaptic NMDA Receptors Mediate Hypoxic

Excitotoxic Death. J. Neurosci. 32, 6732–6742. doi:10.1523/JNEUROSCI.6371-11.2012.

Xu, Y., Ji, R., Wei, R., Yin, B., He, F., Luo, B., 2016. The Efficacy of Hyperbaric Oxygen Therapy on Middle Cerebral Artery Occlusion in Animal Studies: A Meta-Analysis. PLoS One 11, e0148324. doi:10.1371/journal.pone.0148324.

Yam, P.S., Dunn, L.T., Graham, D.I., Dewar, D., McCulloch, J., 2000. NMDA Receptor Blockade Fails to Alter Axonal Injury in Focal Cerebral Ischemia. J. Cereb. Blood Flow Metab. 20, 772–779. doi:10.1097/00004647-200005000-00003.

Yamasaki, T., Kawasaki, H., Nishina, H., 2012. Diverse Roles of JNK and MKK Pathways in the Brain. J. Signal Transduct. 2012, 1–9. doi:10.1155/2012/459265.

Yang, D.D., Kuan, C.-Y., Whitmarsh, A.J., Rinócn, M., Zheng, T.S., Davis, R.J., Rakic, P., Flavell, R.A., 1997. Absence of excitotoxicity-induced apoptosis in the hippocampus of mice lacking the Jnk3 gene. Nature 389, 865–870. doi:10.1038/39899.

Yang, X.-R., Sun, P., Qin, H.-P., Si, P.-P., Sun, X.-F., Zhang, C., 2012. Involvement of MAPK pathways in NMDA-induced apoptosis of rat cortical neurons. Sheng Li Xue Bao 64, 609–16.

Yang, Y., Rosenberg, G.A., 2015. Matrix metalloproteinases as therapeutic targets for stroke. Brain Res. 1623, 30–38. doi:10.1016/j.brainres.2015.04.024.

Yemisci, M., Gursoy-Ozdemir, Y., Vural, A., Can, A., Topalkara, K., Dalkara, T., 2009. Pericyte contraction induced by oxidative-nitrative stress impairs capillary reflow despite successful opening of an occluded cerebral artery. Nat. Med. 15, 1031–1037. doi:10.1038/nm.2022.

Yenari, M.A., Han, H.S., 2012. Neuroprotective mechanisms of hypothermia in brain ischaemia. Nat. Rev. Neurosci. 13, 267–78. doi:10.1038/nrn3174.

Yenari, M.A., Hemmen, T.M., 2010. Therapeutic Hypothermia for Brain Ischemia: Where Have We Come and Where Do We Go? Stroke 41, S72–S74. doi:10.1161/STROKEAHA.110.595371.

Yong, Y., He, L., 2005. SHEsis, a powerful software platform for analyses of linkage disequilibrium, haplotype construction, and genetic association at polymorphism loci. Cell Res. 15, 97–98. doi:10.1038/sj.cr.7290272.

Yu, Y., Han, Q., Ding, X., Chen, Q., Ye, K., Zhang, S., Yan, S., Campbell, B.C. V, Parsons, M.W., Wang, S., Lou, M., 2016. Defining Core and Penumbra in Ischemic Stroke: A Voxel- and Volume-Based Analysis of Whole Brain CT Perfusion. Sci. Rep. 6, 20932. doi:10.1038/srep20932.

Yu, Y.-X., Shen, L., Xia, P., Tang, Y.-W., Bao, L., Pei, G., 2006. Syntaxin 1A promotes the endocytic sorting of EAAC1 leading to inhibition of glutamate transport. J. Cell Sci. 119, 3776–3787. doi:10.1242/jcs.03151.

Yurkewicz, L., Weaver, J., Bullock, M.R., Marshall, L.F., 2005. The Effect of the Selective NMDA Receptor Antagonist Traxoprodil in the Treatment of Traumatic Brain Injury. J. Neurotrauma 22, 1428–1443. doi:10.1089/neu.2005.22.1428.

Zamponi, G.W., 2003. Regulation of presynaptic calcium channels by synaptic proteins. J. Pharmacol. Sci. 92, 79–83.

Zhang, R.L., Chopp, M., Chen, H., Garcia, J.H., 1994. Temporal profile of ischemic tissue damage, neutrophil response, and vascular plugging following permanent and transient (2H) middle cerebral artery occlusion in the rat. J. Neurol. Sci. 125, 3–10.

Zhu, Z., Fu, Y., Tian, D., Sun, N., Han, W., Chang, G., Dong, Y., Xu, X., Liu, Q., Huang, D., Shi, F.-D., 2015. Combination of the Immune Modulator Fingolimod With Alteplase in Acute Ischemic StrokeCLINICAL PERSPECTIVE. Circulation 132, 1104–1112. doi:10.1161/CIRCULATIONAHA.115.016371.

Zipfel, G.J., Babcock, D.J., Lee, J.-M., Choi, D.W., 2000. Neuronal Apoptosis After CNS Injury: The Roles of Glutamate and Calcium. J. Neurotrauma 17, 857–869. doi:10.1089/neu.2000.17.857.

APPENDIX

List of Publications:

[1] **Marcelli**, **S.**, Iannuzzi, F., Ficulle, E., Mango D., Pieraccini, S., Pellegrino, S., Muzzi, M., Ciotti, MT., Sironi, M., Corbo, M., Costa, AS., Guerini, FR., Clerici, M., Pittaluga, A., Chiarugi, A., Nisticò, R., Feligioni, M., 2017. Cerebral Ischemia and excitotoxicity are prevented by selective inhibition of presynaptic JNK2 and STX1a interaction (submitted).

[2] **Marcelli**, **S.**, Ficulle, Piccolo, L., Corbo, M., Feligioni, M., 2017. An overview of the possible therapeutic role of SUMOylation in the treatment of Alzheimer's disease (submitted).

[3] **Marcelli**, **S.**, Iannuzzi, F., Corbo, M., Negri, L., Blandini, F., Nisticò, R., Feligioni, M., 2017. The involvement of post-translational modifications in Alzheimer's disease. Curr. Alzheimer Res. 14, 1. doi:10.2174/1567205014666170505095109.

[4] Mango, D., Braksator, E., Battaglia, G., **Marcelli**, **S.**, Mercuri, N.B., Feligioni, M., Nicoletti, F., Bashir, Z.I., Nisticò, R., 2017. Acid-sensing ion channel 1a is required for mGlu receptor dependent long-term depression in the hippocampus. Pharmacol. Res. 119, 12–19. doi:10.1016/j.phrs.2017.01.028.

[5] **Marcelli**, **S.**, Iannuzzi, F., Ficulle, E., Aquaro, S., Ciechanover, A., Nisticò, R., Feligioni, M., 2016. Involvement of Sumoylation in Alzheimer's disease. Eur J Neurodegener Dis. ISSN: 2279-5855.

[6] **Marcelli**, **S.**, Ficulle, E., Iannuzzi, F., Kövari, E., Nisticò, R., Feligioni, M., 2016. Targeting SUMO-1ylation Contrasts Synaptic Dysfunction in a Mouse Model of Alzheimer's Disease. Mol. Neurobiol. doi:10.1007/s12035-016-0176-9.

[7] Feligioni, M., **Marcelli**, **S.**, Knock, E., Nadeem, U., Arancio, O., E Fraser, P., 2015. SUMO modulation of protein aggregation and degradation. AIMS Mol. Sci. 2, 382–410. doi:10.3934/molsci.2015.4.382.